Supporting information

Mechanistically Orthogonal Radical Strategies Converging on Programmable Site-Selective Halogenation of Quinoxalinones

Chidananda Biswal[a,†], Pravat Nayek[a,†], Sandeepan Maity[a, b,*] and Prasenjit Mal[a,*]

[a]School of Chemical Sciences, National Institute of Science Education and Research (NISER), Bhubaneswar, An OCC of Homi Bhabha National Institute, PO Bhimpur-Padanpur, Via Jatni, District Khurda, Odisha 752050, India.

[b]Department of Chemistry, C. V. Raman Global University, Bidya Nagar, Mahura, Bhubaneswar, Odisha-752054, India.

† Equal contributing authors.

*Corresponding author: Prasenjit Mal, E-mail: pmal@niser.ac.in

Table of contents

GENERAL INFORMATION

Instrumentation. Purifications of difunctionalized quinoxalinones were performed using column chromatography with silica gel (100-200 or 230-400 mesh size) as the stationary phase and mixtures of hexane and ethyl acetate in various ratios as the eluent. NMR spectra were recorded on 400 MHz and 700 MHz Bruker NMR instruments at 25 °C. The chemical shift values are reported in parts per million (ppm) in DMSO-d_6 solvent, referencing residual DMSO (2.50 ppm for ^{1}H and 39.5 ppm for ^{13}C). The peak patterns are designated as follows: s: singlet; d: doublet; t: triplet; q: quartet; m: multiplet. The coupling constants (*J*) are reported in hertz (Hz). High-resolution mass spectra (HRMS) were recorded on an ESI-TOF (time of flight) mass spectrometer. A Thermo-scientific (NICOLET iS5) instrument was used to perform all the FT-IR data under transmittance mode. Infrared (IR) spectral data are reported in wavenumber (cm^{-1}). FT-IR spectra were recorded using an ATR machine (for solid compounds) and on KBr pellets (for liquids), drop-casting a diluted DCM solution. All the photochemical reactions were carried out in a 10 mL quartz tube in a photoreactor that contains four 3W blue LED bulbs. The UV-vis absorption spectra were recorded in a *J*asco V-730 spectrophotometer (Serial number: Ao33661798). The ESR spectra were recorded with a Bruker EMX-microX system at 9.4335 GHz and 298 K. Mass spectra were obtained from Waters XEVO-G2XSQTOF Spectrometer. High-resolution mass spectra (HRMS) were recorded on an electrospray ionization (ESI)-TOF (time of flight) mass spectrometer.

Chemicals. *N*-Bromosuccinimide was purchased from Sigma Aldrich, sodium salts were purchased from TCI, and lithium salts were purchased from Spectrochem. HPLC-grade

dimethylformamide solvent was purchased from Spectrochem. All the commercially available chemicals were used directly without further purification unless mentioned. Perylene diimide (PDI) was synthesized by following the literature report.[1] All quinoxalinone substrates were synthesized following the literature report.[2]

Experimental Setup

All photochemical reactions were performed in a custom-designed photoreactor fitted with four 3W blue LED bulbs as the light source. To prevent excessive heating and maintain near-ambient reaction temperatures, the reactor was equipped with four cooling fans that provided continuous airflow during irradiation.

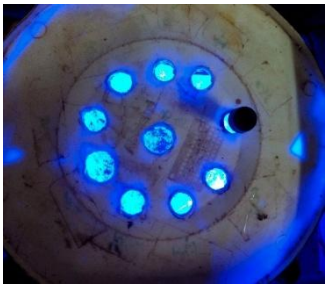

Figure S1. The blue LED photoreactor with four 3W blue LED bulbs.

The sunlight-driven reaction was carried out on the second-floor corridor of the School of Chemical Sciences, NISER Bhubaneswar, India (8 AM to 2 PM, IST).

Figure S2. The reaction set-up in sunlight.

EXPERIMENTAL SECTION

General synthesis procedure for the synthesis of Quinoxalin-2(1*H*)-one derivatives.[2] In a 50 mL round-bottomed flask, *o*-phenylenediamine (200 mg, 1.849 mmol) was dissolved in 15 mL of ethanol, followed by the dropwise addition of ethyl glyoxylate (1.2 equiv, 2.218 mmol). The reaction mixture was then stirred at 80 ˚C for 3 h, followed by stirring at room temperature for 12 h. After the completion of the reaction, the crude reaction mixture was filtered, washed with ethanol, and an off-white solid was obtained after drying under high vacuum, which was directly used in the next step.

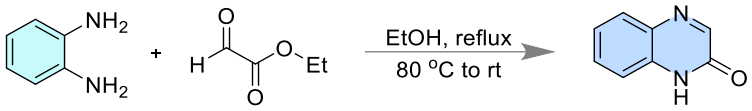

Scheme S1. Synthesis of Quinoxalin-2(1*H*)-one.

General synthesis procedure for the synthesis of *N*-substituted quinoxalin-2(1*H*)-one derivatives.[1] In a 50 mL round-bottomed flask, Quinoxalin-2(1*H*)-one (100 mg, 0.684 mmol) was dissolved in 5 mL of DMF and stirred at room temperature, followed by the addition of K_2CO_3 (1.2 equiv, 0.820 mmol). After 10 min of stirring, methyl iodide (1.5 equiv, 1.026 mmol) was added. After 24 h, the crude mixture was extracted with ethyl acetate, washed with brine, and collected over anhydrous Na_2SO_4, and concentrated using a rotary evaporator. Then the crude residue was purified by column chromatography to obtain the desired 1-methylquinoxalin-2(1*H*)-one derivatives.

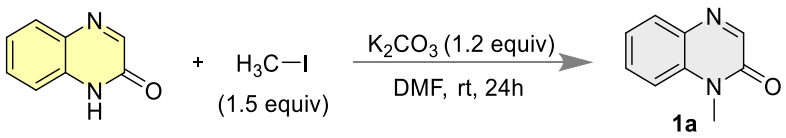

Scheme S2. Synthesis of 1-methylquinoxalin-2(1*H*)-one (**1a**).

General synthesis procedure for oxidative *mono*-bromination using Path-a. In a 10 mL quartz tube, 1-methylquinoxalin-2(1*H*)-one (60 mg), *N*-fluorobenzenesulfonimide (NFSI) (3.5

equiv, 1.312 mmol), NaBr (3.5 equiv, 1.312 mmol) and PDI (3 mol %, 0.011 mmol) were dissolved in 2 mL DMF and exposed to (3W × 4) blue LEDs for 12 h. After the completion of the reaction, the reaction mixture was extracted with ethyl acetate-brine, the organic layer was collected over anhydrous Na_2SO_4 and concentrated using a rotary evaporator. The desired product was isolated using column chromatography with ethyl acetate and hexane as eluents.

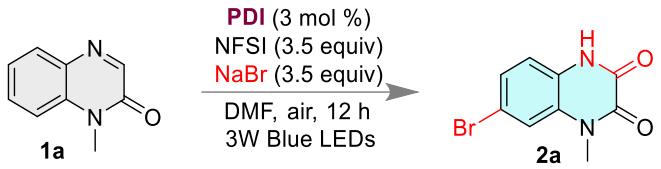

Scheme S3. Synthesis of 7-bromo-1-methyl-1,4-dihydroquinoxaline-2,3-dione **(2a)** using an inorganic bromine source (path-a).

General synthesis procedure for oxidative *mono*-bromination using Path-b. In a 25 mL round-bottomed flask, 1-methylquinoxalin-2(1*H*)-one (60 mg) and *N*-bromosuccinimide (2.5 equiv, 0.937 mmol) were dissolved in 2 mL of DMF and stirred for 10 h in air. After the reaction completion, the solvent was evaporated, the residue was dissolved in ethyl acetate, and washed with brine. The organic layer was collected over anhydrous Na_2SO_4, concentrated, and the mixture was purified using column chromatography with ethyl acetate and hexane as the eluent.

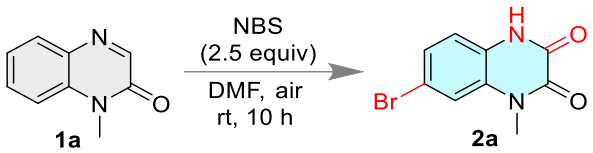

Scheme S4. Synthesis of 7-bromo-1-methyl-1,4-dihydroquinoxaline-2,3-dione **(2a)** using organic bromine source (path-b).

General synthesis procedure for sunlight reaction. In a 10 mL quartz tube, 1-methylquinoxalin-2(1*H*)-one (60 mg), *N*-fluorobenzenesulfonimide (NFSI) (3.5 equiv, 1.312 mmol), NaBr (3.5 equiv, 1.312 mmol) and PDI (3 mol %, 0.011 mmol) were dissolved in 2 mL DMF and exposed to sunlight for 6 h. After the completion of the reaction, the reaction mixture

was extracted with ethyl acetate-brine, the organic layer was collected over anhydrous Na_2SO_4 and concentrated using a rotary evaporator. Then the desired product was purified using column chromatography with ethyl acetate and hexane as eluent.

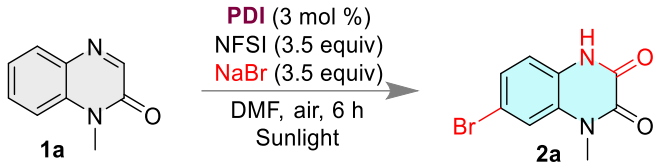

Scheme S5. Synthesis of 7-bromo-1-methyl-1,4-dihydroquinoxaline-2,3-dione **(2a)** using an inorganic bromine source in sunlight.

General synthesis procedure for oxidative dibromination using Path-a. In a 10 mL quartz tube, 1-methylquinoxalin-2(1*H*)-one (**1a**, 60 mg), *N*-fluorobenzenesulfonimide (NFSI) (3.5 equiv, 1.312 mmol), NaBr (9 equiv, 3.374 mmol) and PDI (3 mol %, 0.011 mmol) were dissolved in 3 mL DMF and exposed to (3W × 4) blue LEDs for 12 h. After the completion of the reaction, checked by TLC analysis, the reaction mixture was extracted with ethyl acetate-brine, the organic layer was collected over anhydrous Na_2SO_4 and concentrated using a rotary evaporator. The desired product was purified from the crude reaction mixture using column chromatography with ethyl acetate and hexane as eluents.

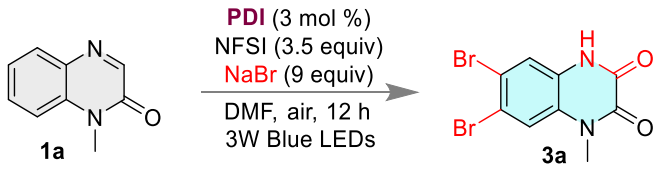

Scheme S6. Synthesis of 6,7-dibromo-1-methyl-1,4-dihydroquinoxaline-2,3-dione **(3a)** using an inorganic bromine source (path-a).

General synthesis procedure for oxidative dibromination using Path-b. In a 25 mL round-bottomed flask, 1-methylquinoxalin-2(1*H*)-one (**1a**, 60 mg) and *N*-bromosuccinimide (8 equiv, 2.998 mmol) were dissolved in 3 mL of DMF and stirred for 10 h in air. After the completion of the reaction, checked by TLC analysis, the reaction mixture was extracted with ethyl acetate-

brine, the organic layer was collected over anhydrous Na_2SO_4 and concentrated using a rotary evaporator. Then the crude reaction mixture was purified using column chromatography with ethyl acetate and hexane as the eluent.

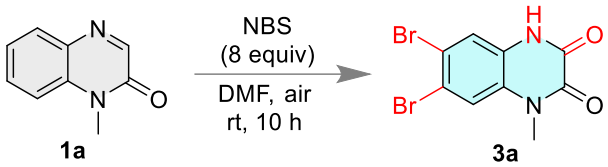

Scheme S7. Synthesis of 6,7-dibromo-1-methyl-1,4-dihydroquinoxaline-2,3-dione **(3a)** using organic bromine source (path-b).

Synthesis Procedure of 6-bromo-1-phenyl-4-(4-(trifluoromethyl)benzyl)-1,4-dihydroquinoxaline-2,3-dione (6a).[3] To a 50 mL round-bottom flask, substrate (60 mg), phenylboronic acid (1.5 equiv, 0.225 mmol), copper acetate (20 mol %, 0.03 mmol), and 1,10-phenanthroline (20 mol %, 0.03 mmol) were dissolved in DMSO (3 mL) and allowed to stir for 24 h at room temperature. After completion of the reaction, which was monitored by TLC, the mixture was extracted with ethyl acetate and water, the organic layer was collected over anhydrous Na_2SO_4, concentrated, and purified using column chromatography (ethyl acetate: hexane)

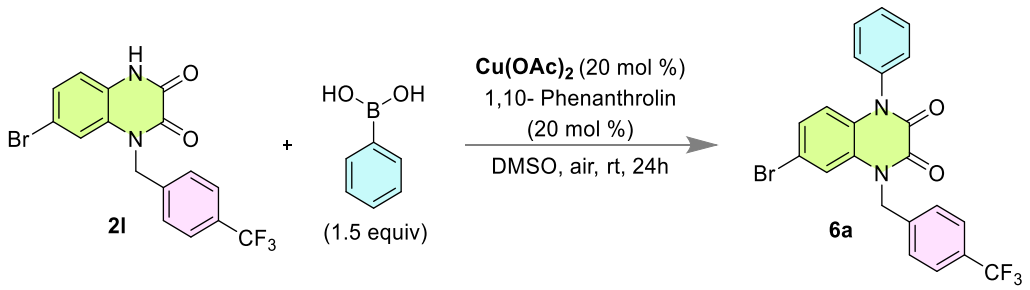

Scheme S8. Synthesis of 6-bromo-1-phenyl-4-(4-(trifluoromethyl)benzyl)-1,4-dihydroquinoxaline-2,3-dione **(6a).**

General Procedure for the synthesis of 1-benzyl-1,4-dihydroquinoxaline-2,3-dione (7a).[4]

To a 15 mL glass vial, substrate (60 mg), Pd/C (10 mol %) were dissolved in 2 mL of THF and allowed to stir for 12 h in the presence of a hydrogen gas balloon. After completion of the reaction, the mixture was extracted with ethyl acetate and water; the organic layer was collected over anhydrous Na_2SO_4, concentrated, and purified through column chromatography using hexane and ethyl acetate.

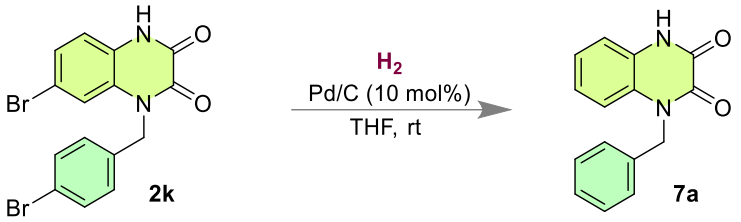

Scheme S9. Synthesis of 1-benzyl-1,4-dihydroquinoxaline-2,3-dione **(7a).**

Optimization of the reaction conditions

(Path-'a', NaBr-mediated pathway).

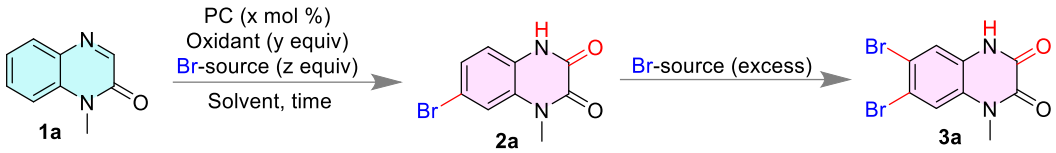

Table S1. Screening of NFSI and NaBr loading.[sa]

Entry	NFSI (equiv)	NaBr (equiv)	Yield **2a** (%)[sh]	Yield **3a** (%)[sh]
01	3	1	trace	-
02	3	2	17	-
03	3	3	37	-
04	3	3.5	40	trace
05	3	4	41	trace
06	3.5	6	27	30

07	1	2	12	-
08	2	3	35	-
09	3	3.5	47	trace
10	**3.5**	**3.5**	**55**	-
11	4	4	47	trace
12	4	6	30	25
13	4	10	trace	45
14	**3.5**	**9**	**15**	**47**
15	10	3.5	trace	-
16	-	3.5	NR	NR

[sa]standard condition: substrate (**1a**, 60 mg), and PDI (20 mol %) in 2 mL DMF irradiated with 3W LEDs for 12 h. [sh]Isolated reaction yield.

First, all the reactions were conducted with a fixed high loading (20 mol %) of the catalyst (PDI). Initially, 3 equiv of NFSI and 1 equiv of NaBr were utilised with **1a**, and we received a trace amount of **2a** (Table S1, entry 1). By increasing the loading of NaBr, the yield of 2a was increased, while a very high loading of NaBr leads to the formation of 3a in a certain amount (entries 2-6). Increasing the loading of NFSI, keeping NaBr fixed at 3.5 equiv, we received the optimum yield for **2a** (entry 10). While keeping the 3.5 equiv loading of NFSI fixed, and using a higher stoichiometry of NaBr we received dibrominated product (**3a**) in optimum yield (entry 14).

Table S2. Screening of solvents.[sb]

Entry	Solvents	Yield **2a** (%)[sh]
01	ACN	40
02	DMSO	NR
03	DCE	NR
04	**DMF**	**55**

05	THF	NR
06	MeOH	25
07	Dry DMF	15
08	DMF:H_2O (9:1)	53
09	DMF:H_2O (7:3)	45

[sb]standard condition: substrate (**1a**, 60 mg), NFSI (3.5 equiv), NaBr (3.5 equiv), and PDI (20 mol %) in 2 mL of solvent irradiated with 3W LEDs for 12 h. [sh]Isolated reaction yield.

After that, the solvent of the reaction was optimized for the formation of **2a** with a fixed loading of NFSI and NaBr (Table S2). All the reactions were conducted with 20 mol % PDI. Although acetonitrile produced 40% of 2a, DMSO or dichloroethane failed (entries 1-3). Normal DMF leads to the maximum generation of **2a** with 55% reaction yield (entry 4), while THF and methanol failed to improve the reaction (entries 5-6). Using dry DMF led to a decrease in reaction yield, highlighting the important role of moisture in the reaction system (entry 7). This observation was further supported by experiments showing that the reaction proceeds smoothly in a 9:1 mixture of DMF and water; increasing the water content beyond this ratio resulted in a reduced product yield (entries 8-9). However, as the reaction proceeded in normal moist DMF, further addition of water was avoided.

Table S3. Screening of the photocatalyst and light source.[sc]

Entry	Photocatalyst (mol %)	Light	Yield **2a** (%)[sh]
01	PDI (20)	Blue LED	56
02	PDI (10)	Blue LED	51
03	**PDI (3)**	**Blue LED**	**55**
04	PDI (1)	Blue LED	22

05	PDI (3)	Green LED	45
06	PDI (3)	White LED	33
07	PDI (3)	Sun light	45[si]
08	-	-	trace
09	Mes-Acr-ClO_4 (3)	Blue LED	44
10	Rose Bengal (3)	Blue LED	trace
11	Eosin Y (3)	Blue LED	35
12	Rhodamine 6G (3)	Blue LED	25

[sc]standard condition: substrate (**1a**, 60 mg), NFSI (3.5 equiv), NaBr (3.5 equiv), and photocatalyst in 2 mL DMF irradiated with 3W LED bulbs for 12 h. [sh]Isolated reaction yield. [si]Reaction performed for 6h.

After optimizing the solvent and reagent, we checked the catalyst loading and light source (Table S3). The loading of PDI can be minimized to as low as 3 mol % from 20 mol %, but less than that leads to a decrease in the reaction yield (entries 1-4). The formation of 2a was not improved in 12W green LEDs or 40W white LEDs (entries 5-6). The formation of 2a was successfully achieved in sunlight with 45% reaction yield (entry 7). The reaction without light or a photocatalyst leads to a trace amount of formation of 2a (entry 8). Some standard organic photocatalysts, like Fukuzumi, Rose Bengal, or Eosin Y, also failed to improve the reaction yield (entries 9-12).

Table S4. Screening of the atmosphere and time.[sd]

Entry	Atmosphere	Time (h)	Yield **2a** (%)[sh]
01	Ar	12	56
02	**air**	**12**	**55**
03	O_2	12	51

04	air	24	56
05	air	6	38
06	air	8	45

[sd]standard condition: substrate (60 mg), NFSI (3.5 equiv), NaBr (3.5 equiv), and PDI (3 mol %) in 2 mL DMF irradiated with 3W LEDs. [sh]Isolated reaction yield.

The, we checked the role of the atmospheric environment in the reaction system. Our initial trial suggested that the reaction proceeded with a similar reaction yield in both an aerial environment and in argon, eliminating the role of aerial oxygen in the reaction (entries 1-2). Also, we performed a reaction in an O_2 environment and found no prominent effect (entry 3). The reaction requires a minimum of 12 h; shorter reaction times lead to decreased yield, while extending the reaction to 24 h does not result in any further improvement in yield (entries 4-6).

Optimization of the reaction conditions (Path-'b', NBS-mediated pathway).

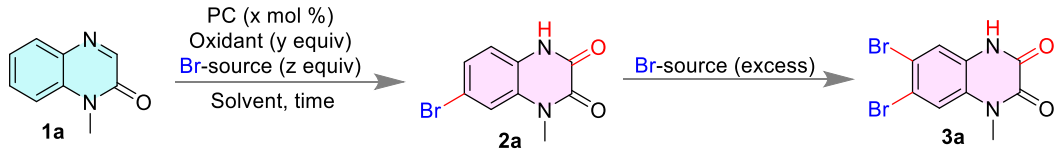

Table S5. Screening of Br-source.[se]

Entry	Br-source (equiv)	Photocatalyst (mol %)	Oxidant (equiv)	Yield 2a (%)[sh]	Yield 3a (%)[sh]
01	NBSA (3.5)	PDI (3)	NFSI (3.5)	33	-
02	CBr_4 (3.5)	PDI (3)	NFSI (3.5)	NR	NR
03	TBIA (3.5)	PDI (3)	NFSI (3.5)	NR	NR
04	DBIA (3.5)	PDI (3)	NFSI (3.5)	52	-
05	NBS (3.5)	PDI (3)	NFSI (3.5)	61	11
06	NBS (1)	-	-	Trace	-
07	**NBS (2.5)**	-	-	**75**	-
08	NBS (3)	-	-	67	trace
09	NBS (5)	-	-	52	35

10	**NBS (8)**	**-**	**-**	**10**	**56**
11	NBS (10)	-	-	15	47

[se]standard condition: substrate (**1a**, 60 mg), and Br-source in 2 mL DMF stirred at room temperature for 10-12 h. [sh]Isolated reaction yield.

Initially, we replaced the inorganic halide with several organic bromine sources to evaluate their effectiveness in the reaction (Table S5). Fragile bromine sources such as tribromoisocyanuric acid (TBIA) and carbon tetrabromide (CBr_4) resulted in no observable reaction, whereas, somewhat surprisingly, dibromoisocyanuric acid (DBIA) afforded **2a** in 52% yield (entries 2–5). Although *N*-bromosaccharin (NBSA) failed to improve the reaction yield (entry 1), *N*-bromosuccinimide (NBS) provided **2a** in 61% yield along with a trace amount of **3a** (entry 5). Further investigation revealed that, in the NBS-based system, the catalyst is not required; bromine radicals generated in the polar solvent (Figure S3) are sufficient to drive the reaction. Under these conditions, the yield of **2a** increased to a maximum of 75% when 2.5 equiv of NBS were used (entry 7). In contrast, increasing the NBS loading to 9 equiv favored the formation of **3a**, which was obtained in up to 56% yield (entries 8-10). However, further increases in NBS resulted in mixtures of **2a** and **3a** with an uncontrolled ratio.

Table S6. Screening of solvents.[sf]

Entry	Solvents	Yield 2a (%)[sh]
01	ACN	Trace
02	DMSO	NR
03	DCE	NR
04	1,4 dioxane	Trace
05	**DMF**	**75**
06	MeOH	57
07	DCM	32

08	THF	NR

[sf]standard condition: substrate (**1a**, 60 mg), and NBS (2.5 equiv) in 2 mL of solvent stirred at room temperature for 10 h. [sh]Isolated reaction yield.

For the NBS-based pathway, we also optimized the solvents of the reaction and found that DMF shows superior activity compared to other solvents (Table S6, entries 1-8).

Table S7. Screening of atmosphere and time.[sg]

Entry	Atmosphere	Time	Yield 2a (%)[sh]
01	air	12	72
02	Ar	12	64
03	O_2	12	66
04	**air**	**10**	**75**
05	air	5	59
06	air	24	77

[sg]standard condition: substrate (60 mg, 0.375 mmol), and NBS (2.5 equiv) in 2 mL DMF stirred at room temperature. [sh]Isolated reaction yield.

Then, we optimized the atmospheric effect in the NBS-mediated pathway (Table S7). Initial investigation demonstrated that the reaction shows slightly better performance in air, compared to argon or in a pure oxygen environment, possibly due to the presence of moisture in the reaction system (entries 1-3). The, we optimized the duration of the reaction and found that a minimum of 10 h was needed for optimum yield of **2a** (entries 4-6).

Bromine radical generation in DMF from NBS.[5] To examine whether bromine radicals are generated upon the addition of NBS to DMF, 60 mg of NBS was dissolved in 2 mL of DMF,

and the mixture was stirred for 6 h. During this period, the initially colourless solution gradually turned yellow, suggesting the in situ formation of molecular bromine.

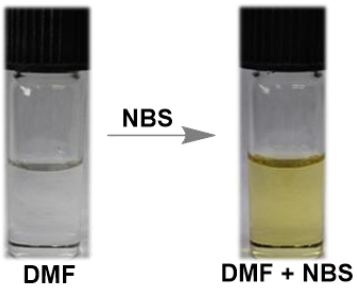

Figure S3. The color changes from colorless to yellow upon the addition of NBS to DMF.

EPR Quenching Experiment with TEMPO. To further probe the presence of radical species, an EPR quenching experiment was conducted using TEMPO. In a 25 mL round-bottom flask, 60 mg of TEMPO was dissolved in 2 mL of DMF, followed by the addition of 2 equivalents of NBS. EPR spectra were recorded at certain intervals. A gradual decrease in the characteristic EPR signal of TEMPO, a stable free radical, was observed over time, indicating quenching of TEMPO and supporting the generation of radical species in the reaction mixture.

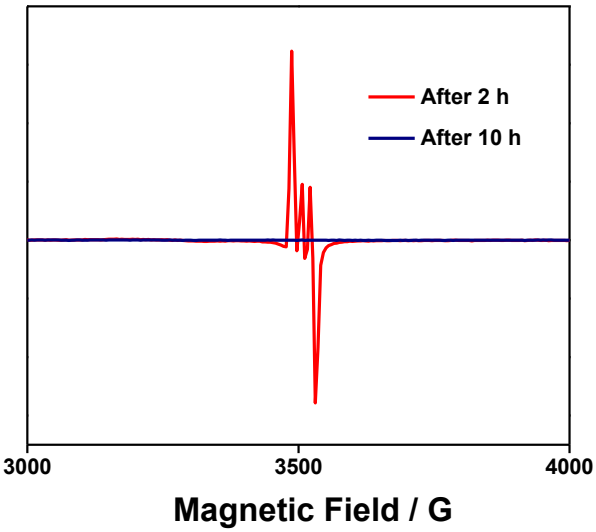

Figure S4. The EPR-quenching experiment of TEMPO.

Radical scavenging reaction procedure by TEMPO, BHT, 1,1-DPE. In a 10 mL quartz tube, 1-methylquinoxalin-2(1*H*)-one (**1a**, 60 mg), *N*-fluorobenzenesulfonimide (3.5 equiv, 1.312 mmol), NaBr (3.5 equiv, 1.312 mmol), and PDI (3 mol %, 0.011 mmol) were dissolved in 2 mL DMF, followed by the addition of 4 equiv of radical scavengers (TEMPO, BHT, 1,1-DPE) in the reaction mixture. Then the reaction mixture was irradiated with 3W blue LEDs for 12 h in air. After that, the reaction mixture was directly sent for mass spectrometric analysis. Similarly, radical scavenging experiments were conducted for the NBS-mediated pathway (path-b) as well.

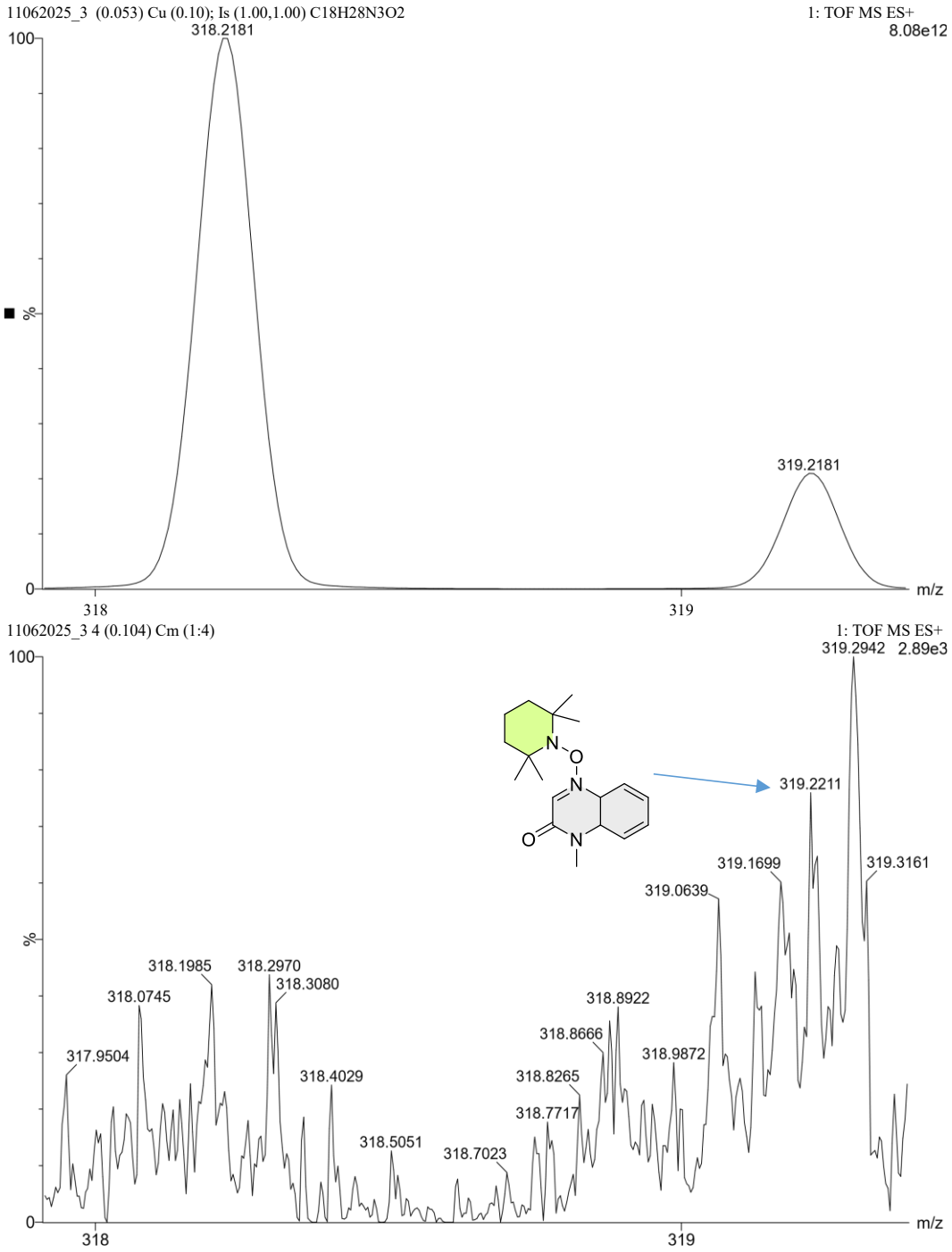

Figure S5. HRMS spectra of TEMPO trapped quinoxalinone radical.

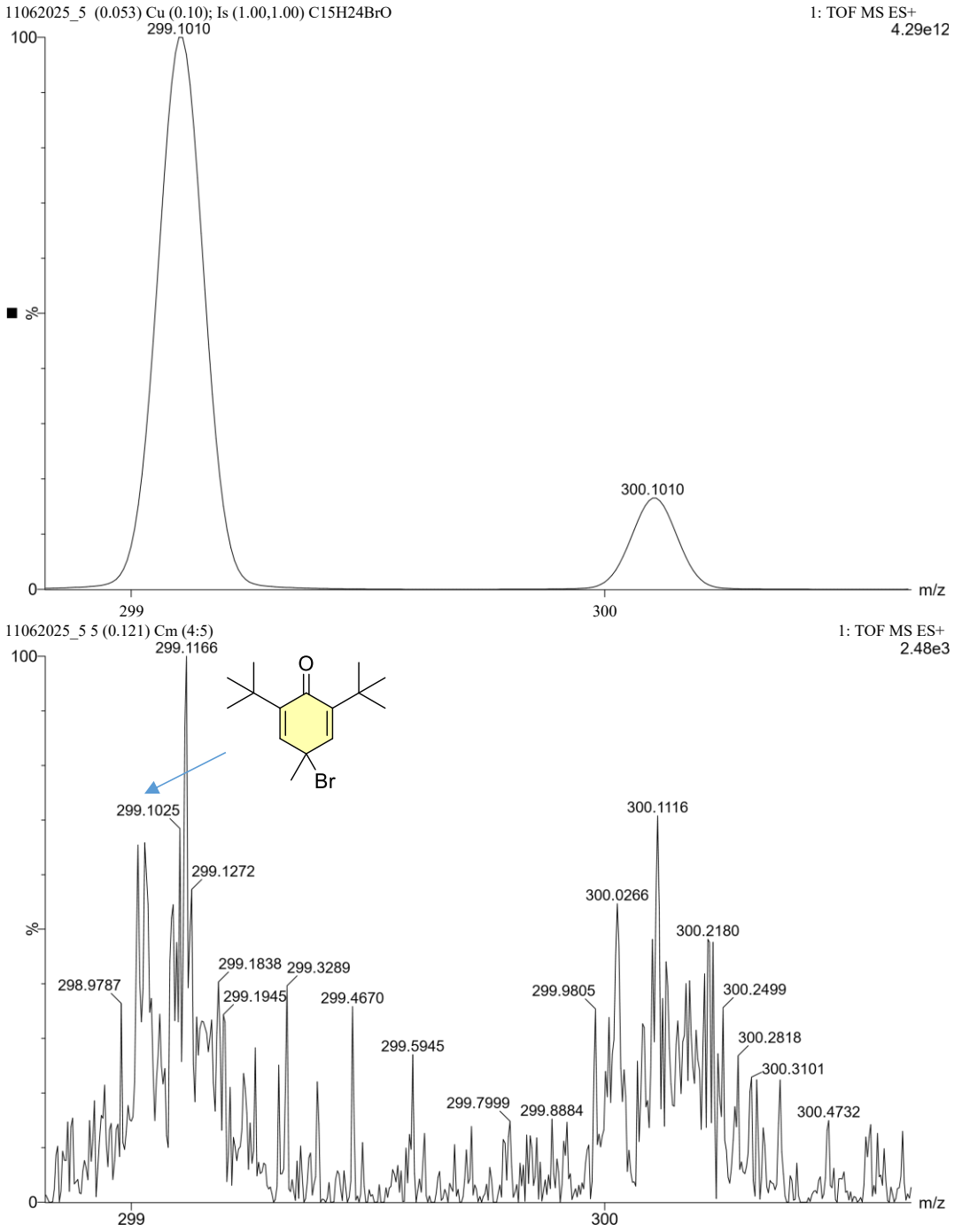

Figure S6. HRMS spectra of BHT trapped bromine radical.

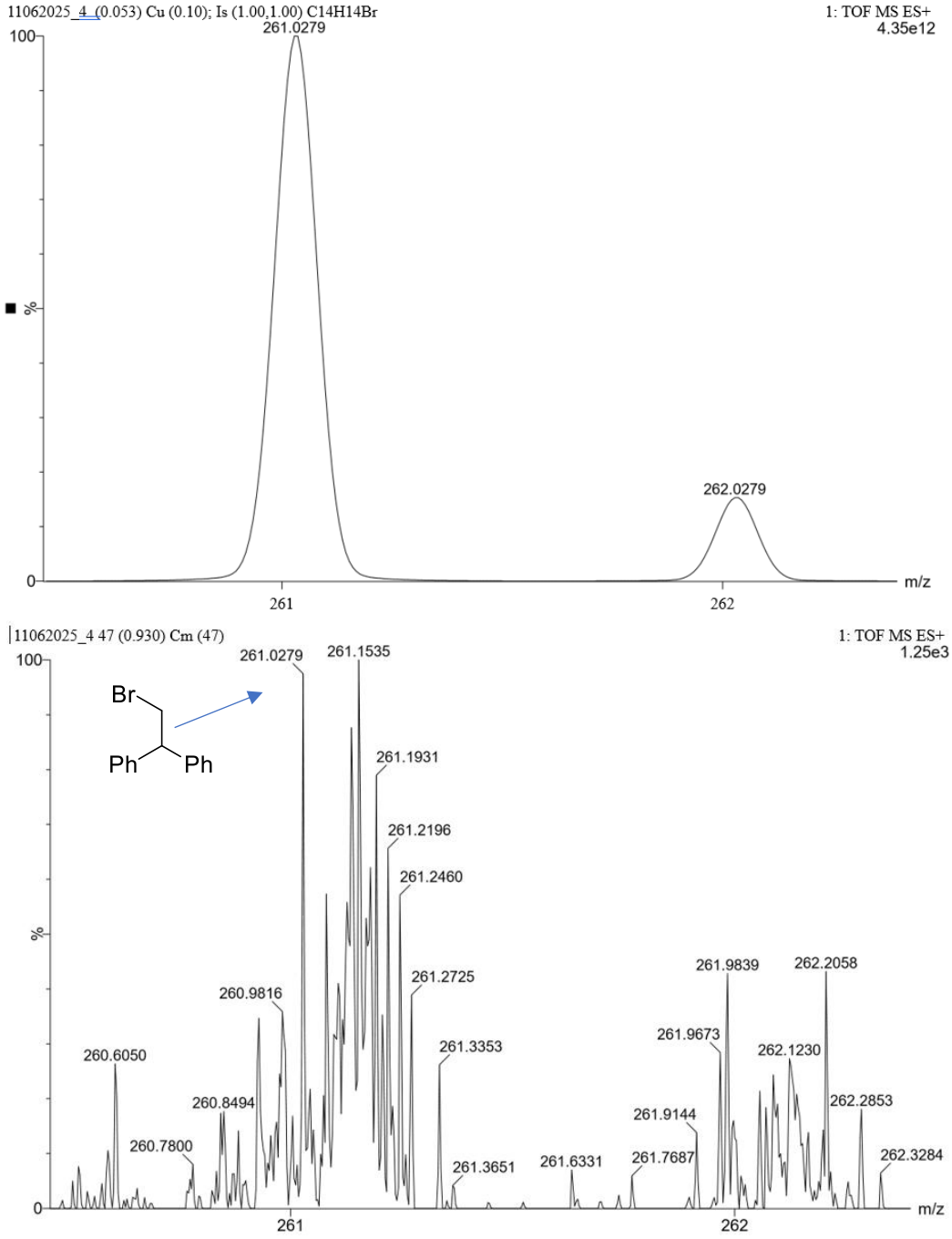

Figure S7. HRMS spectra of 1,1-DPE trapped bromine radical.

The isotopic labelling experiment with $H_2{}^{18}O$. In a 10 mL quartz tube, 1-methylquinoxalin-2(1*H*)-one (**1a**, 60 mg), *N*-fluorobenzenesulfonimide (3.5 equiv, 1.312 mmol), NaBr (3.5 equiv, 1.312 mmol), ^{18}O isotope-labelled water ($H_2{}^{18}O$) (67 μL, 10 equiv), and PDI (3 mol %, 0.011 mmol) were dissolved in 2 mL DMF and exposed to 3W blue LEDs for 12 h. After the reaction was completed, the organic layer was extracted with ethyl acetate, collected over anhydrous Na_2SO_4, concentrated, and directly used for mass spectrometric analysis.

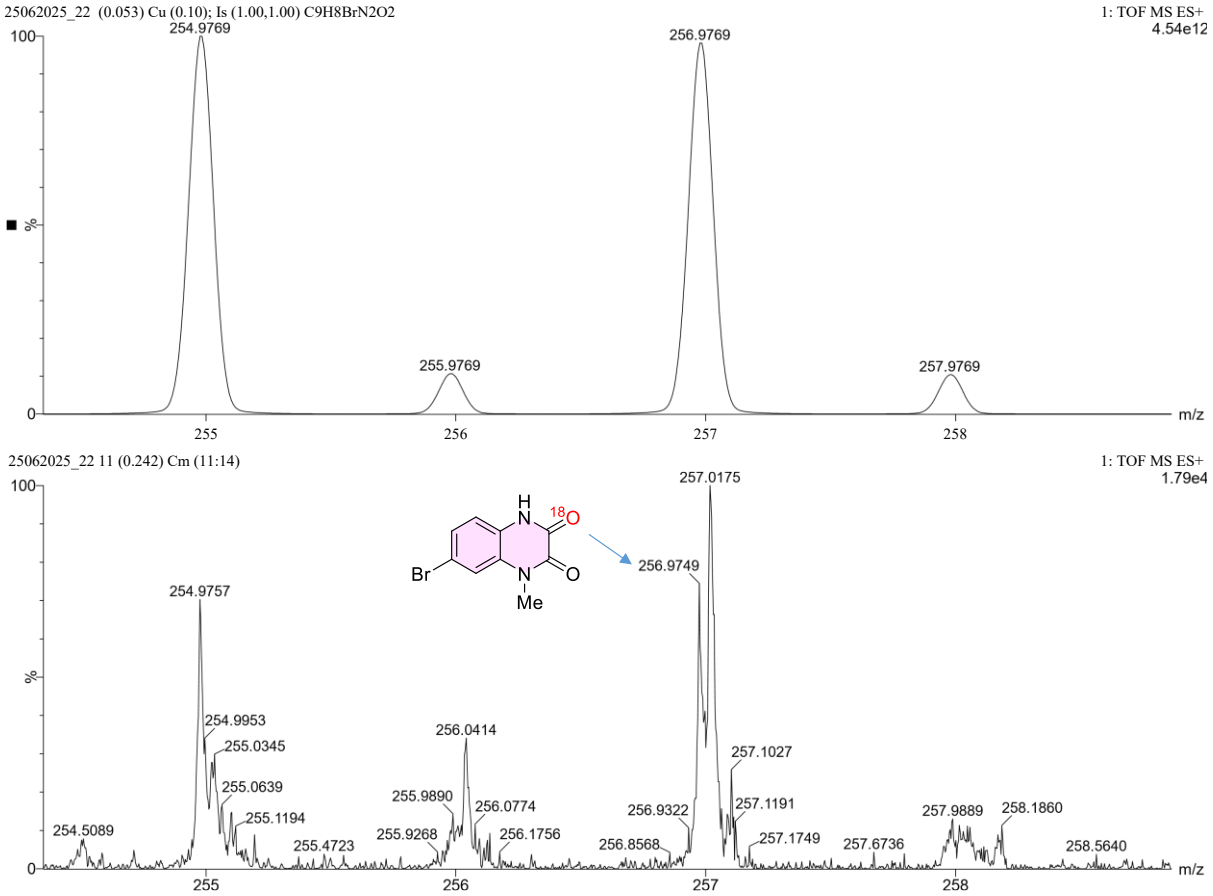

Figure S8. HRMS spectra of $H_2{}^{18}O$ reaction.

Fluorescence (PL) quenching experiment. The photoluminescence quenching study of the PDI-photocatalyst was conducted based on Stern-Volmer kinetics, using 1-methylquinoxalin-2(1*H*)-one as the emission quencher. The probe sample was prepared by dissolving 1 mg PDI in 2 mL DMF. Then, 10 μL of this concentrated solution was diluted with DMF to make a total

volume of 2 mL. Then, the quencher with a concentration of 1 mM (in DMF) was added to the probe solution with a 5 µL increment, and the emission spectra were recorded. Based on the emission quenching, a corresponding Stern-Volmer plot was plotted, which indicated a dynamic nature of quenching. We have also calculated the rate of quenching by the following formula……

$I_0/I = k_q . \tau . [C]$,

where I_0 = initial fluorescence intensity; I = fluorescence intensity after addition of the quencher; k_q = rate of quenching; τ = average excited state lifetime of the photocatalyst; C = concentration of the quencher.

By using the average excited state lifetime of 4 ns for the excited PDI molecule, we found k_q in the order of 10^{13} M^{-1} sec^{-1}.

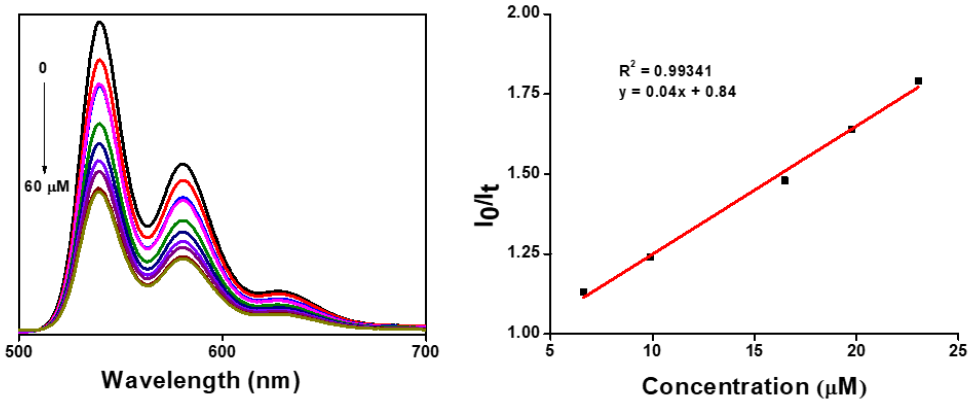

Figure S9. PL quenching experiment of PDI with the gradual addition of **1a** and the Stern-Volmer plot.

Spin-trapping experiment with DMPO.[6] In a 10 mL quartz tube, 1-methylquinoxalin-2(1*H*)-one (**1a**, 60 mg), *N*-fluorobenzenesulfonimide (3.5 equiv, 1.312 mmol), NaBr (3.5 equiv, 1.312 mmol), DMPO (0.4 equiv, 20 µL), and PDI (3 mol %, 0.011 mmol) were dissolved in 2 mL DMF and exposed to 3W Blue LEDs for 30 minutes. Afterward, 200 µL of the reaction mixture was withdrawn using a syringe and transferred into an oven-dried EPR tube, and the EPR

spectrum was recorded immediately. The '*g*' value (or *g*-factor) for DMPO-based oxygen-centred radical intermediate usually appears at a higher value (typically around 2.004-2.005) compared to a free-electron (*g* = 2.00232).[7] This increase in the *g*-factor is associated with the higher electronegativity of oxygen, which promotes localization of the unpaired electron on the oxygen atom and enhances spin-orbit coupling effects, leading to a positive shift in the observed *g*-value.

C-C cross-coupling of 7-bromo-1-(4-(tert-butyl)benzyl)-1,4-dihydroquinoxaline-2,3-dione (2i).[4] In a 15 mL presser tube, 60 mg of 7-bromo-1-(4-(*tert*-butyl)benzyl)-1,4-dihydroquinoxaline-2,3-dione (**2i**), 2 equiv of *para*-tolyl boronic acid, and 1.5 equiv of K_2CO_3 were taken. Then, a mixture of DMF, ethanol and water were added following a ratio of (1.5:1.5:1) and the reaction was heated at 110 ˚C for 24 h after degassing with argon. After 24 h, the reaction mixture was extracted with ethyl acetate-brine, the organic layer was collected over anhydrous Na_2SO_4 and concentrated using a rotary evaporator. Then the desired product was purified using column chromatography with ethyl acetate and hexane as eluent. However, the product and the starting material exhibited very similar polarity, rendering them indistinguishable by TLC analysis and difficult to separate using conventional column chromatography. Despite purification attempts, the isolated material consisted of a mixture of **2i** and the C-C cross coupled product (**8a**) in an approximate ratio of 1:0.15 (Figure S131-132). Also, after running the reaction for 72 h, the starting material was not fully consumed.

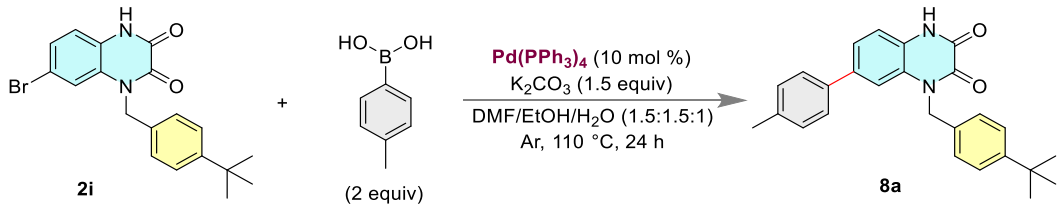

Scheme S10. C-C cross-coupling of 7-bromo-1-(4-(tert-butyl)benzyl)-1,4-dihydroquinoxaline-2,3-dione **(2i)**.

Crystallographic Information

Crystal measurement. The crystal data were collected with Rigaku (Model: XtaLAB Supernova) equipped with an APEX CCD detector and an INCOATEC micro source (Cu-Kα radiation, λ = 1.54184 Å). SAINT+[8] and SADABS[9] were used to integrate the intensities and to correct the absorption, respectively. The structure was resolved by direct methods and refined on F^2 with SHELXL-97.[10] ORTEP drawing of the compound **2f** shows an ellipsoid contour at the 50 % probability level.

Crystallization of 2f. In a 5 mL glass vial, 10 mg of 1-benzyl-7-bromo-1,4-dihydroquinoxaline-2,3-dione (**2f**) was dissolved by using a mixture of ethyl acetate (1 mL) and hexane (1 mL). After that, the solution was allowed to stand for slow evaporation to obtain fine-quality crystals.

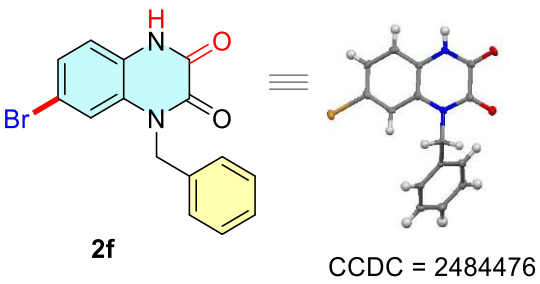

Figure S10. Crystal structure of **2f** (50% ellipsoid probability).

Table S8. Crystal data and structure refinement for **2f.**

CCDC No	2484476
Empirical formula	$C_{15}H_{10}BrN_2O_2$
Formula weight	330.16

Temperature/K	100.01(10)
Crystal system	Monoclinic
Space group	$P2_1/c$
a/Å	7.4693(6)
b/Å	10.4315(11)
c/Å	16.4870(17)
α/°	90
β/°	99.938(9)
γ/°	90
Volume/Å^3	1265.3(2)
Z	4
ρ_{calc}g/cm^3	1.733
μ/mm^{-1}	3.251
F(000)	660.0
Crystal size/mm^3	0.2 × 0.2 × 0.2
Radiation	Mo Kα (λ = 0.71073)
2Θ range for data collection/°	6.778 to 59.032
Index ranges	$-9 \leq h \leq 8$, $-13 \leq k \leq 12$, $-20 \leq l \leq 22$
Reflections collected	12707
Independent reflections	2894 [R_{int} = 0.0905, R_{sigma} = 0.0834]
Data/restraints/parameters	2894/0/181

Goodness-of-fit on F^2	1.061
Final R indexes [I>=2σ (I)]	R_1 = 0.0474, wR_2 = 0.1046
Final R indexes [all data]	R_1 = 0.0735, wR_2 = 0.1136
Largest diff. peak/hole / e $Å^{-3}$	1.32/-0.54

Calculation of the Gibbs free-energy change (ΔG) for the mechanistic process

Calculation of $E_{0,0}$

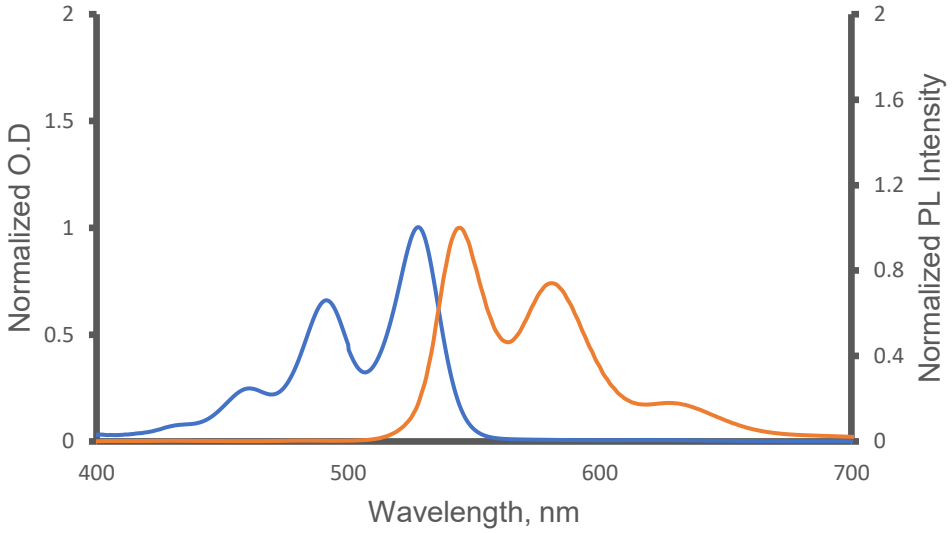

Intersecting point ($E_{0,0}$) = 535 nm = 53.2 kcal/mol

Free energy change of electron transfer from substrate (1a) to excited PDI

$$\Delta G = 23.06(E_{red} - E_{ox}) - E_{0,0}$$

$$\Delta G = 23.06\,[-0.37 - (-1.9)] - 53.2\ kcal/mol$$

$$\Delta G = 35.28 - 53.2\ kcal/mol$$

$$\Delta G = -17.91\ kcal/mol$$

E_{red} = Reduction potential of PDI/PDI(RA) vs SCE

E_{ox} = Reduction potential of substrate vs SCE

Free energy change of electron transfer from PDI radical anion to NFSI

$$\Delta G = 23.06\,(E_{red} - E_{ox})$$

$$\Delta G = 23.06\big(-0.6 - (-0.37)\big)\ kcal/mol$$

$$\Delta G = 23.06 \times -0.23\ kcal/mol$$

$$\Delta G = -5.3\ kcal/mol$$

E_{red} = reduction potential of NFSI vs SCE

E_{ox} = reduction potential of PDI/PDI(RA) vs SCE

From this calculation, the negative value of the Gibbs free energy change (ΔG) clearly states that both the electron transfer processes, from the substrate to the excited PDI photocatalyst and from PDI radical anion to the NFSI, are thermodynamically favourable processes.

CHARACTERIZATION DATA

1-Methylquinoxalin-2(1*H*)-one (1a).[11] R_f = 0.2 (10% ethyl acetate in hexane); white solid;

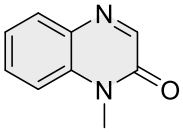

yield 80%; ^{1}H NMR (400 MHz, $CDCl_3$) δ 8.32 (s, 1H), 7.89 (dd, *J* = 7.9, 1.4 Hz, 1H), 7.61 (s, 1H), 7.37 (td, *J* = 8.6, 2.3 Hz, 2H), 3.71 (s, 3H); $^{13}C\{^1H\}$ NMR (100 MHz, $CDCl_3$) δ 155.2, 150.4, 133.5, 133.4, 131.2, 130.7, 123.9, 113.9, 28.9.

1-Ethylquinoxalin-2(1*H*)-one (1b).[11] R_f = 0.2 (5% ethyl acetate in hexane); white solid; yield

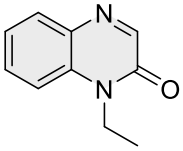

78%; ^{1}H NMR (400 MHz, $CDCl_3$) δ 8.31 (s, 1H), 7.90 (dd, *J* = 7.9, 1.4 Hz, 1H), 7.60 (m, *J* = 8.6, 7.3, 1.5 Hz, 1H), 7.39 – 7.34 (m, 2H), 4.32 (q, *J* = 7.2 Hz, 2H), 1.39 (t, *J* = 7.2 Hz, 3H); $^{13}C\{^1H\}$ NMR (100 MHz, $CDCl_3$) δ 154.8, 150.5, 133.9, 132.3, 131.2, 130.9, 123.7, 113.8, 37.1, 12.6.

1-Hexylquinoxalin-2(1*H*)-one (1c).[12] R_f = 0.2 (5% ethyl acetate in hexane); yellow liquid;

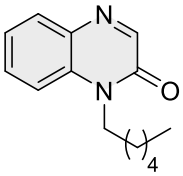

yield 71%; ^{1}H NMR (700 MHz, $CDCl_3$) δ 8.33 – 8.21 (m, 1H), 7.88 – 7.84 (m, 1H), 7.57 (td, *J* = 7.3, 1.8 Hz, 1H), 7.33 (dd, *J* = 4.0, 3.1 Hz, 2H), 4.21 (d, *J* = 7.7 Hz, 2H), 1.73 (dd, *J* = 5.3, 2.3 Hz, 2H), 1.44 (s, 2H), 1.32 (d, *J* = 2.5 Hz, 3H), 1.23 (s, 1H), 0.88 (dd, *J* = 5.9, 3.8 Hz, 3H); ^{13}C{^{1}H} NMR (175 MHz, $CDCl_3$) δ 154.9, 150.4, 133.7, 132.5, 131.0, 130.8, 123.6, 113.9, 42.1, 31.5, 27.3, 26.7, 22.6, 14.1.

1-Decylquinoxalin-2(1*H*)-one (1d). R_f = 0.2 (5% ethyl acetate in hexane); yellow liquid; yield

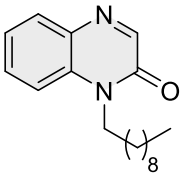

74%; ^{1}H NMR (700 MHz, $CDCl_3$) δ 8.28 – 8.25 (m, 1H), 7.88 – 7.84 (m, 1H), 7.56 (d, *J* = 4.8 Hz, 1H), 7.32 (dd, *J* = 7.1, 3.7 Hz, 2H), 4.22 – 4.19 (m, 2H), 1.75 – 1.71 (m, 2H), 1.43 (d, *J* = 3.9 Hz, 2H), 1.34 (d, *J* = 4.0 Hz, 2H), 1.24 (s, 10H), 0.86 (dd, *J* = 6.7, 3.7 Hz, 3H); ^{13}C{^{1}H} NMR (175 MHz, $CDCl_3$) δ 154.9, 150.4, 133.7, 132.5, 131.0, 130.8, 123.6, 113.9, 42.1, 31.9, 29.6, 29.39, 29.36, 27.4, 27.1, 22.7, 14.2, 14.1.

Ethyl 2-(2-oxoquinoxalin-1(2*H*)-yl)acetate (1e).[11] R_f = 0.3 (10% ethyl acetate in hexane);

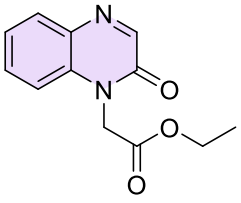

yellow solid; yield 66%; ^{1}H NMR (400 MHz, $CDCl_3$) δ 8.34 (s, 1H), 7.91 (dd, *J* = 8.0, 1.2 Hz, 1H), 7.59 – 7.54 (m, 1H), 7.39 – 7.35 (m, 1H), 7.10 (d, *J* = 8.4 Hz, 1H), 5.02 (s, 2H), 4.24 (q, *J* = 7.1 Hz, 2H), 1.27 (s, 3H); ^{13}C{^{1}H} NMR (100 MHz, $CDCl_3$) δ 167.0, 154.7, 150.1, 133.5, 132.5, 131.4, 131.0, 124.2, 113.4, 62.3, 43.3, 14.2.

1-Benzylquinoxalin-2(1*H*)-one (1f).[11] R_f = 0.2 (10% ethyl acetate in hexane); white solid;

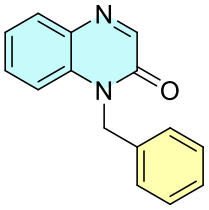

yield 70%; ^{1}H NMR (400 MHz, $CDCl_3$) δ 8.33 (s, 1H), 7.82 (dd, *J* = 8.0, 1.5 Hz, 1H), 7.39 (m, *J* = 8.6, 7.5, 1.5 Hz, 1H), 7.25 – 7.15 (m, 7H), 5.42 (s, 2H); ^{13}C{^{1}H} NMR (100 MHz, $CDCl_3$) δ 155.3, 150.4, 135.1, 133.8, 132.7, 131.1, 130.8, 129.1, 127.9, 127.0, 123.9, 114.8, 45.7.

1-(4-Methylbenzyl)quinoxalin-2(1*H*)-one (1g).[11] R_f = 0.3 (10% ethyl acetate in hexane);

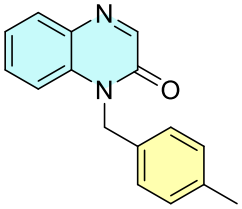

brown solid; yield 73%; ^{1}H NMR (400 MHz, $CDCl_3$) δ 8.40 (s, 1H), 7.88 (d, *J* = 7.4 Hz, 1H), 7.47 (t, *J* = 7.7 Hz, 1H), 7.31 (t, *J* = 7.5 Hz, 2H), 7.13 (d, *J* = 3.7 Hz, 4H), 5.45 (s, 2H), 2.30 (s, 3H); ^{13}C{^{1}H} NMR (100 MHz, $CDCl_3$) δ 155.3, 150.4, 137.7, 133.8, 132.7, 132.0, 131.2, 130.7, 129.8, 127.0, 123.9, 114.8, 45.5, 21.2.

1-(4-Isopropylbenzyl)quinoxalin-2(1*H*)-one (1h).[13] R_f = 0.2 (10% ethyl acetate in hexane);

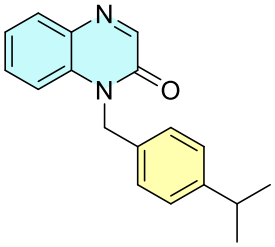

brown solid; yield 75%; ^{1}H NMR (400 MHz, $CDCl_3$) δ 8.42 (s, 1H), 7.94 – 7.88 (m, 1H), 7.51 – 7.46 (m, 1H), 7.31 (dd, *J* = 12.4, 4.7 Hz, 2H), 7.17 (s, 4H), 5.46 (s, 2H), 2.86 (m, 1H), 1.20 (d, *J* = 6.9 Hz, 6H); ^{13}C{^{1}H} NMR (100 MHz, $CDCl_3$) δ 155.3, 150.5, 148.7, 133.7, 132.8, 132.4, 131.2, 130.7, 127.2, 127.0, 123.9, 114.9, 45.5, 33.9, 24.0.

1-(4-(Tert-butyl)benzyl)quinoxalin-2(1*H*)-one (1i).[13] R_f = 0.3 (15% ethyl acetate in hexane);

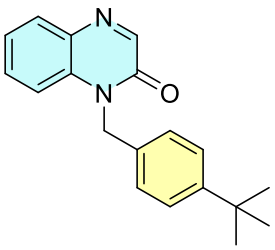

brown solid; yield 70%; ^{1}H NMR (400 MHz, $CDCl_3$) δ 8.40 (s, 1H), 7.91 – 7.87 (m, 1H), 7.51 – 7.46 (m, 1H), 7.33 (d, *J* = 8.4 Hz, 4H), 7.18 (d, *J* = 8.3 Hz, 2H), 5.46 (s, 2H), 1.27 (s, 9H); ^{13}C{^{1}H} NMR (100 MHz,

$CDCl_3$) δ 155.3, 150.9, 150.5, 133.8, 132.8, 132.0,131.2, 130.7, 126.8, 126.0, 123.9, 114.9, 45.4, 34.6, 31.4.

1-(4-Fluorobenzyl)quinoxalin-2(1*H*)-one (1j).[13] R_f = 0.2 (10% ethyl acetate in hexane); off-

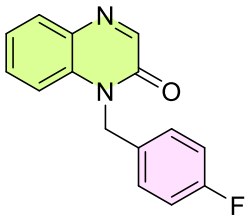

white solid; yield 69%; ^{1}H NMR (400 MHz, $CDCl_3$) δ 8.38 (s, 1H), 7.88 (dd, *J* = 8.0, 1.4 Hz, 1H), 7.49 – 7.45 (m, 1H), 7.34 – 7.29 (m, 1H), 7.26 – 7.20 (m, 3H), 7.01 – 6.96 (m, 2H), 5.43 (s, 2H); ^{13}C{^{1}H} NMR (100 MHz, $CDCl_3$) δ 162.38 (d, $^1J_{C\text{-}F}$ = 246.9 Hz), 155.2, 150.4, 133.8, 132.5, 131.0 (d, $^2J_{C\text{-}F}$ = 35.1 Hz), 128.8 (d, $^3J_{C\text{-}F}$ = 8.7 Hz), 124.1, 116.2, 115.9, 114.5, 45.0.

1-(4-Bromobenzyl)quinoxalin-2(1*H*)-one (1k).[13] R_f = 0.2 (5% ethyl acetate in hexane);

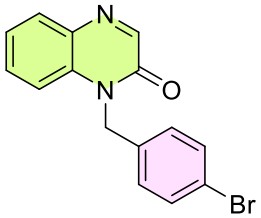

yellow solid; yield 74%; ^{1}H NMR (400 MHz, $CDCl_3$) δ 8.40 (s, 1H), 7.90 (dd, *J* = 8.0, 1.4 Hz, 1H), 7.49 – 7.43 (m, 3H), 7.36 – 7.32 (m, 1H), 7.22 (d, *J* = 8.4 Hz, 1H), 7.13 (d, *J* = 8.5 Hz, 2H), 5.43 (s, 2H); ^{13}C{^{1}H} NMR (100 MHz, $CDCl_3$) δ 155.2, 150.4, 134.2, 133.8, 132.5, 132.3, 131.3, 130.9, 128.8, 124.1, 121.9, 114.5, 45.1.

1-(4-(Trifluoromethyl)benzyl)quinoxalin-2(1*H*)-one (1l).[13] R_f = 0.2 (15% ethyl acetate in

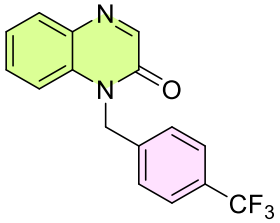

hexane); brown solid; yield 75%; ^{1}H NMR (400 MHz, $CDCl_3$) δ 8.41 (s, 1H), 7.92 (dd, *J* = 8.0, 1.3 Hz, 1H), 7.58 (d, *J* = 8.2 Hz, 2H), 7.51 – 7.46 (m, 1H), 7.34 (dd, *J* = 11.4, 4.5 Hz, 3H), 7.19 (d, *J* = 8.3 Hz, 1H), 5.54 (s, 2H); ^{13}C{^{1}H} NMR (100 MHz, $CDCl_3$) δ 155.1, 150.3, 139.1, 133.8, 132.4, 131.4, 131.0, 130.5, 130.2, 127.3, 126.1 (q, $J_{C\text{-}F}$ = 3.8 Hz), 125.3, 124.2, 122.6, 114.4, 45.3.

1-(3-Chlorobenzyl)quinoxalin-2(1*H*)-one (1m).[14] R_f = 0.2 (10% ethyl acetate in hexane);

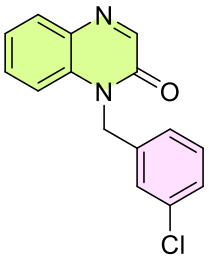

white solid; yield 79%; ^{1}H NMR (700 MHz, $CDCl_3$) δ 8.46 (s, 1H), 7.96 (d, *J* = 7.9 Hz, 1H), 7.54 (t, *J* = 7.7 Hz, 1H), 7.39 (t, *J* = 7.6 Hz, 1H), 7.29 (dd, *J* = 16.2, 4.4 Hz, 4H), 7.17 (s, 1H), 5.50 (s, 2H); ^{13}C{^{1}H} NMR (175 MHz, $CDCl_3$) δ 155.2, 150.3, 137.1, 135.1, 133.8, 132.5, 131.4, 130.9, 130.4, 128.3, 127.1, 125.1, 124.2, 114.5, 45.2.

4-((2-Oxoquinoxalin-1(2*H*)-yl)methyl)benzonitrile (1n).[12] R_f = 0.3 (10% ethyl acetate in hexane); white solid; yield 71%; ^{1}H NMR (700 MHz, $CDCl_3$) δ 8.53 (s, 1H), 8.01 (d, *J* = 8.2 Hz, 1H), 7.82 (d, *J* = 8.3 Hz, 1H), 7.66 (d, *J* = 7.3 Hz, 3H), 7.60 (d, *J* = 7.8 Hz, 2H), 7.57 (t, *J* = 7.6 Hz, 1H), 5.57 (s, 2H); ^{13}C{^{1}H} NMR (175 MHz, $CDCl_3$) δ 160.4, 156.5, 141.7, 140.0, 139.2, 132.4, 130.4, 129.1, 128.4, 127.2, 127.0, 118.7, 111.9, 66.9.

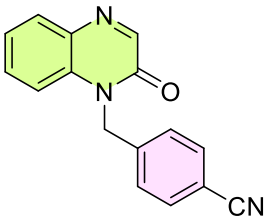

1-Phenylquinoxalin-2(1*H*)-one (1o).[15] R_f = 0.5 (25% ethyl acetate in hexane); yellow solid; yield 64%; ^{1}H NMR (400 MHz, $CDCl_3$) δ 8.29 (s, 1H), 7.83 (d, *J* = 7.8 Hz, 1H), 7.54 (t, *J* = 6.6 Hz, 2H), 7.49 (d, *J* = 6.1 Hz, 1H), 7.30 (dd, *J* = 10.7, 4.8 Hz, 1H), 7.23 (d, *J* = 7.9 Hz, 3H), 6.66 (d, *J* = 8.3 Hz, 1H); ^{13}C{^{1}H} NMR (100 MHz, $CDCl_3$) δ 154.9, 151.1, 135.4, 134.1, 133.3, 130.9, 130.5, 130.2, 129.8, 128.3, 124.1, 115.8.

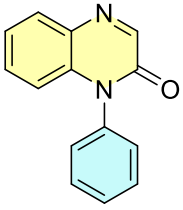

1-(2-Iodobenzyl)quinoxalin-2(1*H*)-one (1p).[16] R_f = 0.3 (5% ethyl acetate in hexane); white solid; yield 71%; ^{1}H NMR (400 MHz, $CDCl_3$) δ 8.57 (s, 1H), 8.04 (dd, *J* = 8.2, 1.2 Hz, 1H), 7.91 (m, *J* = 8.2, 5.1, 0.9 Hz, 2H), 7.73 – 7.67 (m, 1H), 7.62 – 7.55 (m, 2H), 7.39 (td, *J* = 7.6, 1.0 Hz, 1H), 7.06 (td, *J* = 7.7, 1.6 Hz,

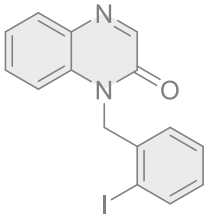

1H), 5.56 (s, 2H). ^{13}C {^{1}H} NMR (100 MHz, $CDCl_3$) δ 156.9, 140.4, 139.7, 139.6, 139.3, 138.9, 130.4, 130.1, 129.9, 129.1, 128.5, 127.5, 126.9, 98.8, 72.1.

1-Allylquinoxalin-2(1*H*)-one (1q).[17] R_f = 0.3 (10% ethyl acetate in hexane); brown solid; yield

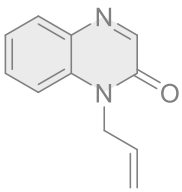

79%; ^{1}H NMR (700 MHz, $CDCl_3$) δ 8.21 (s, 1H), 7.78 (d, *J* = 8.0 Hz, 1H), 7.47 (dd, *J* = 8.3, 7.4 Hz, 1H), 7.25 – 7.22 (m, 2H), 5.87 – 5.82 (m, 1H), 5.18 (d, *J* = 10.5 Hz, 1H), 5.07 (d, *J* = 17.3 Hz, 1H), 4.81 – 4.79 (m, 2H); ^{13}C {^{1}H} NMR (175 MHz, $CDCl_3$) δ 154.4, 150.0, 133.3, 132.3, 130.9, 130.4, 130.3, 123.6, 118.0, 114.3, 44.0.

1-(Prop-2-yn-1-yl)quinoxalin-2(1*H*)-one (1r).[4] R_f = 0.4 (20% ethyl acetate in hexane); brown

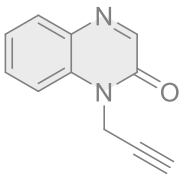

solid; yield 76%; ^{1}H NMR (400 MHz, $CDCl_3$) δ 8.31 (s, 1H), 7.90 (d, *J* = 8.0 Hz, 1H), 7.63 (t, *J* = 7.3 Hz, 1H), 7.50 (d, *J* = 8.4 Hz, 1H), 7.39 (dd, *J* = 11.2, 4.1 Hz, 1H), 5.04 (d, *J* = 2.5 Hz, 2H), 2.30 (t, *J* = 2.5 Hz, 1H). ^{13}C {^{1}H} NMR (100 MHz, $CDCl_3$) δ 154.1, 150.1, 133.7, 131.8, 131.3, 130.8, 124.3, 114.5, 76.6, 73.5, 31.3.

Quinoxalin-2(1*H*)-one (1s).[4] R_f = 0.1 (20% ethyl acetate in hexane); brown solid; yield 75%;

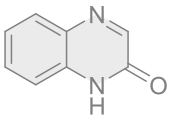

^{1}H NMR (700 MHz, DMSO-d_6) δ 12.41 (s, 1H), 8.15 (s, 1H), 7.75 (dd, *J* = 8.0, 1.0 Hz, 1H), 7.52 (dd, *J* = 11.2, 4.2 Hz, 1H), 7.30 – 7.27 (m, 2H).

1,6-Dimethylquinoxalin-2(1*H*)-one (1t). R_f = 0.5 (25% ethyl acetate in hexane); brown solid;

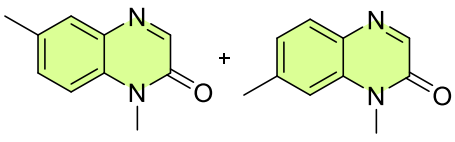

yield 70%; ^{1}H NMR (400 MHz, $CDCl_3$) δ 8.29 (s, 1H), 8.24 (s, 1H), 7.75 (d, *J* = 8.1 Hz, 1H), 7.67 (s, 1H), 7.41 (dd, *J* = 8.5, 1.6 Hz, 1H), 7.23 (d, *J* = 8.5 Hz, 1H), 7.18 (d, *J* = 8.1 Hz, 1H), 7.13 (s, 1H), 3.68

(s, 6H), 2.53 (s, 3H), 2.46 (s, 3H); $^{13}C\{^{1}H\}$ NMR (100 MHz, $CDCl_3$) δ 155.2, 155.0, 150.3, 149.1, 142.1, 133.8, 133.5, 133.3, 132.4, 131.8, 130.4, 130.3, 128.6, 125.2, 114.1, 113.7, 29.8, 28.9, 22.3, 20.7; HRMS (ESI-TOF) m/z: $[M + H]^+$ calcd for $C_{10}H_{11}N_2O$ 175.0871; found 175.0880.

6-Methyl-1-octylquinoxalin-2(1*H*)-one (1u). R_f = 0.3 (10% ethyl acetate in hexane); brown

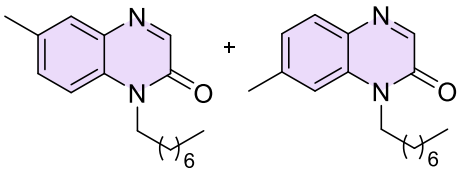

liquid; yield 74%; ^{1}H NMR (400 MHz, $CDCl_3$) δ 8.26 (s, 1H), 8.21 (s, 1H), 7.74 (d, *J* = 8.1 Hz, 1H), 7.66 (s, 1H), 7.39 (d, *J* = 8.6 Hz, 1H), 7.22 (d, *J* = 8.6 Hz, 1H), 7.15 (d, *J* = 8.2 Hz, 1H), 7.10 (s, 1H), 4.22 – 4.17 (m, 4H), 2.51 (s, 3H), 2.44 (s, 3H), 1.77 – 1.70 (m, 4H), 1.44 (dd, *J* = 14.6, 7.4 Hz, 4H), 1.27 (s, 15H), 0.87 (dd, *J* = 6.3, 5.8 Hz, 7H); $^{13}C\{^{1}H\}$ NMR (100 MHz, $CDCl_3$) δ 155.1, 154.9, 150.4, 149.2, 141.9, 133.7, 133.5, 132.5, 132.3, 132.0, 130.6, 130.5, 130.3, 125.0, 113.9, 113.7, 42.1, 42.0, 31.9, 29.4, 29.3, 29.2, 27.4, 27.3, 27.08, 27.06, 22.7, 22.3, 20.7, 14.2.

1-Benzyl-6-methylquinoxalin-2(1*H*)-one (1v).[13] R_f = 0.2 (10% ethyl acetate in hexane); white

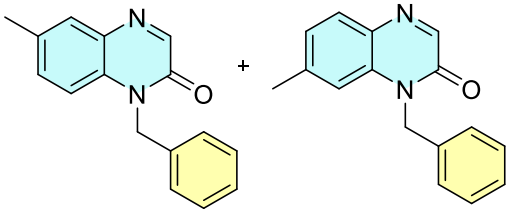

solid; yield 75%; ^{1}H NMR (400 MHz, $CDCl_3$) δ 8.32 (s, 1H), 8.27 (s, 0.62H), 7.71 – 7.61 (m, 2H), 7.24 (dd, *J* = 7.6, 6.2 Hz, 5H), 7.20 – 7.14 (m, 7H), 7.09 (d, *J* = 8.6 Hz, 2H), 5.41 (s, 4H), 2.34 (d, *J* = 3.7 Hz, 6H); $^{13}C\{^{1}H\}$ NMR (100 MHz, $CDCl_3$) δ 150.4, 149.2, 135.2, 133.9, 132.4, 130.5, 130.4, 129.1, 127.9, 127.0, 114.8, 114.5, 45.7, 31.1.

1-Benzyl-6-bromoquinoxalin-2(1*H*)-one (1w).[13] R_f = 0.2 (10% ethyl acetate in hexane); 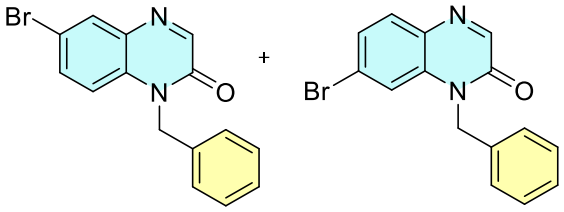
brown solid; yield 72%; ^{1}H NMR (400 MHz, $CDCl_3$) δ 8.40 (s, 1H), 8.38 (s, 0.64H), 8.04 (d, J = 2.3 Hz, 1H), 7.74 (d, J = 8.4 Hz, 0.77H), 7.54 (dd, J = 9.0, 2.3 Hz, 1H), 7.44 (dd, J = 3.8, 1.8 Hz, 1H), 7.41 (d, J = 1.9 Hz, 0.39H), 7.37 – 7.26 (m, 7H), 7.22 (dd, J = 8.0, 6.5 Hz, 3H), 7.14 (d, J = 9.0 Hz, 1H), 5.46 (s, 2H), 5.43 (s, 1.47H); ^{13}C {^{1}H} NMR (100 MHz, $CDCl_3$) δ 154.8, 151.5, 150.5, 134.6, 134.5, 134.5, 133.9, 133.7, 133.0, 132.5, 131.9, 131.7, 129.2, 129.2, 128.13, 128.06, 127.2, 127.0, 126.9, 125.4, 117.7, 116.5, 116.2, 45.7.

1-(4-Bromobenzyl)-6-methylquinoxalin-2(1*H*)-one (1x). R_f = 0.2 (10% ethyl acetate in 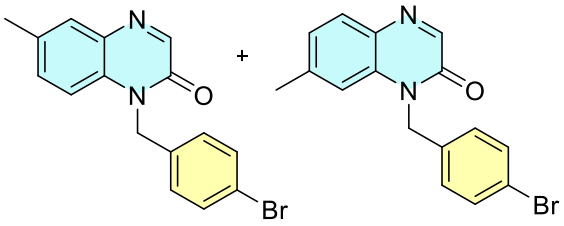
hexane); brown solid; yield 79%; ^{1}H NMR (400 MHz, $CDCl_3$) δ 8.37 (s, 0.75H), 8.32 (s, 1H), 7.77 (d, J = 8.2 Hz, 1H), 7.69 (s, 0.87H), 7.44 (dd, J = 8.3, 6.0 Hz, 4H), 7.29 (dd, J = 8.5, 1.7 Hz, 1H), 7.16 – 7.09 (m, 6H), 6.99 (s, 1H), 5.41 (s, 4H), 2.42 (s, 6H); ^{13}C{^{1}H} NMR (100 MHz, $CDCl_3$) δ 155.3, 155.1, 150.3, 149.1, 142.2, 134.3, 134.3, 134.1, 133.8, 132.5, 132.4, 132.3, 132.2, 132.0, 130.7, 130.6, 130.5, 130.2, 128.8, 128.7, 125.5, 121.8, 114.5, 114.2, 45.1, 45.0, 22.3, 20.7; HRMS (ESI-TOF) m/z: $[M + H]^+$ calcd for $C_{16}H_{14}BrN_2O$ 329.0290; found 329.0286.

7-Bromo-1-methyl-1,4-dihydroquinoxaline-2,3-dione (2a).[12] R_f = 0.3 (40% ethyl acetate in 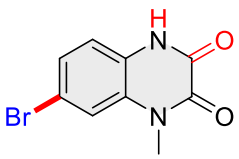
hexane); pink solid; yield 76% (72 mg); ^{1}H NMR (400 MHz, DMSO-d_6) δ 12.09 (s, 1H), 7.51 (d, J = 1.9 Hz, 1H), 7.33 (dd, J = 8.5, 2.0 Hz, 1H), 7.08 (d, J = 8.5 Hz, 1H), 3.48 (s, 3H); ^{13}C{^{1}H} NMR (100 MHz, DMSO-d_6) δ 155.1, 153.3, 128.8, 126.0, 125.0, 117.5, 117.0, 114.8, 29.8.

7-Bromo-1-ethyl-1,4-dihydroquinoxaline-2,3-dione (2b). R_f = 0.3 (40% ethyl acetate in hexane); pink solid; yield 72% (66 mg); mp 180-183 ˚C; ^{1}H NMR (400 MHz, DMSO-d_6) δ 12.09 (s, 1H), 7.56 (d, J = 1.8 Hz, 1H), 7.33 (dd, J = 8.5, 1.9 Hz, 1H), 7.11 (d, J = 8.5 Hz, 1H), 4.15 – 4.09 (m, 2H), 1.18 (s, 3H); ^{13}C{^{1}H} NMR (100 MHz, DMSO-d_6) δ 154.7, 153.3, 127.5, 126.0, 125.3, 117.4, 117.1, 115.1, 37.5, 11.93; IR (ATR) ῡ 3071, 2922, 1708, 1664, 824 cm^{-1}; HRMS (ESI-TOF) m/z: [M + H]$^+$ calcd for $C_{10}H_{10}BrN_2O_2$ 268.9926; found 268.9906.

7-Bromo-1-hexyl-1,4-dihydroquinoxaline-2,3-dione (2c). R_f = 0.2 (30% ethyl acetate in hexane); pink solid; yield 81% (68 mg); mp > 200 ˚C; ^{1}H NMR (400 MHz, DMSO-d_6) δ 12.09 (s, 1H), 7.53 (d, J = 1.9 Hz, 1H), 7.33 (dd, J = 8.5, 1.9 Hz, 1H), 7.10 (d, J = 8.5 Hz, 1H), 4.10 – 4.03 (m, 2H), 1.56 (dd, J = 14.9, 7.7 Hz, 2H), 1.37 – 1.26 (m, 6H), 0.86 (t, J = 7.0 Hz, 3H); ^{13}C{^{1}H} NMR (100 MHz, DMSO-d_6) δ 154.9, 153.3, 127.7, 126.0, 125.3, 117.4, 117.2, 115.0, 42.1, 30.9, 26.3, 25.8, 22.0, 13.9; IR (ATR) ῡ 3076, 2922, 1715, 1666, 831 cm^{-1}; HRMS (ESI-TOF) m/z: [M + H]$^+$ calcd for $C_{14}H_{18}BrN_2O_2$ 325.0552; found 325.0545.

7-Bromo-1-decyl-1,4-dihydroquinoxaline-2,3-dione (2d). R_f = 0.3 (25% ethyl acetate in hexane); pink solid; yield 60% (47 mg); mp 143-146 ˚C; ^{1}H NMR (400 MHz, DMSO-d_6) δ 12.10 (s, 1H), 7.53 (d, J = 1.8 Hz, 1H), 7.33 (dd, J = 8.5, 1.9 Hz, 1H), 7.10 (d, J = 8.5 Hz, 1H), 4.09 – 4.04 (m, 2H), 1.60 – 1.53 (m, 2H), 1.23 (d, J = 4.9 Hz, 14H), 0.85 (t, J = 6.8 Hz, 3H); ^{13}C{^{1}H} NMR (100 MHz, DMSO-d_6) δ 154.9, 153.3, 127.7, 126.1, 125.3, 117.4, 117.2, 115.0, 42.2, 31.2, 28.9, 28.9, 28.7, 28.7, 26.3, 26.1, 22.1, 14.0; IR (ATR) ῡ 3133, 2919, 2851, 1696, 1390 cm^{-1}; HRMS (ESI-TOF) m/z: [M + Na]$^+$ calcd for $C_{18}H_{25}BrN_2O_2Na$ 403.0997; found 403.0987.

Ethyl 2-(7-bromo-2,3-dioxo-3,4-dihydroquinoxalin-1(2*H*)-yl)acetate (2e). R_f = 0.2 (30% ethyl acetate in hexane); orange liquid; yield 53% (44 mg); ^{1}H NMR (400 MHz, DMSO-d_6) δ 12.29 (s, 1H), 7.61 (d, J = 1.9 Hz, 1H), 7.38 (dd, J = 8.5, 1.8 Hz, 1H), 7.14 (d, J = 8.5 Hz, 1H), 4.97 (s, 2H), 4.17 (q, J = 7.1 Hz, 2H), 0.85 (t, J = 6.8 Hz, 3H); ^{13}C{^{1}H} NMR (100 MHz, DMSO-d_6) δ 167.5, 155.1, 152.9, 127.9, 126.6, 124.9, 117.5, 117.5, 115.2, 61.3, 29.0, 14.0; IR (KBr) ῡ 3145, 2916, 1714, 1675, 832 cm^{-1}; HRMS (ESI-TOF) m/z: [M + Na]$^+$ calcd for $C_{12}H_{11}BrN_2O_4Na$ 348.9800; found 348.9806.

1-Benzyl-7-bromo-1,4-dihydroquinoxaline-2,3-dione (2f).[4] R_f = 0.3 (40% ethyl acetate in hexane); pink solid; yield 67% (56 mg); ^{1}H NMR (400 MHz, DMSO-d_6) δ 12.19 (s, 1H), 7.32 (t, J = 7.4 Hz, 7H), 7.12 (d, J = 8.7 Hz, 1H), 5.37 (s, 2H); ^{13}C {^{1}H} NMR (175 MHz, DMSO-d_6) δ 155.6, 153.5, 135.4, 128.7, 127.8, 127.4, 126.6, 126.2, 125.5, 117.8, 117.4, 114.7, 45.6.

7-Bromo-1-(4-methylbenzyl)-1,4-dihydroquinoxaline-2,3-dione (2g). R_f = 0.2 (40% ethyl acetate in hexane); yellow solid; yield 71% (58 mg); mp > 200 ˚C; ^{1}H NMR (400 MHz, DMSO-d_6) δ 12.18 (s, 1H), 7.30 (d, J = 7.5 Hz, 2H), 7.19 (d, J = 8.1 Hz, 2H), 7.15 – 7.10 (m, 3H), 5.32 (s, 2H), 2.26 (s, 3H); ^{13}C{^{1}H} NMR (100 MHz, DMSO-d_6) δ 155.5, 153.4, 136.5, 132.3, 129.3, 127.8, 126.6, 126.2, 125.4, 117.9, 117.3, 114.6, 45.3, 20.6; IR (ATR) ῡ 3069, 2919, 1709, 1667, 832 cm^{-1}; HRMS (ESI-TOF) m/z: [M + Na]$^+$ calcd for $C_{16}H_{13}BrN_2O_2Na$ 367.0058; found 367.0020.

7-Bromo-1-(4-isopropylbenzyl)-1,4-dihydroquinoxaline-2,3-dione (2h). R_f = 0.2 (40% ethyl acetate in hexane); pink solid; yield 61% (49 mg); mp > 200 °C; ^{1}H NMR (400 MHz, DMSO-d_6) δ 12.18 (s, 1H), 7.37 (d, J = 1.9 Hz, 1H), 7.31 (dd, J = 8.5, 1.9 Hz, 1H), 7.24 – 7.18 (m, 4H), 7.12 (d, J = 8.5 Hz, 1H), 5.33 (s, 2H), 2.89-2.79 (m, 1H), 1.16 (d, J = 6.9 Hz, 6H); ^{13}C{^{1}H} NMR (100 MHz, DMSO-d_6) δ 155.5, 153.4, 147.5, 132.8, 127.9, 126.7, 126.6, 126.2, 125.4, 117.8, 117.4, 114.7, 45.5, 33.1, 23.8; IR (ATR) ῡ 3221, 2956, 1704, 1678, 829 cm^{-1}; HRMS (ESI-TOF) m/z: [M + Na]$^+$ calcd for $C_{18}H_{17}BrN_2O_2Na$ 395.0371; found 395.0356.

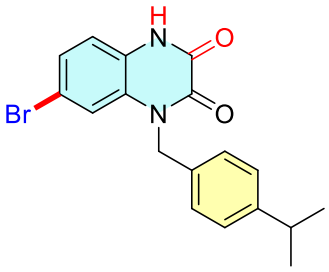

7-Bromo-1-(4-(tert-butyl)benzyl)-1,4-dihydroquinoxaline-2,3-dione (2i). R_f = 0.2 (40% ethyl acetate in hexane); pink solid; yield 70% (55 mg); mp > 200 °C; ^{1}H NMR (400 MHz, DMSO-d_6) δ 12.19 (s, 1H), 7.39 (d, J = 1.9 Hz, 1H), 7.35 (d, J = 8.4 Hz, 2H), 7.31 (dd, J = 8.5, 1.9 Hz, 1H), 7.22 (d, J = 8.4 Hz, 2H), 7.12 (d, J = 8.5 Hz, 1H), 5.33 (s, 2H), 1.24 (s, 9H); ^{13}C{^{1}H} NMR (100 MHz, DMSO-d_6) δ 155.5, 153.4, 149.7, 132.4, 127.9, 126.5, 126.2, 125.4, 125.4, 117.8, 117.4, 114.7, 45.2, 34.21, 31.0; IR (ATR) ῡ 3076, 2957, 1698, 1375 cm^{-1}; HRMS (ESI-TOF) m/z: [M + Na]$^+$ calcd for $C_{19}H_{19}BrN_2O_2Na$ 409.0528; found 409.0551.

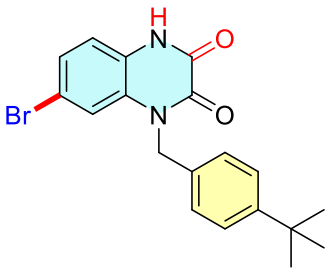

7-Bromo-1-(4-fluorobenzyl)-1,4-dihydroquinoxaline-2,3-dione (2j). R_f = 0.2 (40% ethyl acetate in hexane); pink solid; yield 73% (60 mg); mp > 200 °C; ^{1}H NMR (400 MHz, DMSO-d_6) δ 12.17 (s, 1H), 7.38 (dd, J = 8.6, 5.5 Hz, 2H), 7.33 – 7.29 (m, 2H), 7.15 (dd, J = 15.3, 6.5 Hz, 3H), 5.35

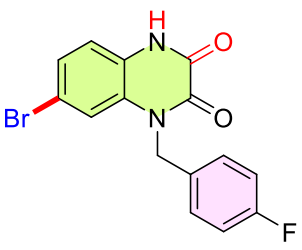

(s, 2H); $^{13}C\{^{1}H\}$ NMR (100 MHz, DMSO-d_6) δ 161.4 (d, $^{1}J_{C\text{-}F}$ = 242.3 Hz), 155.6, 153.4, 131.5 (d, $^{4}J_{C\text{-}F}$ = 3.2 Hz), 128.8 (d, $^{3}J_{C\text{-}F}$ = 8.2 Hz), 127.8, 126.2, 125.5, 117.5 (d, $^{2}J_{C\text{-}F}$ = 32.0 Hz), 115.6, 115.3, 114.6, 44.9; IR (ATR) ῡ 3242, 2921, 1695, 1659 cm^{-1}; HRMS (ESI-TOF) m/z: $[M + Na]^+$ calcd for $C_{15}H_{10}{}^{81}BrFN_2O_2Na$ 372.9807; found 372.9815.

7-Bromo-1-(4-bromobenzyl)-1,4-dihydroquinoxaline-2,3-dione (2k). R_f = 0.2 (30% ethyl acetate in hexane); orange solid; yield 76% (59 mg); mp > 200 ˚C; ^{1}H NMR (400 MHz, DMSO-d_6) δ 12.17 (s, 1H), 7.52 (d, J = 8.5 Hz, 2H), 7.33 – 7.27 (m, 4H), 7.12 (d, J = 8.3 Hz, 1H), 5.34 (s, 2H); $^{13}C\{^{1}H\}$ NMR (100 MHz, DMSO-d_6) δ 155.6, 153.4, 135.0, 131.5, 129.0, 127.8, 126.3, 125.5, 120.4, 117.6, 117.4, 114.6, 45.0; IR (ATR) ῡ 2918, 2851, 1682, 796 cm^{-1}; HRMS (ESI-TOF) m/z: $[M + H]^+$ calcd for $C_{15}H_{11}Br_2N_2O_2$ 410.9187; found 410.9184.

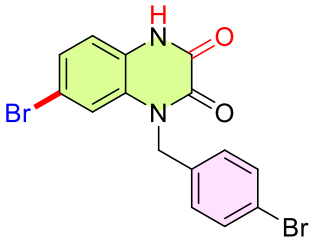

7-Bromo-1-(4-(trifluoromethyl)benzyl)-1,4-dihydroquinoxaline-2,3-dione (2l). R_f = 0.2 (30 % ethyl acetate in hexane); white solid; yield 69% (54 mg); mp > 200 ˚C; ^{1}H NMR (400 MHz, DMSO-d_6) δ 12.19 (s, 1H), 7.70 (d, J = 8.2 Hz, 2H), 7.55 (d, J = 8.1 Hz, 2H), 7.32 (dd, J = 4.4, 2.5 Hz, 2H), 7.13 (d, J = 9.0 Hz, 1H), 5.47 (s, 2H); $^{13}C\{^{1}H\}$ NMR (100 MHz, DMSO-d_6) δ 155.6, 153.4, 140.4, 127.8, 127.5, 126.3, 125.6, 125.4 (q, $J_{C\text{-}F}$ = 3.6 Hz), 117.5, 117.4, 114.7, 45.3; IR (ATR) ῡ 3145, 2918, 1713, 1666, 1110 cm^{-1}; HRMS (ESI-TOF) m/z: $[M + Na]^+$ calcd for $C_{16}H_{10}BrF_3N_2O_2Na$ 420.9775; found 420.9770.

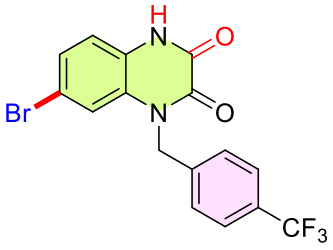

7-Bromo-1-(3-chlorobenzyl)-1,4-dihydroquinoxaline-2,3-dione (2m). R_f = 0.2 (30% ethyl acetate in hexane); colorless liquid; yield 80% (64 mg); ^{1}H NMR (400 MHz, DMSO-d_6) δ 12.14 (s, 1H), 7.45 (s, 1H), 7.37 – 7.32 (m, 2H), 7.32 – 7.27 (m, 3H), 7.12 (d, J = 8.3 Hz, 1H), 5.36 (s, 2H); ^{13}C{^{1}H} NMR (100 MHz, DMSO-d_6) δ 155.7, 153.5, 138.1, 133.4, 130.5, 127.9, 127.4, 126.6, 126.2, 125.6, 125.4, 117.6, 117.4, 114.6, 45.2; IR (KBr) ῡ 3152, 3081, 1709, 1655 cm^{-1}; HRMS (ESI-TOF) m/z: [M + Na]$^+$ calcd for $C_{15}H_{10}N_2O_2{}^{81}BrClNa$ 388.9512; found 388.9491.

4-((7-Bromo-2,3-dioxo-3,4-dihydroquinoxalin-1(2*H*)-yl)methyl)benzonitrile (2n). R_f = 0.2 (30% ethyl acetate in hexane); white solid; yield 56% (45 mg); mp > 200 °C; ^{1}H NMR (400 MHz, DMSO-d_6) δ 12.17 (s, 1H), 7.81 (d, J = 8.3 Hz, 2H), 7.53 (d, J = 8.3 Hz, 2H), 7.32 (dd, J = 8.5, 1.8 Hz, 1H), 7.27 (d, J = 1.8 Hz, 1H), 7.13 (d, J = 8.5 Hz, 1H), 5.45 (s, 2H); ^{13}C{^{1}H} NMR (100 MHz, DMSO-d_6) δ 155.7, 153.5, 141.4, 132.5, 127.8, 127.6, 126.4, 125.6, 118.7, 117.5, 117.4, 114.7, 110.1, 45.5; IR (ATR) ῡ 3068, 2920, 1700, 1596, 1399 cm^{-1}; HRMS (ESI-TOF) m/z: [M + Na]$^+$ calcd for $C_{16}H_{10}BrN_3O_2Na$ 377.9854; found 377.9872.

7-Bromo-1-phenyl-1,4-dihydroquinoxaline-2,3-dione (2o). R_f = 0.2 (40% ethyl acetate in hexane); colorless liquid; yield 59% (50 mg); ^{1}H NMR (400 MHz, DMSO-d_6) δ 12.20 (s, 1H), 7.65 (t, J = 7.4 Hz, 2H), 7.59 (d, J = 7.3 Hz, 1H), 7.42 – 7.39 (m, 2H), 7.32 (dd, J = 8.5, 2.0 Hz, 1H), 7.17 (d, J = 8.5 Hz, 1H), 6.32 (d, J = 2.0 Hz, 1H); ^{13}C{^{1}H} NMR (100 MHz, DMSO-d_6) δ 155.0, 154.0, 136.1, 130.3, 130.27, 129.4, 128.5, 126.0, 125.3, 117.5, 117.4, 114.1; IR (KBr) ῡ 2918, 2851, 1682,

1378 cm^{-1}; HRMS (ESI-TOF) m/z: $[M + H]^+$ calcd for $C_{14}H_{10}BrN_2O_2$ 316.9926; found 316.9943.

1-Benzyl-7-chloro-1,4-dihydroquinoxaline-2,3-dione (2a'). R_f = 0.3 (40% ethyl acetate in hexane); pink liquid; yield 66% (48 mg); ^1H NMR (400 MHz, DMSO-d_6) δ 12.19 (s, 1H), 7.32 (q, J = 6.6 Hz, 4H), 7.29 – 7.24 (m, 1H), 7.22 – 7.17 (m, 3H), 5.38 (s, 2H); $^{13}C\{^1H\}$ NMR (100 MHz, DMSO-d_6) δ 155.6, 153.4, 135.4, 128.7, 127.6, 127.3, 126.9, 126.6, 125.1, 123.4, 117.0, 115.1, 45.6; IR (KBr) ῡ 3078, 2954, 2920, 1700, 1660 cm^{-1}; HRMS (ESI-TOF) m/z: $[M + H]^+$ calcd for $C_{15}H_{12}ClN_2O_2$ 287.0587; found 287.0618.

7-Chloro-1-(4-isopropylbenzyl)-1,4-dihydroquinoxaline-2,3-dione (2b'). R_f = 0.3 (40% ethyl acetate in hexane); pink solid; yield 69% (49 mg); mp > 200 °C; ^1H NMR (400 MHz, DMSO-d_6) δ 12.19 (s, 1H), 7.26 (s, 1H), 7.22 (t, J = 6.7 Hz, 4H), 7.18 (s, 2H), 5.33 (s, 2H), 2.87-2.80 (m, 1H), 1.16 (d, J = 6.9 Hz, 6H); $^{13}C\{^1H\}$ NMR (100 MHz, DMSO-d_6) δ 155.5, 153.4, 147.5, 132.8, 127.6, 126.9, 126.7, 126.6, 125.0, 123.4, 117.1, 115.1, 45.3, 33.1, 23.8; IR (ATR) ῡ 3155, 2957, 1703, 1374 cm^{-1}; HRMS (ESI-TOF) m/z: $[M + Na]^+$ calcd for $C_{18}H_{17}ClN_2O_2Na$ 351.0876; found 351.0857.

1-(4-(Tert-butyl)benzyl)-7-chloro-1,4-dihydroquinoxaline-2,3-dione (2c'). R_f = 0.3 (40% ethyl acetate in hexane); pink solid; yield 67% (47 mg); mp > 200 °C; ^{1}H NMR (400 MHz, DMSO-d_6) δ 12.19 (s, 1H), 7.34 (d, J = 8.4 Hz, 2H), 7.28 (s, 1H), 7.23 (d, J = 8.3 Hz, 2H), 7.19 (s, 2H), 5.33 (s, 2H), 1.24 (s, 9H); ^{13}C{^{1}H} NMR (100 MHz, DMSO-d_6) δ 155.5, 153.4, 149.7, 132.4, 127.6, 126.9, 126.5, 125.4, 125.0, 123.4, 117.1, 115.1, 45.7, 34.2, 31.1; IR (ATR) ῡ 3082, 2957, 1700, 1373 cm^{-1}; HRMS (ESI-TOF) m/z: [M + Na]$^+$ calcd for $C_{19}H_{19}ClN_2O_2Na$ 365.1033; found 365.1014.

7-Chloro-1-(4-fluorobenzyl)-1,4-dihydroquinoxaline-2,3-dione (2d'). R_f = 0.3 (40% ethyl acetate in hexane); pink solid; yield 72% (51 mg); mp > 200 °C; ^{1}H NMR (400 MHz, DMSO-d_6) δ 12.16 (s, 1H), 7.38 (dd, J = 8.6, 5.5 Hz, 2H), 7.22 (d, J = 4.5 Hz, 1H), 7.17 (dd, J = 15.0, 5.9 Hz, 4H), 5.35 (s, 2H); ^{13}C{^{1}H} NMR (100 MHz, DMSO-d_6) δ 161.4 (d, $^1J_{C\text{-}F}$ = 242.7 Hz), 155.6, 153.4, 131.5 (d, $^4J_{C\text{-}F}$ = 2.9 Hz), 128.8 (d, $^3J_{C\text{-}F}$ = 7.9 Hz), 127.5, 126.9, 125.1, 123.4, 117.0, 115.6 (d, $^2J_{C\text{-}F}$ = 21.36 Hz) 115.0, 44.9; ^{19}F NMR (376 MHz, DMSO-d_6) δ -115.2; IR (ATR) ῡ 3025, 2883, 1677, 1600, 1498 cm^{-1}; HRMS (ESI-TOF) m/z: [M + Na]$^+$ calcd for $C_{15}H_{10}ClFN_2O_2Na$ 327.0313; found 327.0310.

7-Bromo-1,6-dimethyl-1,4-dihydroquinoxaline-2,3-dione (2t). R_f = 0.2 (30% ethyl acetate in hexane); pink solid; yield 63% (58 mg); mp > 200 °C; ^{1}H NMR (700 MHz, DMSO-d_6) δ 12.03 (s, 1H), 11.97 (s, 1H), 7.51 (s, 1H), 7.35 (s, 1H), 7.30 (s, 1H), 7.06 (s, 1H), 3.47 (d, J = 3.2 Hz, 6H), 2.36 (s, 3H), 2.31 (s, 3H); ^{13}C{^{1}H} NMR (100 MHz, DMSO-d_6) δ 155.1, 154.9, 153.5,

153.3, 132.0, 131.6, 126.9, 126.7, 125.1, 124.9, 118.1, 117.9, 117.4, 117.4, 117.1, 116.8, 29.8, 29.0, 22.0, 21.8; IR (ATR) $\bar{\upsilon}$ 3038, 2917, 1663, 1367, 1309 cm^{-1}; HRMS (ESI-TOF) m/z: $[M + H]^+$ calcd for $C_{10}H_{10}{}^{81}BrN_2O_2$ 270.9926; found 270.9956.

7-Bromo-6-methyl-1-octyl-1,4-dihydroquinoxaline-2,3-dione (2u). R_f = 0.2 (30% ethyl

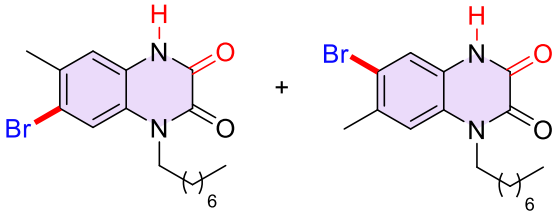

acetate in hexane); pink solid; yield 65% (52 mg); mp 168-171 ˚C; ^1H NMR (400 MHz, DMSO-d_6) δ 12.05 (s, 1H), 7.52 (s, 1H), 7.08 (s, 1H), 4.09 – 4.01 (m, 2H), 2.31 (s, 3H), 1.62 – 1.52 (m, 2H), 1.36 – 1.28 (m, 4H), 1.26 – 1.22 (m, 6H), 0.85 (t, J = 6.8 Hz, 3H); $^{13}C\{^1H\}$ NMR (100 MHz, DMSO-d_6) δ 154.7, 153.5, 132.1, 125.6, 125.3, 117.8, 117.6, 117.2, 42.1, 31.2, 28.65, 28.57, 26.3, 26.1, 22.1, 21.8, 14.0; IR (ATR) $\bar{\upsilon}$ 3133, 2919, 1696, 1391 cm^{-1}; HRMS (ESI-TOF) m/z: $[M + H]^+$ calcd for $C_{17}H_{24}BrN_2O_2$ 367.1021; found 367.1023.

1-Benzyl-7-bromo-6-methyl-1,4-dihydroquinoxaline-2,3-dione (2v). R_f = 0.2 (30% ethyl

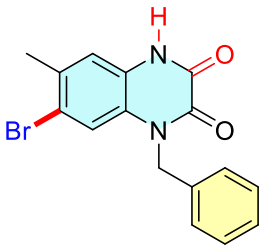

acetate in hexane); colorless liquid; yield 66% (54 mg); ^1H NMR (400 MHz, DMSO-d_6) δ 12.09 (s, 1H), 7.35 (s, 1H), 7.33 – 7.29 (m, 4H), 7.28 – 7.23 (m, 1H), 7.21 (s, 1H), 5.34 (s, 2H), 2.24 (s, 3H); $^{13}C\{^1H\}$ NMR (100 MHz, DMSO-d_6) δ 155.5, 153.4, 135.6, 131.5, 128.6, 127.3, 126.7, 126.0, 125.3, 118.3, 117.7, 117.3, 45.6, 22.1; IR (KBr) $\bar{\upsilon}$ 3139, 2918, 1674, 1380, 727 cm^{-1}; HRMS (ESI-TOF) m/z: $[M + Na]^+$ calcd for $C_{16}H_{13}BrN_2O_2Na$ 368.0058; found 368.0087.

1-Benzyl-6,7-dibromo-1,4-dihydroquinoxaline-2,3-dione (2w). R_f = 0.2 (40% ethyl acetate

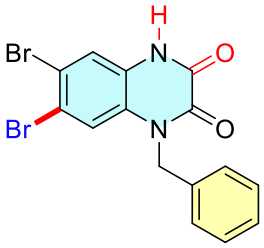

in hexane); pink solid; yield 71% (55 mg); mp > 200 ˚C; ^{1}H NMR (700 MHz, DMSO-d_6) δ 12.19 (s, 1H), 7.45 (d, J = 13.2 Hz, 2H), 7.32 (dd, J = 13.8, 7.4 Hz, 4H), 7.27 (t, J = 7.0 Hz, 1H), 5.36 (s, 2H); ^{13}C{^{1}H} NMR (175 MHz, DMSO-d_6) δ 155.4, 153.4, 135.2, 128.7, 127.4, 127.3, 126.9, 126.6, 119.7, 119.4, 117.3, 116.6, 45.7; IR (ATR) ῡ 3230, 2918, 1708, 1658, 791 cm^{-1}; HRMS (ESI-TOF) m/z: [M + H]$^+$ calcd for $C_{15}H_{11}Br_2N_2O_2$ 408.9187; found 408.9191.

7-Bromo-1-(4-bromobenzyl)-6-methyl-1,4-dihydroquinoxaline-2,3-dione (2x). R_f = 0.3

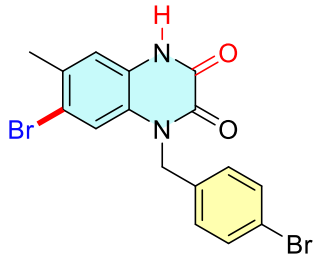

(40% ethyl acetate in hexane); white solid; yield 70% (54 mg); mp > 200 ˚C; ^{1}H NMR (400 MHz, DMSO-d_6) δ 12.13 (s, 1H), 7.52 (d, J = 8.4 Hz, 2H), 7.32 – 7.26 (m, 3H), 7.09 (s, 1H), 5.33 (s, 2H), 2.27 (s, 3H); ^{13}C{^{1}H} NMR (100 MHz, DMSO-d_6) δ 155.4, 153.6, 135.0, 132.3, 131.5, 129.0, 125.6, 125.6, 120.4, 118.3, 117.2, 117.2, 45.0, 21.8; IR (ATR) ῡ 3231, 2917, 1689, 1657, 1381 cm^{-1}; HRMS (ESI-TOF) m/z: [M + H]$^+$ calcd for $C_{16}H_{13}{}^{81}Br_2N_2O_2$ 424.9344; found 424.9355.

6,7-Dibromo-1-methyl-1,4-dihydroquinoxaline-2,3-dione (3a).[18] R_f = 0.4 (40% ethyl acetate

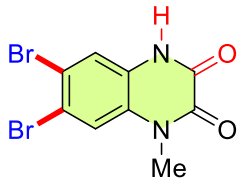

in hexane); white solid; yield 56% (70 mg); ^{1}H NMR (700 MHz, DMSO-d_6) δ 11.13 (s, 1H), 7.68 (s, 1H), 7.56 (s, 1H), 3.49 (s, 3H); ^{13}C{^{1}H} NMR (175 MHz, DMSO-d_6) δ 154.7, 153.6, 129.9, 128.7, 121.2, 118.6, 117.3, 114.9, 30.31.

6,7-Dibromo-1-decyl-1,4-dihydroquinoxaline-2,3-dione (3b). R_f = 0.4 (25% ethyl acetate in

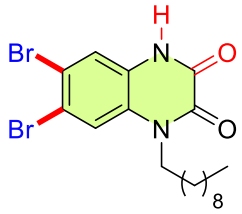

hexane); pink solid; yield 60% (57 mg); mp 172-175 ˚C; ^{1}H NMR (400 MHz, DMSO-d_6) δ 12.11 (s, 1H), 7.68 (s, 1H), 7.42 (s, 1H), 4.08 – 4.02 (m, 2H), 1.55 (dd, J = 14.1, 7.0 Hz, 2H), 1.23 (s, 14H), 0.84 (t, J = 6.8 Hz, 3H); ^{13}C{^{1}H} NMR (100 MHz, DMSO-d_6) δ 154.7, 153.2, 127.2, 126.7, 119.4, 119.1, 117.0, 116.9, 42.3, 31.3, 28.92, 28.90, 28.70, 28.69, 26.2, 26.1, 22.1, 14.0; IR (ATR) ῡ 3120, 2919, 1696, 1389, 1299 cm^{-1}; HRMS (ESI-TOF) m/z: [M + H]$^+$ calcd for $C_{18}H_{25}Br_2N_2O_2$ 459.0283; found 459.0258.

1-Benzyl-6,7-dibromo-1,4-dihydroquinoxaline-2,3-dione (3c). R_f = 0.3 (40% ethyl acetate

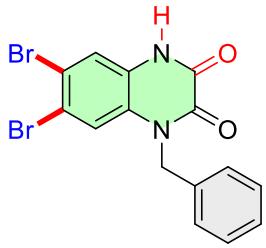

in hexane); pink solid; yield 66% (68 mg); mp > 200 ˚C; ^{1}H NMR (700 MHz, DMSO-d_6) δ 12.19 (s, 1H), 7.47 (s, 1H), 7.45 (s, 1H), 7.35 – 7.30 (m, 4H), 7.27 (t, J = 6.9 Hz, 1H), 5.36 (s, 2H); ^{13}C{^{1}H} NMR (175 MHz, DMSO-d_6) δ 155.4, 153.4, 135.2, 128.7, 127.4, 127.3, 126.9, 126.6, 119.7, 119.3, 117.2, 116.5, 45.6; IR (ATR) ῡ 3230, 2918, 1708, 1658 cm^{-1}; HRMS (ESI-TOF) m/z: [M + H]$^+$ calcd for $C_{15}H_{11}Br_2N_2O_2$ 408.9187; found 408.9191.

6,7-Dibromo-1-(4-fluorobenzyl)-1,4-dihydroquinoxaline-2,3-dione (3d). R_f = 0.3 (40%

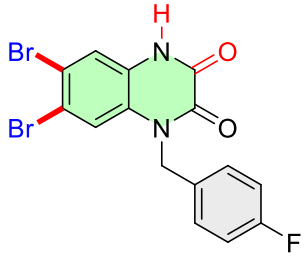

ethyl acetate in hexane); pink solid; yield 68% (68 mg); mp > 200 ˚C; ^{1}H NMR (400 MHz, DMSO-d_6) δ 12.17 (s, 1H), 7.47 (s, 1H), 7.44 (s, 1H), 7.38 (dd, J = 8.6, 5.5 Hz, 2H), 7.16 (t, J = 8.9 Hz, 2H), 5.34 (s, 2H); ^{13}C{^{1}H} NMR (100 MHz, DMSO-d_6) δ 161.4 (d, $^1J_{C\text{-}F}$ = 242.8 Hz), 155.4, 153.4, 131.3 (d, $^4J_{C\text{-}F}$ = 2.9 Hz), 128.8 (d, $^3J_{C\text{-}F}$ = 8.6 Hz), 127.2, 127.0, 119.4 (d, $^2J_{C\text{-}F}$ = 22.7 Hz), 117.3, 116.6, 115.6, 115.3, 45.0; IR (ATR) ῡ 3113, 3058, 1704, 1510,

1389 cm^{-1}; HRMS (ESI-TOF) m/z: $[M + H]^+$ calcd for $C_{15}H_{10}Br_2FN_2O_2$ 426.9093; found 426.9115.

1-Benzyl-6,7-dichloro-1,4-dihydroquinoxaline-2,3-dione (3a'). R_f = 0.5 (40% ethyl acetate

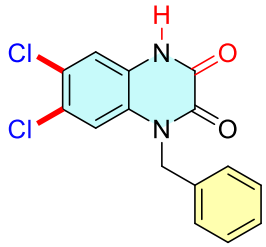

in hexane); pink solid; yield 71% (58 mg); ^1H NMR (400 MHz, DMSO-d_6) δ 12.20 (s, 1H), 7.38 (s, 1H), 7.33 (d, J = 5.9 Hz, 5H), 7.27 (dd, J = 6.2, 2.3 Hz, 1H), 5.37 (s, 2H); $^{13}C\{^1H\}$ NMR (100 MHz, DMSO-d_6) δ 155.3, 153.4, 135.2, 128.7, 127.4, 126.75, 126.66, 126.4, 125.2, 124.5, 116.8, 116.4, 45.7; IR (ATR) ῡ 3223, 2956, 2919, 1706, 1662 cm^{-1}; HRMS (ESI-TOF) m/z: $[M + Na]^+$ calcd for $C_{15}H_{10}Cl_2N_2O_2Na$ 343.0017; found 343.0023.

6,7-Dichloro-1-(4-fluorobenzyl)-1,4-dihydroquinoxaline-2,3-dione (3b'). R_f = 0.5 (40%

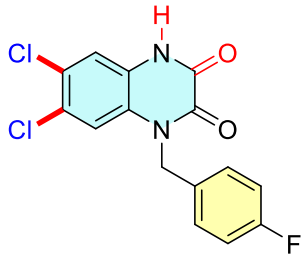

ethyl acetate in hexane); pink solid; yield 58% (46 mg); mp > 200 °C; ^1H NMR (400 MHz, DMSO-d_6) δ 11.61 (s, 1H), 7.44 (d, J = 2.0 Hz, 1H), 7.40 (dd, J = 8.2, 5.6 Hz, 2H), 7.20 – 7.12 (m, 3H), 5.36 (s, 2H); $^{13}C\{^1H\}$ NMR (100 MHz, DMSO-d_6) δ 161.4 (d, $^1J_{C\text{-}F}$ = 242.7 Hz), 155.3, 153.7, 131.2 (d, $^4J_{C\text{-}F}$ = 2.6 Hz), 128.8 (d, $^3J_{C\text{-}F}$ = 7.8 Hz), 128.7, 126.8, 123.3, 122.9, 115.4 (d, $^2J_{C\text{-}F}$ = 21.4 Hz), 114.3, 45.5; ^{19}F NMR (376 MHz, DMSO-d_6) δ -115.27; IR (ATR) ῡ 3069, 2918, 1690, 1587, 811 cm^{-1}; HRMS (ESI-TOF) m/z: $[M + H]^+$ calcd for $C_{15}H_{10}Cl_2FN_2O_2$ 339.0103; found 339.0117.

6,7-Dichloro-1-(4-isopropylbenzyl)-1,4-dihydroquinoxaline-2,3-dione (3c'). R_f = 0.4 (40%

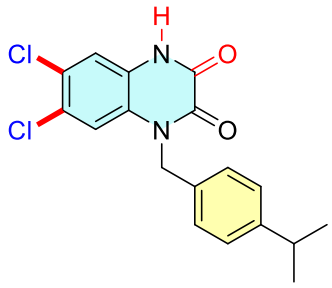

ethyl acetate in hexane); pink liquid; yield 62% (48 mg); ^{1}H NMR (400 MHz, DMSO-d_6) δ 12.21 (s, 1H), 7.44 (s, 1H), 7.32 (s, 1H), 7.21 (d, J = 7.4 Hz, 4H), 5.32 (s, 2H), 2.88 – 2.81 (m, 1H), 1.16 (d, J = 6.9 Hz, 6H); ^{13}C{^{1}H} NMR (100 MHz, DMSO-d_6) δ 155.3, 153.4, 147.5, 132.6, 126.79, 126.77, 126.6, 126.4, 125.2, 124.6, 116.8, 116.4, 45.5, 33.1, 23.8; IR (KBr) ῡ 3122, 2955, 2921, 1702, 1391 cm^{-1}; HRMS (ESI-TOF) m/z: [M + Na]$^+$ calcd for $C_{18}H_{16}Cl_2N_2O_2Na$ 385.0486; found 385.0497.

1-(4-(Tert-butyl)benzyl)-6,7-dichloro-1,4-dihydroquinoxaline-2,3-dione (3d'). R_f = 0.4

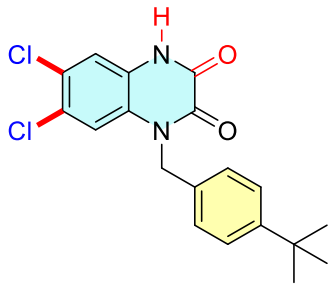

(40% ethyl acetate in hexane); pink solid; yield 70% (54 mg); mp > 200 ˚C; ^{1}H NMR (400 MHz, DMSO-d_6) δ 12.22 (s, 1H), 7.46 (s, 1H), 7.36 – 7.32 (m, 3H), 7.23 (d, J = 8.4 Hz, 2H), 5.32 (s, 2H), 1.24 (s, 9H); ^{13}C{^{1}H} NMR (100 MHz, DMSO-d_6) δ 155.2, 153.3, 149.8, 132.2, 126.8, 126.5, 126.3, 125.4, 125.2, 124.6, 116.8, 116.4, 45.4, 34.2, 31.1; IR (ATR) ῡ 3146, 2955, 1703, 1657, 1387 cm^{-1}; HRMS (ESI-TOF) m/z: [M + H]$^+$ calcd for $C_{19}H_{19}Cl_2N_2O_2$ 377.0824; found 377.0818.

(1R,2S,5R)-2-Isopropyl-5-methylcyclohexyl 4-((7-bromo-2,3-dioxo-3,4-

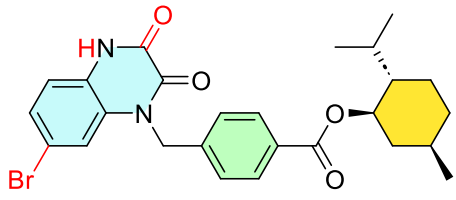

dihydroquinoxalin-1(2H)-yl)methyl)benzoate (2y). R_f = 0.1 (30% ethyl acetate in hexane); white solid; yield 72% (54 mg); mp > 200 ˚C; ^{1}H NMR (400 MHz, DMSO-d_6) δ 12.22 (s, 1H), 7.90 (d, J = 8.2 Hz, 2H), 7.46 (d, J = 8.1 Hz, 2H), 7.32 – 7.28 (m, 2H), 7.13 (d, J = 8.4 Hz, 1H), 5.45 (d, J = 3.9 Hz, 2H), 4.83 – 4.76 (m, 1H), 1.96 (d, J = 11.7 Hz, 1H),

1.87 – 1.81 (m, 1H), 1.64 (d, J = 11.7 Hz, 2H), 1.49 (t, J = 11.2 Hz, 2H), 1.05 (dd, J = 11.5, 6.0 Hz, 2H), 0.85 (dd, J = 10.4, 6.9 Hz, 7H), 0.71 (d, J = 6.9 Hz, 3H); $^{13}C\{^1H\}$ NMR (100 MHz, DMSO-d_6) δ 164.9, 155.6, 153.4, 141.0, 129.5, 129.1, 127.8, 127.0, 126.4, 125.5, 117.6, 117.5, 114.7, 74.1, 46.6, 45.5, 33.7, 30.9, 26.2, 23.3, 21.9, 20.4, 16.5; HRMS (ESI-TOF) m/z: $[M + H]^+$ calcd for $C_{26}H_{30}BrN_2O_4$ 513.1389; found 513.1373.

6-Bromo-1-phenyl-4-(4-(trifluoromethyl)benzyl)-1,4-dihydroquinoxaline-2,3-dione (6a).

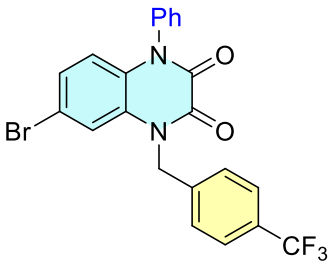

R_f = 0.4 (40% ethyl acetate in hexane); white solid; yield 75 % (54 mg); mp >200 ˚C; ^1H NMR (400 MHz, DMSO-d_6) δ 7.75 (d, J = 8.3 Hz, 2H), 7.69 – 7.64 (m, 4H), 7.59 (t, J = 7.4 Hz, 1H), 7.46 – 7.42 (m, 2H), 7.39 (d, J = 2.0 Hz, 1H), 7.22 (dd, J = 8.8, 2.0 Hz, 1H), 6.33 (d, J = 8.8 Hz, 1H), 5.57 (s, 2H); $^{13}C\{^1H\}$ NMR (175 MHz, DMSO-d_6) δ 155.0, 153.6, 140.4, 136.3, 130.3, 129.4, 128.7, 128.6, 128.1, 127.9, 127.6, 126.1, 125.5 (q, $J_{C\text{-}F}$ = 3.6 Hz), 125.0, 123.5, 117.8, 115.5, 45.7; ^{19}F NMR (376 MHz, DMSO- d_6) δ -60.84.

HRMS (ESI-TOF) m/z: $[M + H]^+$ calcd for $C_{22}H_{15}BrF_3N_2O_2$ 475.0269; found 475.0230.

1-Benzyl-1,4-dihydroquinoxaline-2,3-dione (7a).[4] R_f = 0.3 (50% ethyl acetate in hexane);

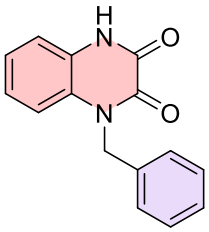

yellow solid; yield 69 % (25 mg); ^1H NMR (700 MHz, DMSO-d_6) δ 12.12 (s, 1H), 7.32-7.29 (m, 4H), 7.25 (t, J = 6.4 Hz, 1H), 7.20 (d, J = 7.9 Hz, 1H), 7.17 (d, J = 8.3 Hz, 1H), 7.13 (t, J = 7.6 Hz, 1H), 7.06 (t, J = 7.7 Hz, 1H), 5.38 (s, 2H); ^{13}C NMR (175 MHz, DMSO-d_6) δ 155.8, 153.7, 135.8, 128.7, 127.3, 126.7, 126.3, 125.9, 123.7, 123.2, 115.7, 115.5, 45.6.

NMR Spectra

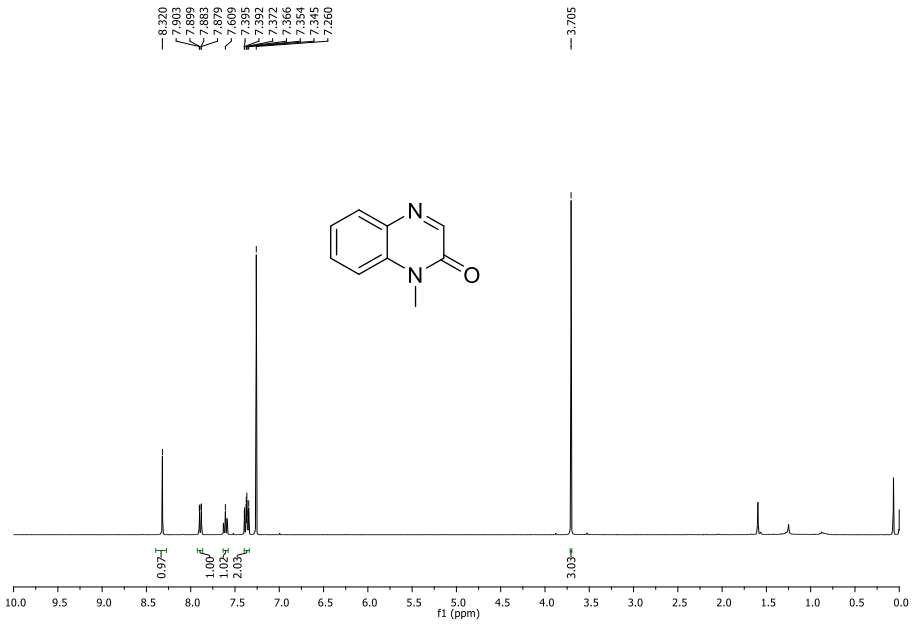

Figure S11. ^{1}H NMR (400 MHz, $CDCl_3$) of 1-methylquinoxalin-2(1*H*)-one **(1a)**

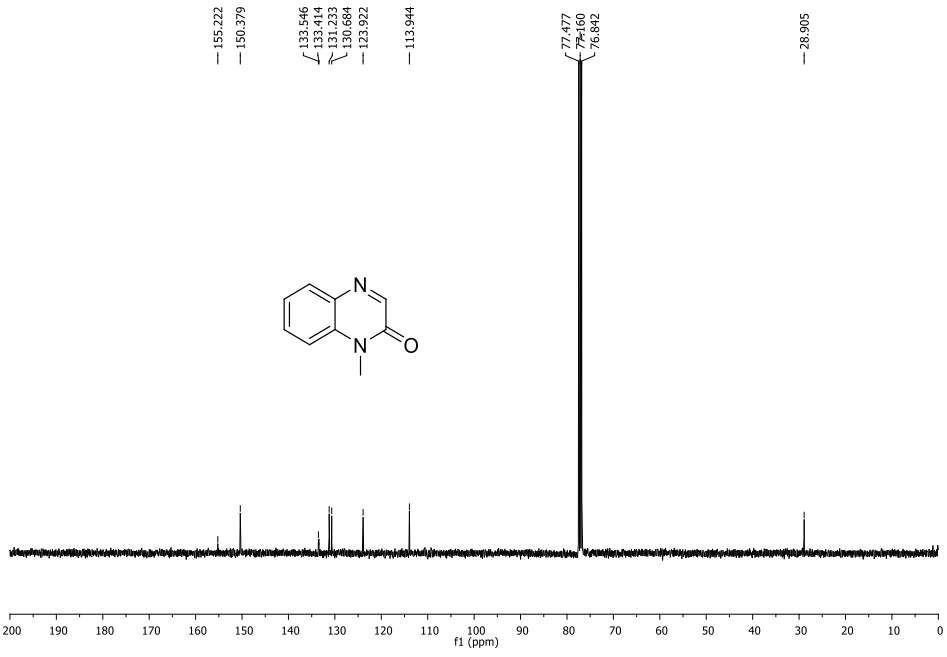

Figure S12. ^{13}C{^{1}H} NMR (100 MHz, $CDCl_3$) of 1-methylquinoxalin-2(1*H*)-one **(1a)**

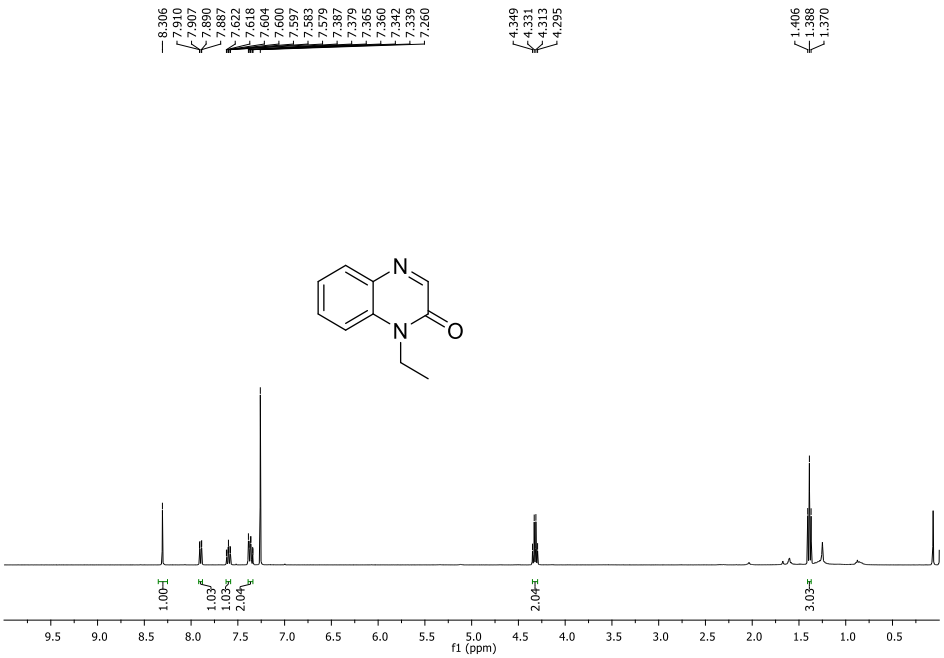

Figure S13. ^{1}H NMR (400 MHz, $CDCl_3$) of 1-ethylquinoxalin-2(1*H*)-one **(1b)**

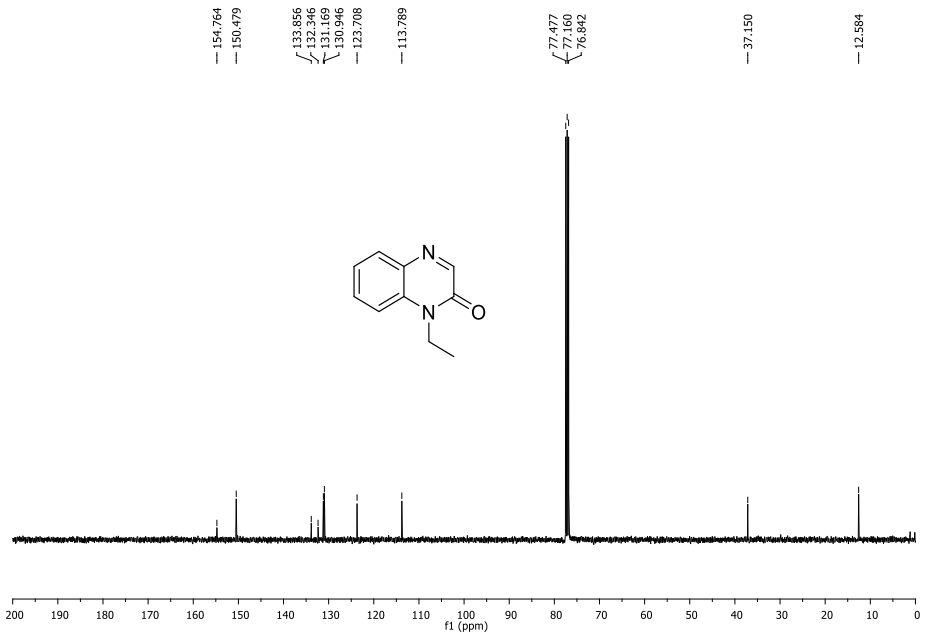

Figure S14. ^{13}C{^{1}H} NMR (100 MHz, $CDCl_3$) of 1-ethylquinoxalin-2(1*H*)-one **(1b)**

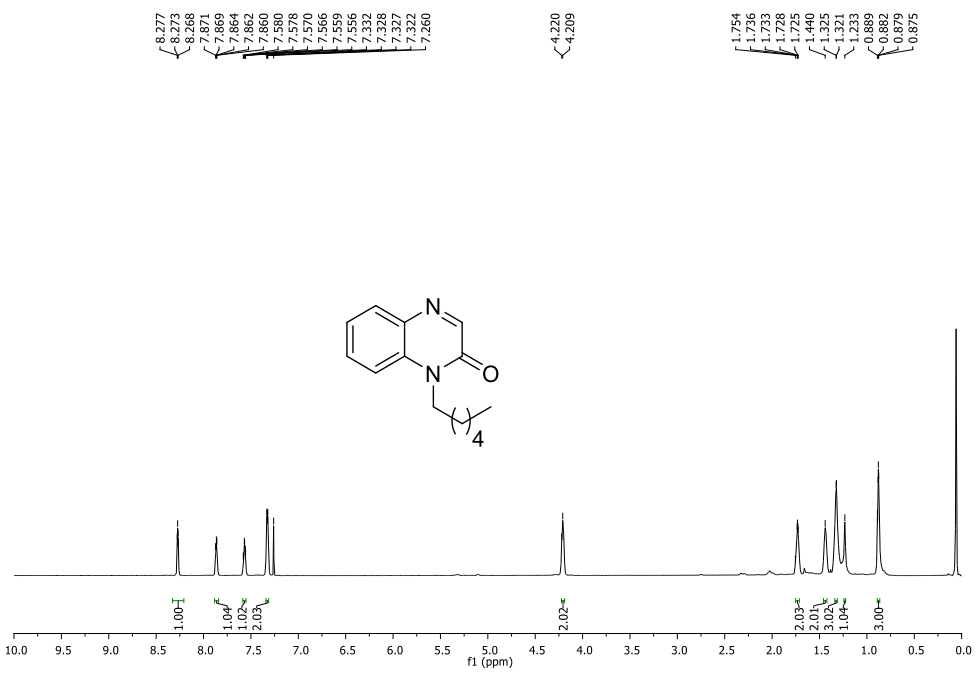

Figure S15. ^{1}H NMR (700 MHz, $CDCl_3$) of 1-hexylquinoxalin-2(1*H*)-one **(1c)**

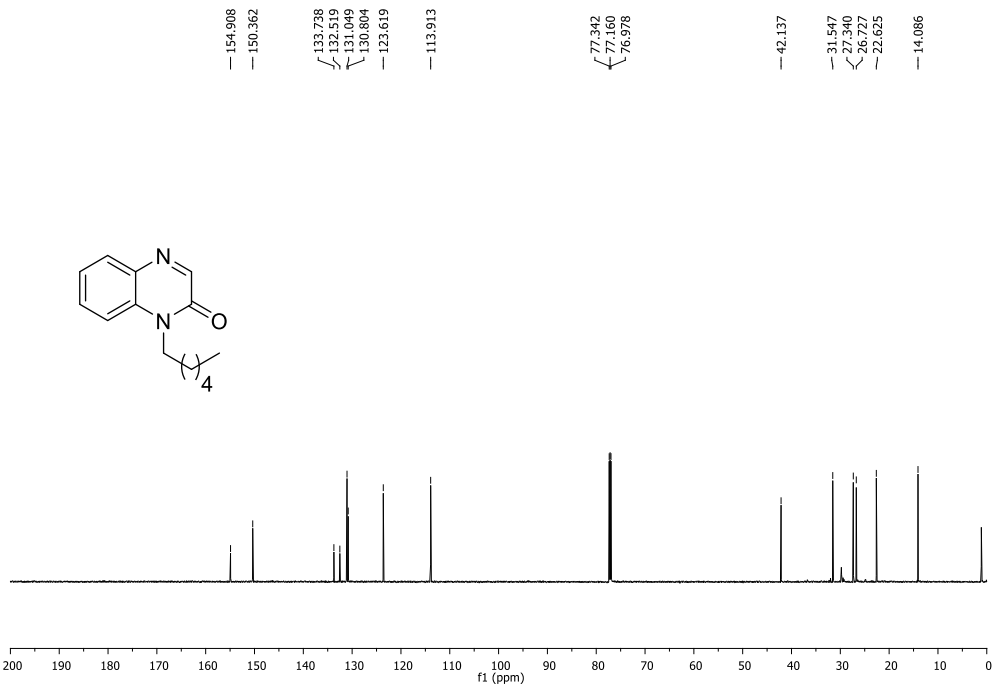

Figure S16. ^{13}C{^{1}H} NMR (175 MHz, $CDCl_3$) of 1-hexylquinoxalin-2(1*H*)-one **(1c)**

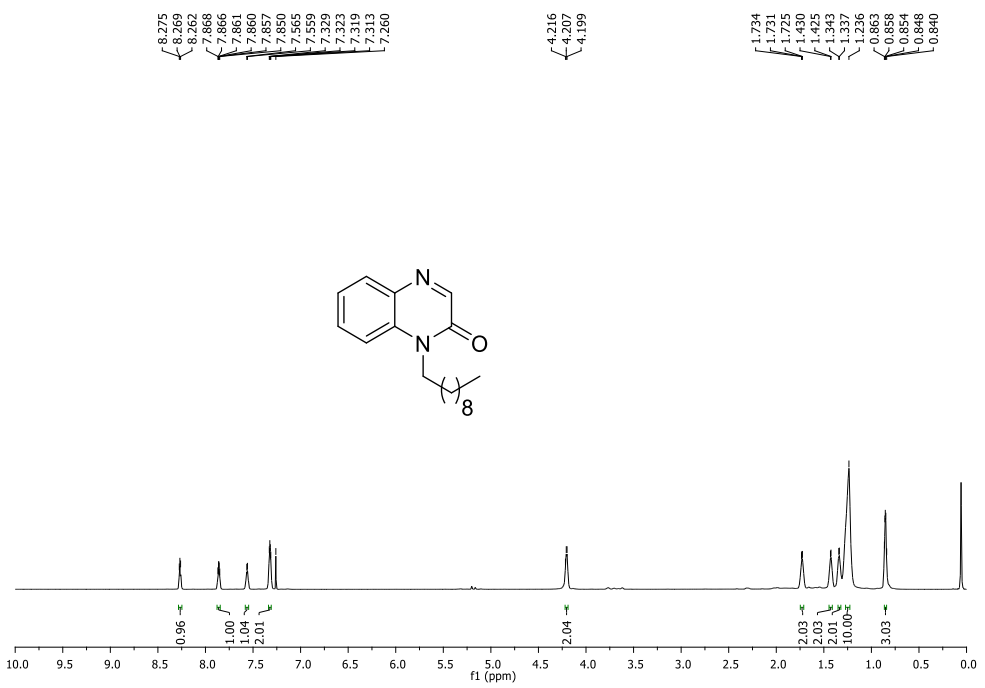

Figure S17. ^{1}H NMR (700 MHz, $CDCl_3$) of 1-decylquinoxalin-2(1*H*)-one **(1d)**

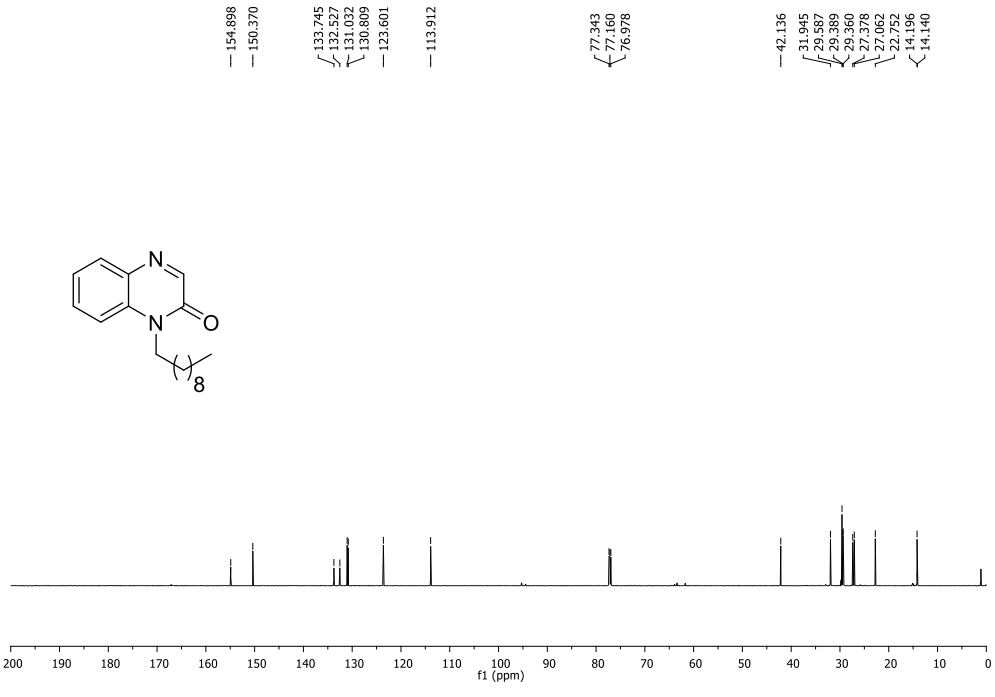

Figure S18. ^{13}C{^{1}H} NMR (175 MHz, $CDCl_3$) of 1-decylquinoxalin-2(1*H*)-one **(1d)**

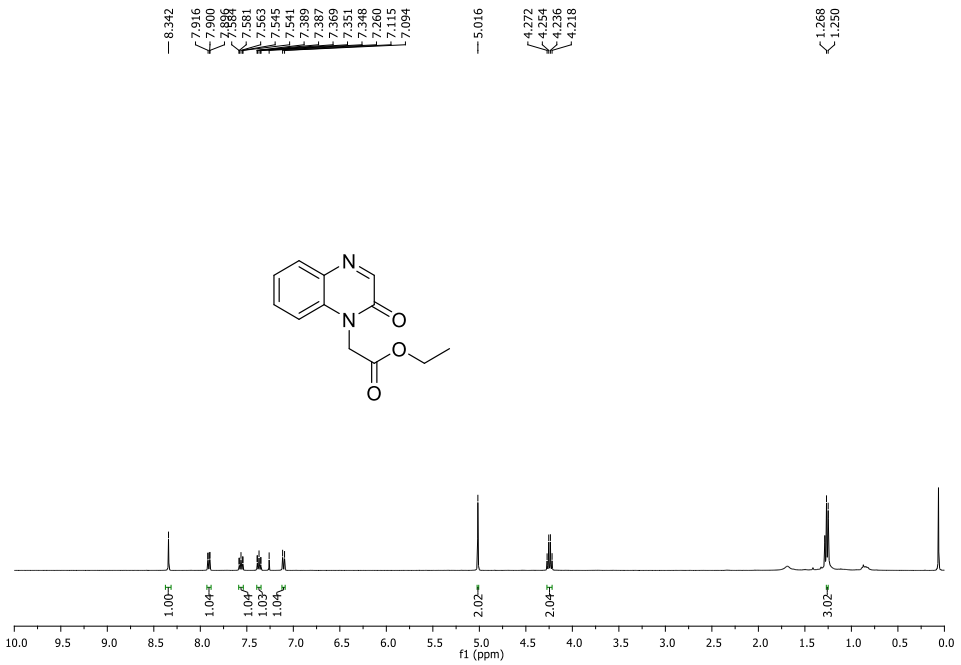

Figure S19. ^{1}H NMR (400 MHz, $CDCl_3$) of ethyl 2-(2-oxoquinoxalin-1(2*H*)-yl)acetate **(1e).**

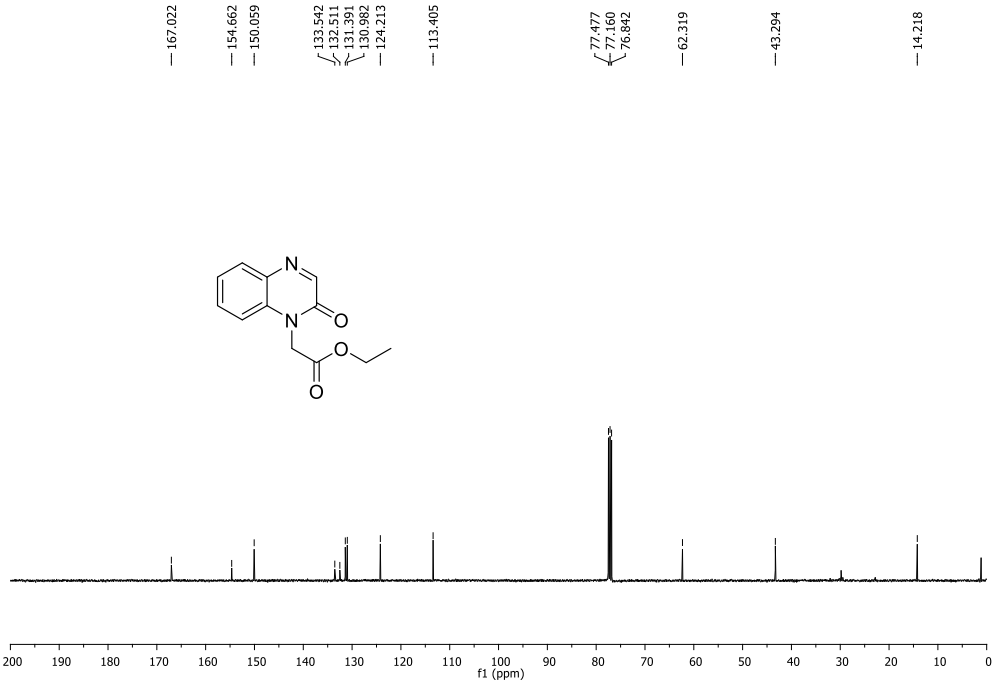

Figure S20. ^{13}C{^{1}H} NMR (100 MHz, $CDCl_3$) of ethyl 2-(2-oxoquinoxalin-1(2*H*)-yl)acetate **(1e)**

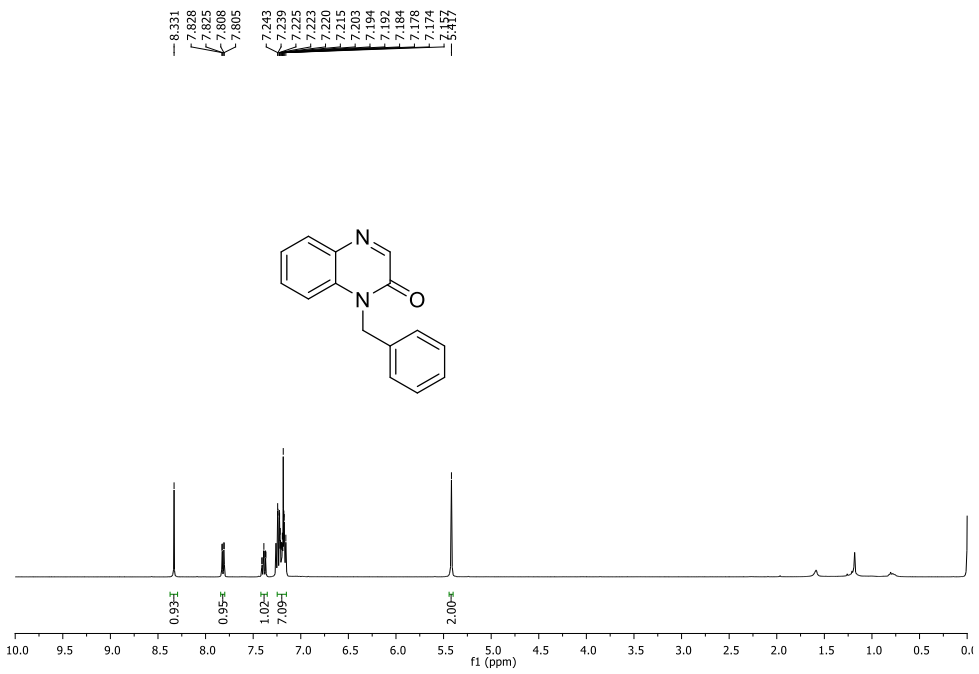

Figure S21. ^{1}H NMR (400 MHz, $CDCl_3$) of 1-benzylquinoxalin-2(1*H*)-one **(1f)**

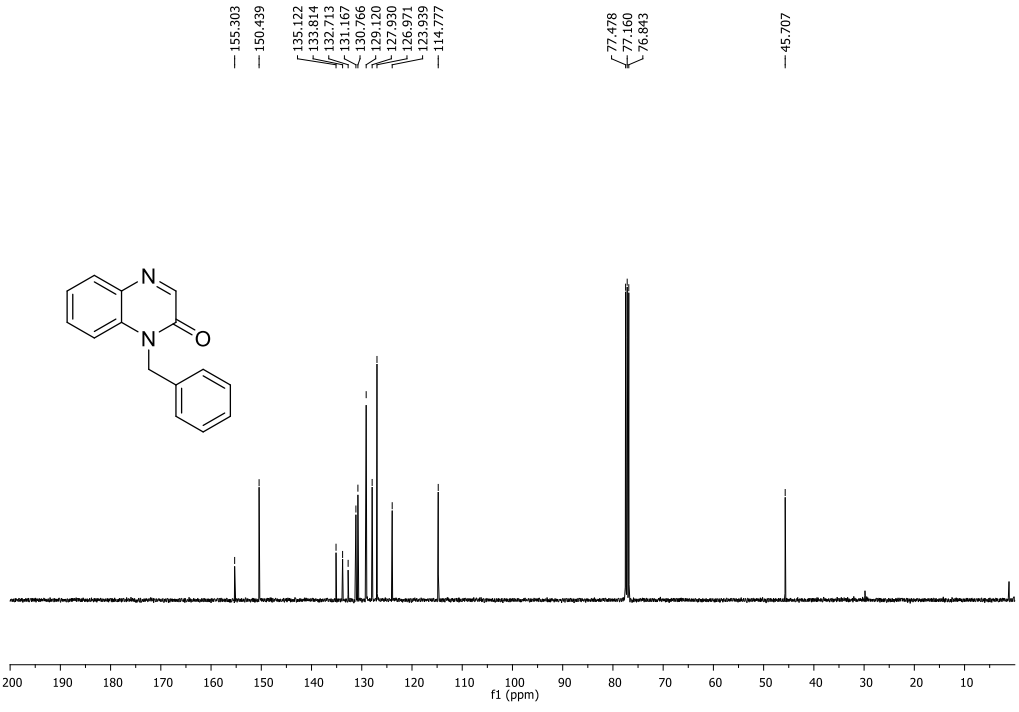

Figure S22. ^{13}C{^{1}H} NMR (100 MHz, $CDCl_3$) of 1-benzylquinoxalin-2(1*H*)-one **(1f)**

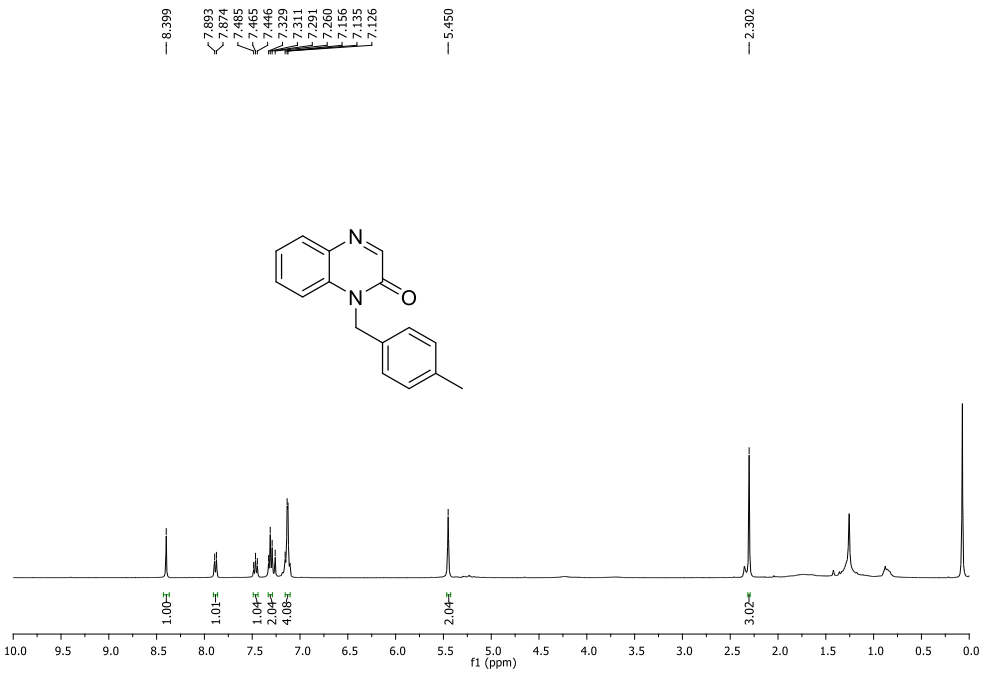

Figure S23. ^{1}H NMR (400 MHz, $CDCl_3$) of 1-(4-methylbenzyl)quinoxalin-2(1*H*)-one **(1g)**

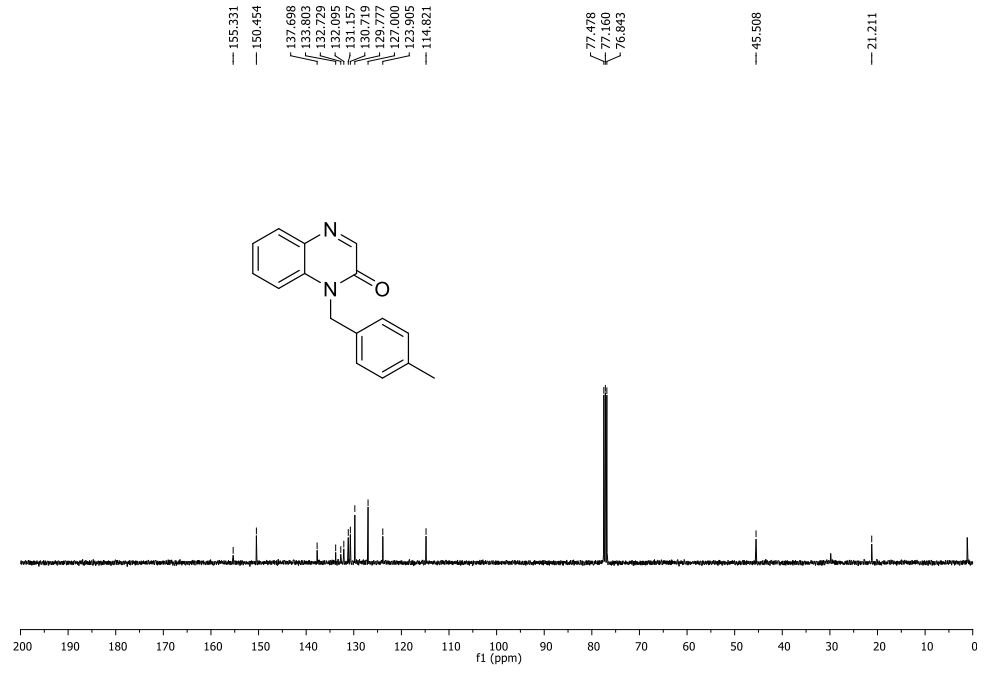

Figure S24. $^{13}C\{^{1}H\}$ NMR (100 MHz, $CDCl_3$) of 1-(4-methylbenzyl)quinoxalin-2(1*H*)-one **(1g)**

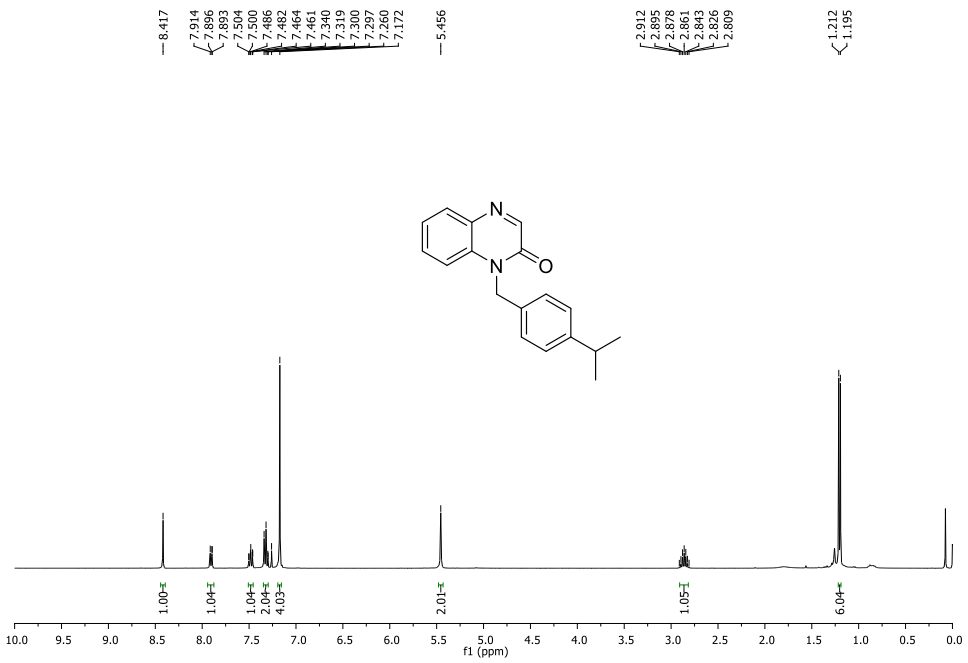

Figure S25. ^{1}H NMR (400 MHz, $CDCl_3$) of 1-(4-isopropylbenzyl)quinoxalin-2(1*H*)-one **(1h)**

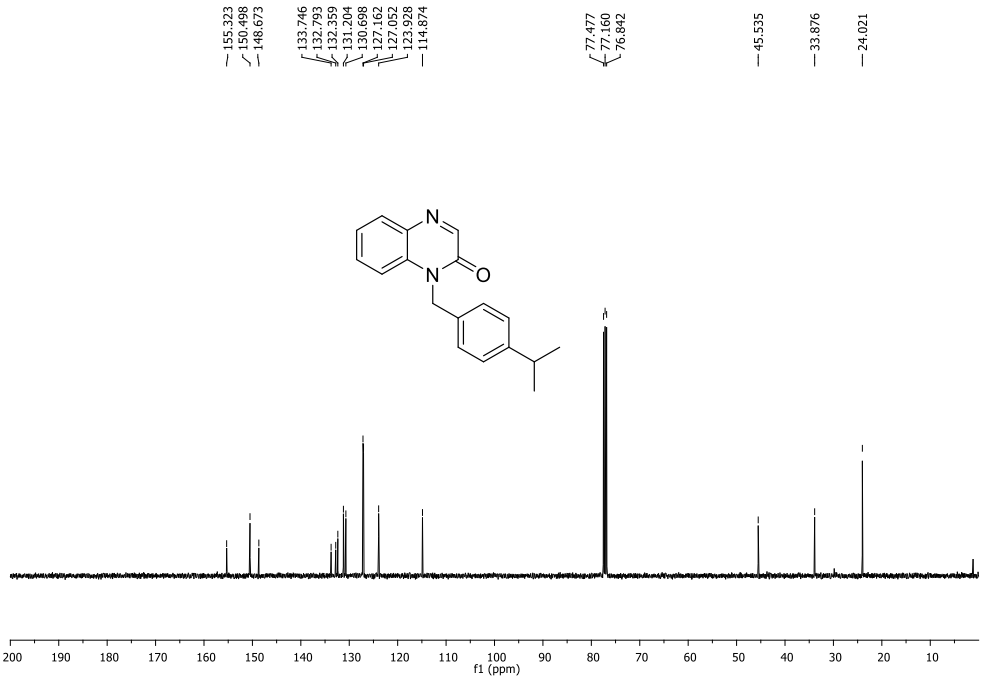

Figure S26. ^{13}C{^{1}H} NMR (100 MHz, $CDCl_3$) of 1-(4-isopropylbenzyl)quinoxalin-2(1*H*)-one **(1h)**

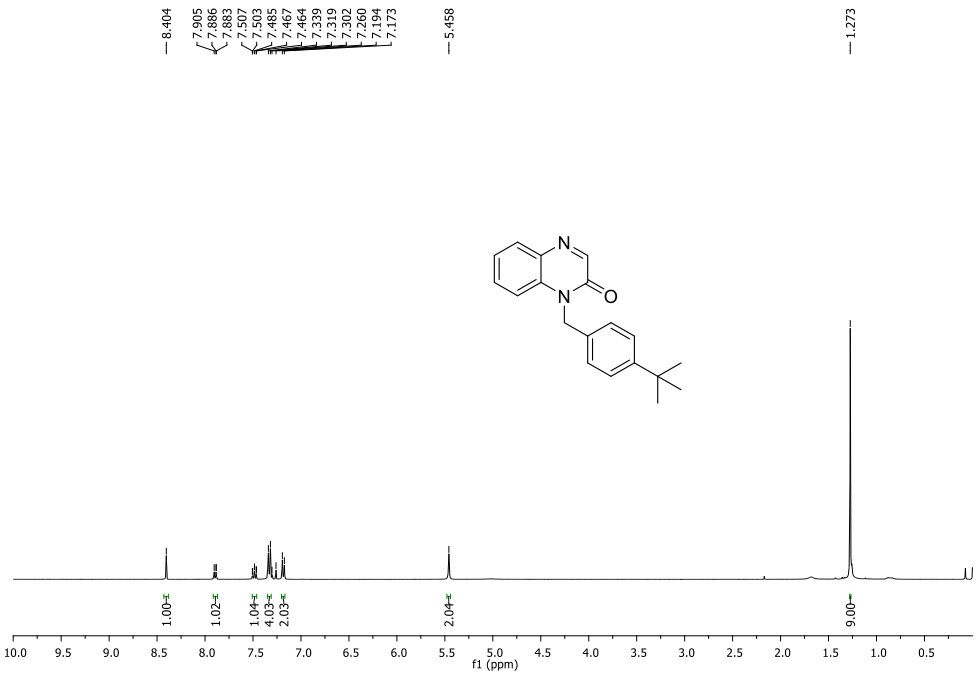

Figure S27. ^{1}H NMR (400 MHz, $CDCl_3$) of 1-(4-(*tert*-butyl)benzyl)quinoxalin-2(1*H*)-one **(1i)**

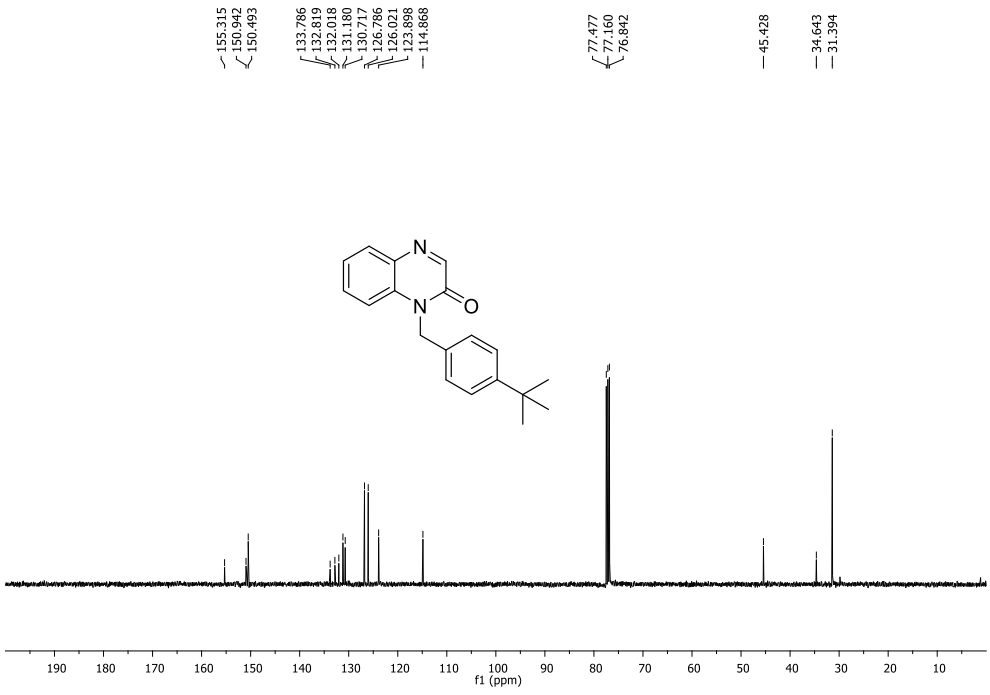

Figure S28. ^{13}C{^{1}H} NMR (100 MHz, $CDCl_3$) of 1-(4-(*tert*-butyl)benzyl)quinoxalin-2(1*H*)-one **(1i)**

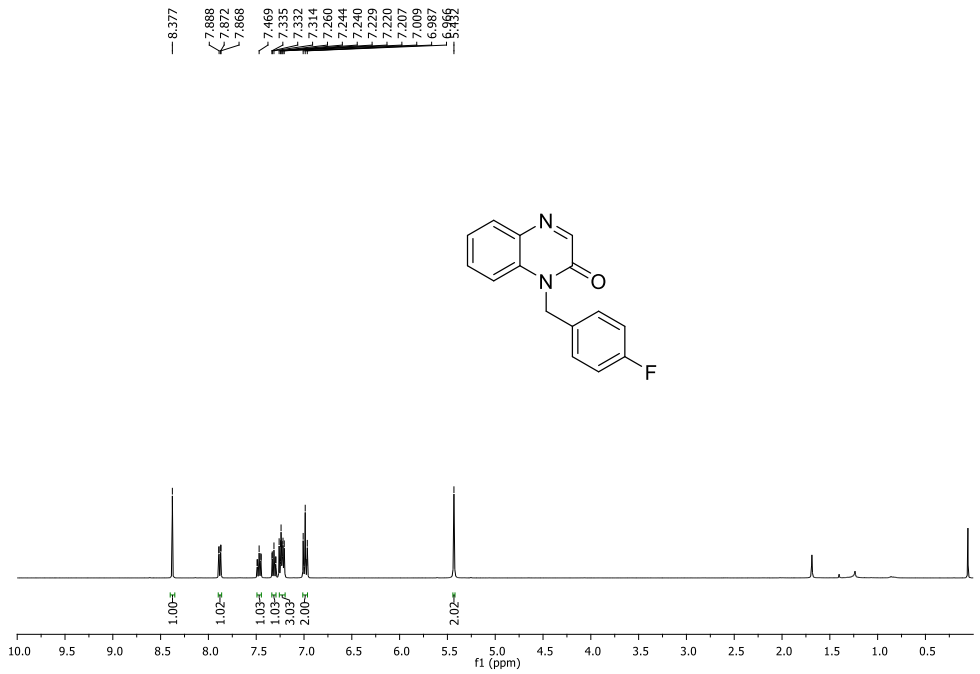

Figure S29. ^{1}H NMR (400 MHz, $CDCl_3$) of 1-(4-fluorobenzyl)quinoxalin-2(1*H*)-one **(1j)**

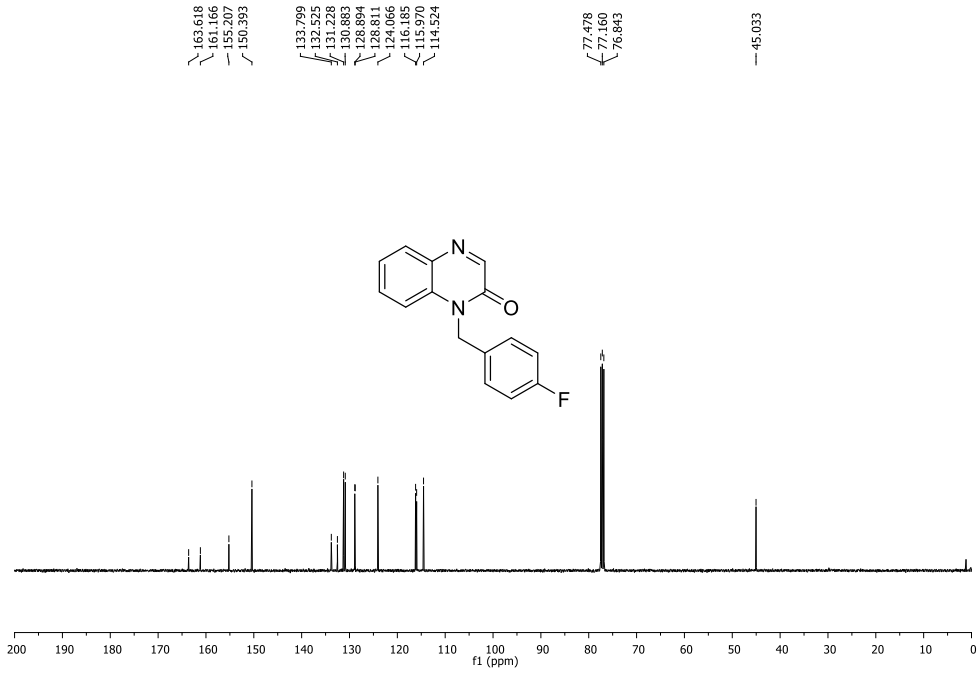

Figure S30. ^{13}C{^{1}H} NMR (100 MHz, $CDCl_3$) of 1-(4-fluorobenzyl)quinoxalin-2(1*H*)-one **(1j)**

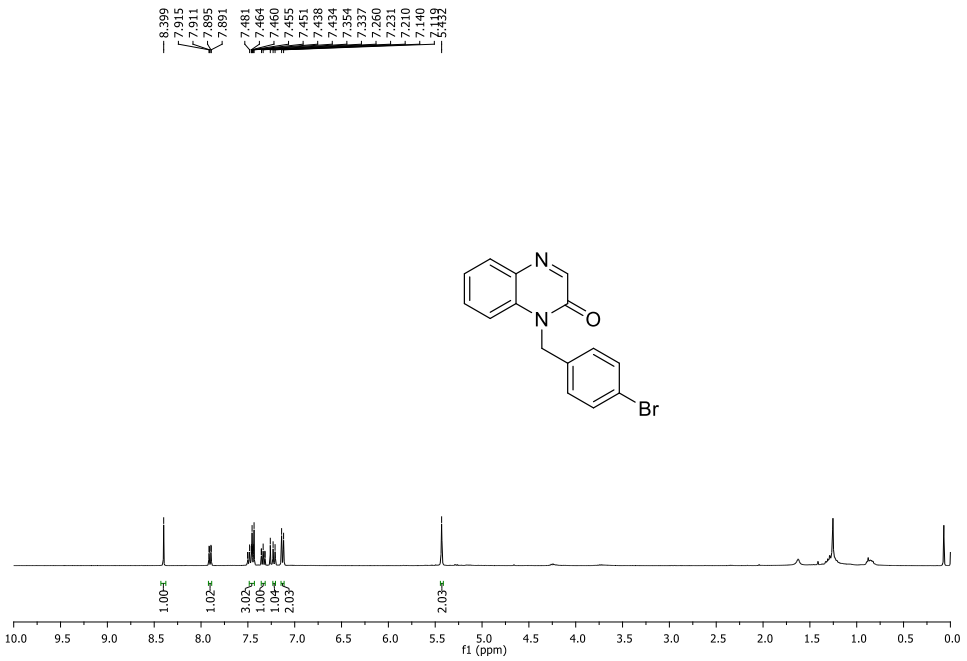

Figure S31. ^{1}H NMR (400 MHz, $CDCl_3$) of 1-(4-bromobenzyl)quinoxalin-2(1*H*)-one **(1k)**

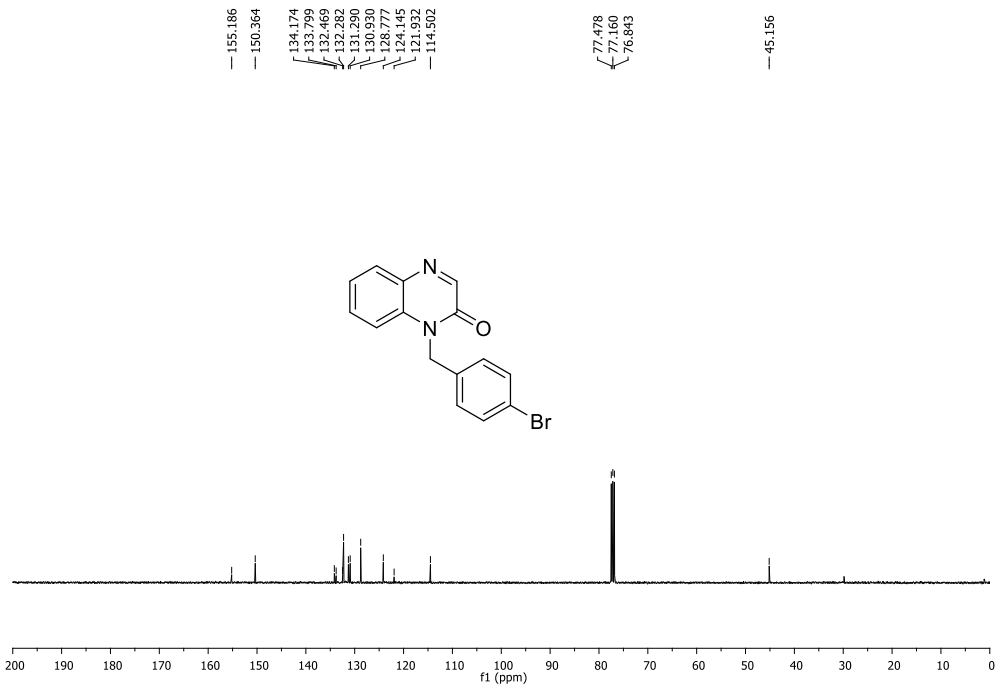

Figure S32. $^{13}C\{^{1}H\}$ NMR (100 MHz, $CDCl_3$) of 1-(4-bromobenzyl)quinoxalin-2(1*H*)-one **(1k)**

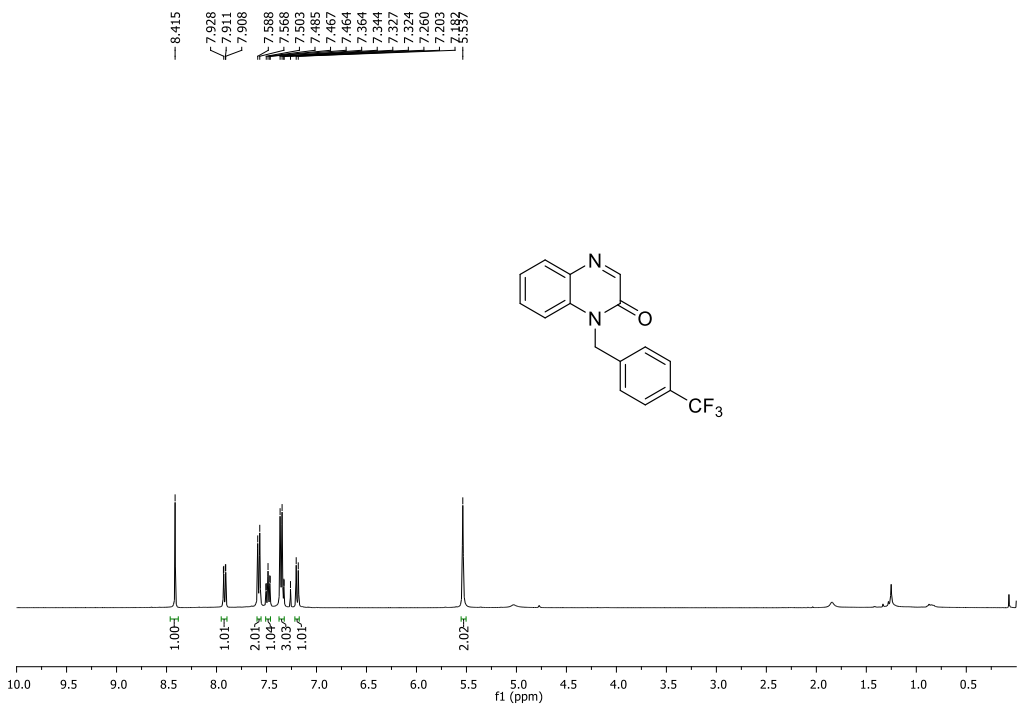

Figure 33. ^{1}H NMR (400 MHz, $CDCl_3$) of 1-(4-(trifluoromethyl)benzyl)quinoxalin-2(1*H*)-one **(1l)**

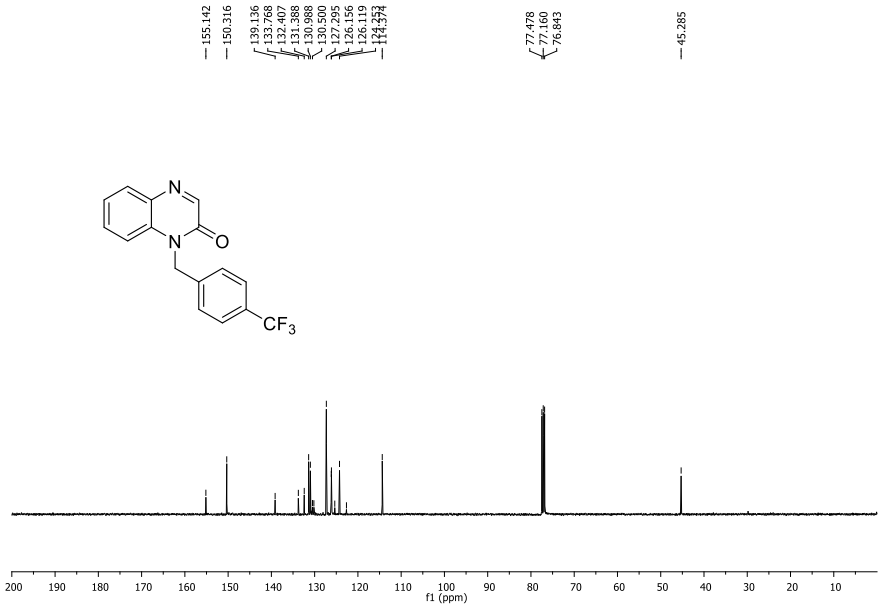

Figure S34. ^{13}C{^{1}H} NMR (100 MHz, $CDCl_3$) of 1-(4-(trifluoromethyl)benzyl)quinoxalin-2(1*H*)-one **(1l)**

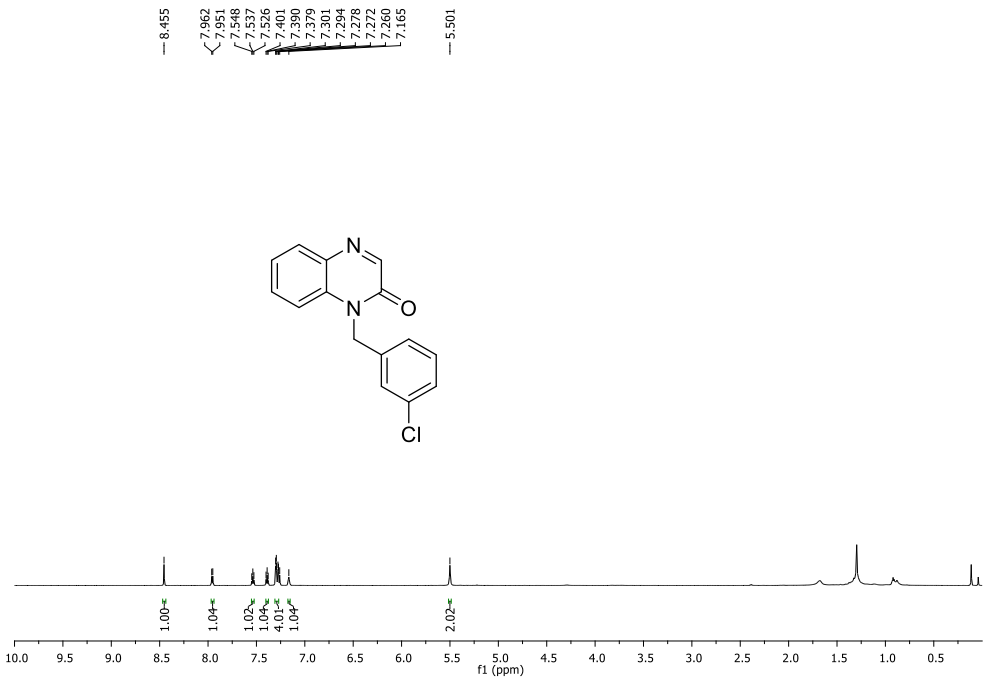

Figure S35. ^{1}H NMR (700 MHz, $CDCl_3$) of 1-(3-chlorobenzyl)quinoxalin-2(1*H*)-one **(1m)**

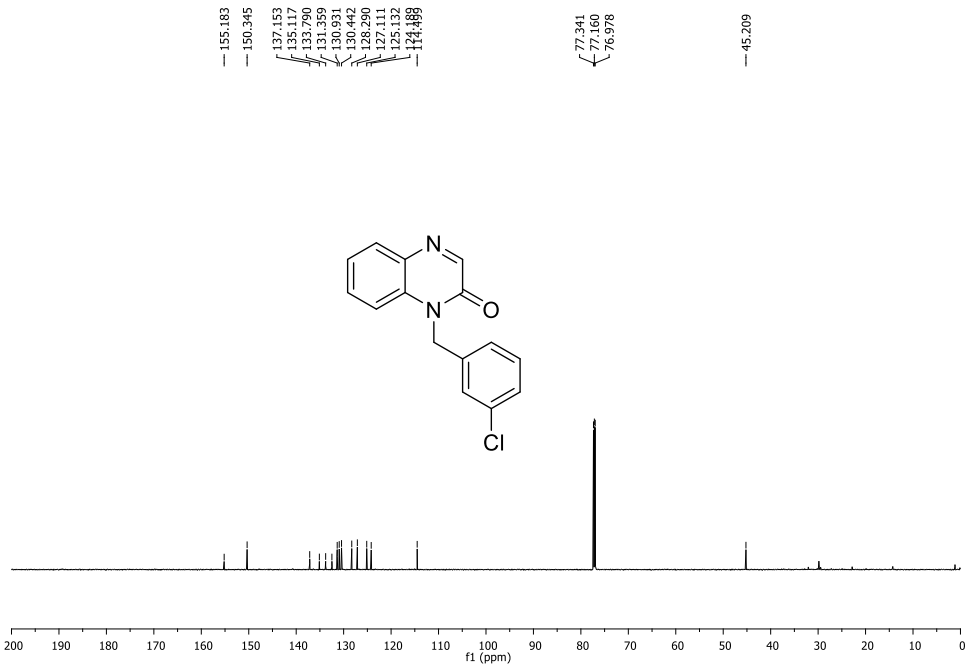

Figure S36. $^{13}C\{^{1}H\}$ NMR (175 MHz, $CDCl_3$) of 1-(3-chlorobenzyl)quinoxalin-2(1*H*)-one **(1m)**

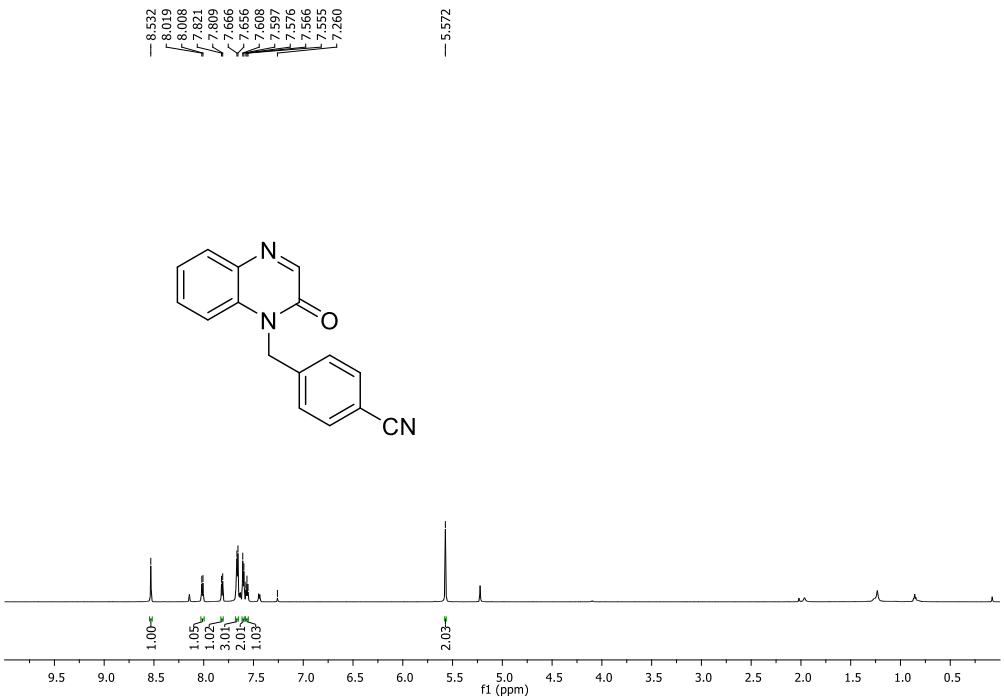

Figure S37. ^{1}H NMR (700 MHz, $CDCl_3$) of 4-((2-oxoquinoxalin-1(2*H*)-yl)methyl)benzonitrile **(1n)**

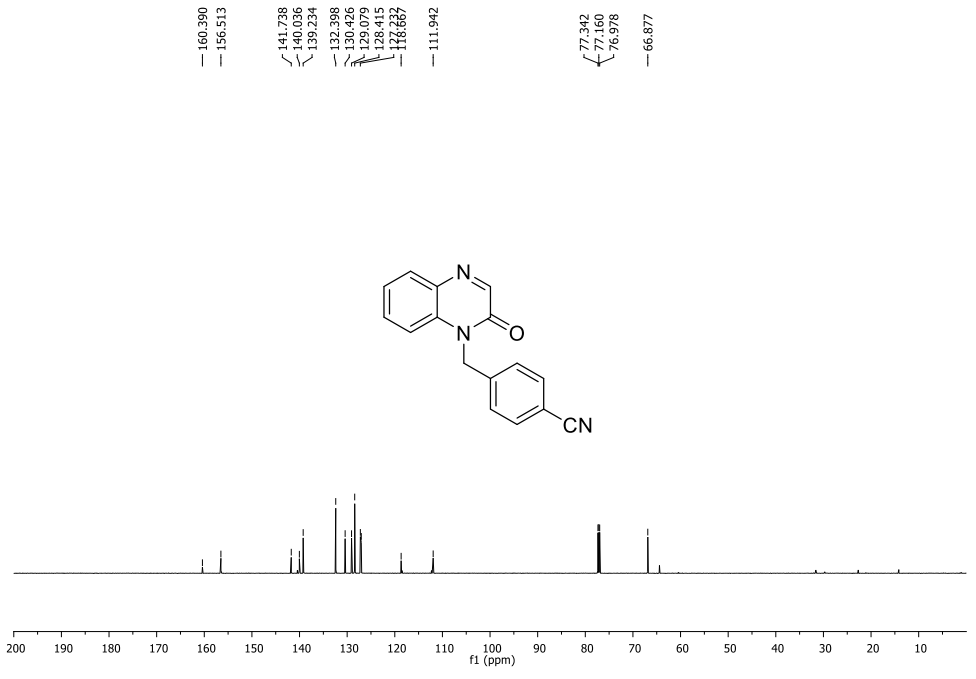

Figure S38. ^{13}C{^{1}H} NMR (175 MHz, $CDCl_3$) of 4-((2-oxoquinoxalin-1(2*H*)-yl)methyl)benzonitrile **(1n)**

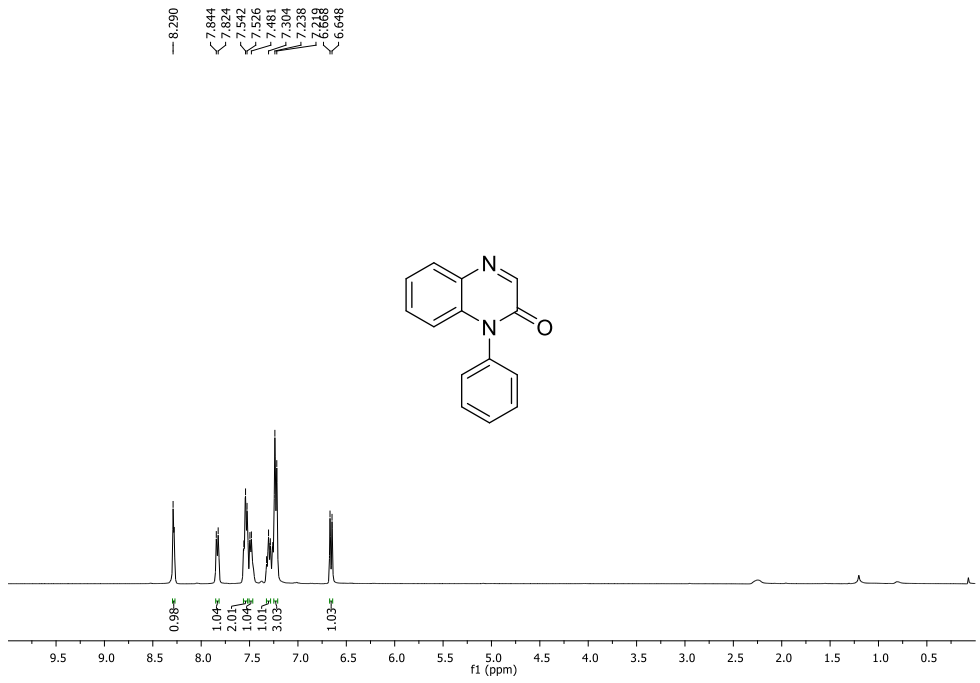

Figure S39. ^{1}H NMR (400 MHz, $CDCl_3$) of 1-phenylquinoxalin-2(1*H*)-one **(1o)**

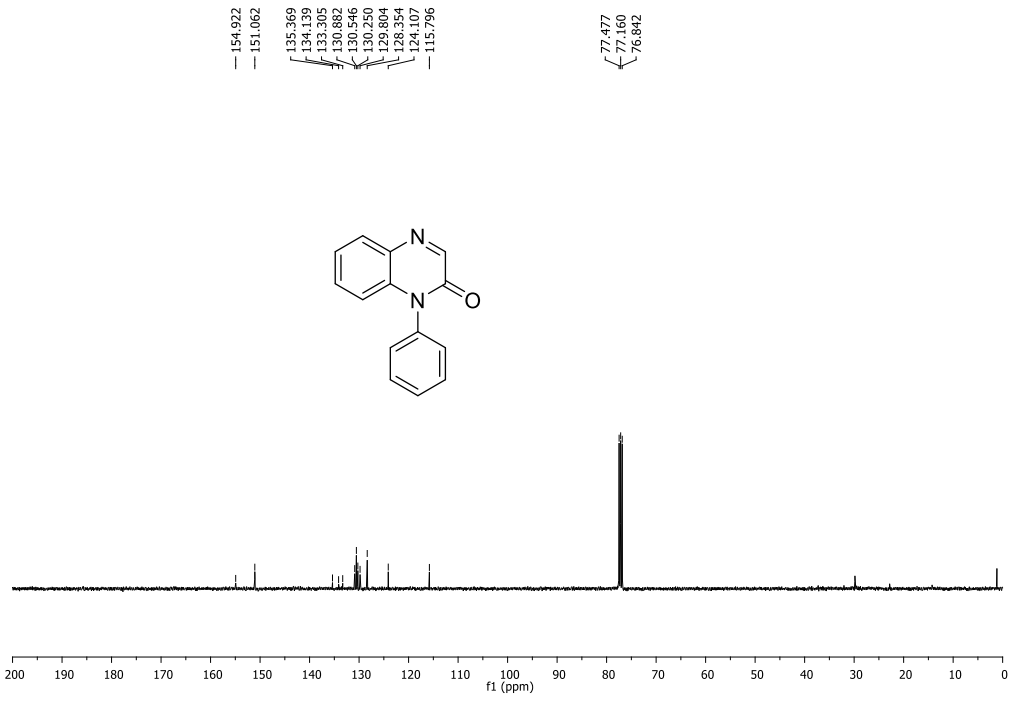

Figure S40. $^{13}C\{^{1}H\}$ NMR (100 MHz, $CDCl_3$) of 1-phenylquinoxalin-2(1*H*)-one **(1o)**

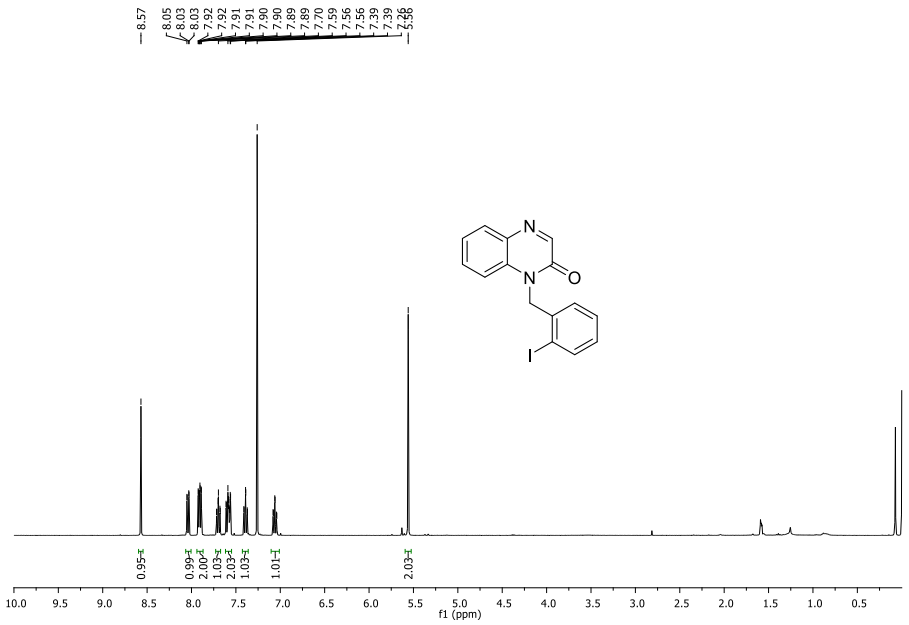

Figure S41. ^{1}H NMR (400 MHz, $CDCl_3$) of 1-(2-Iodobenzyl)quinoxalin-2(1*H*)-one (**1p**)

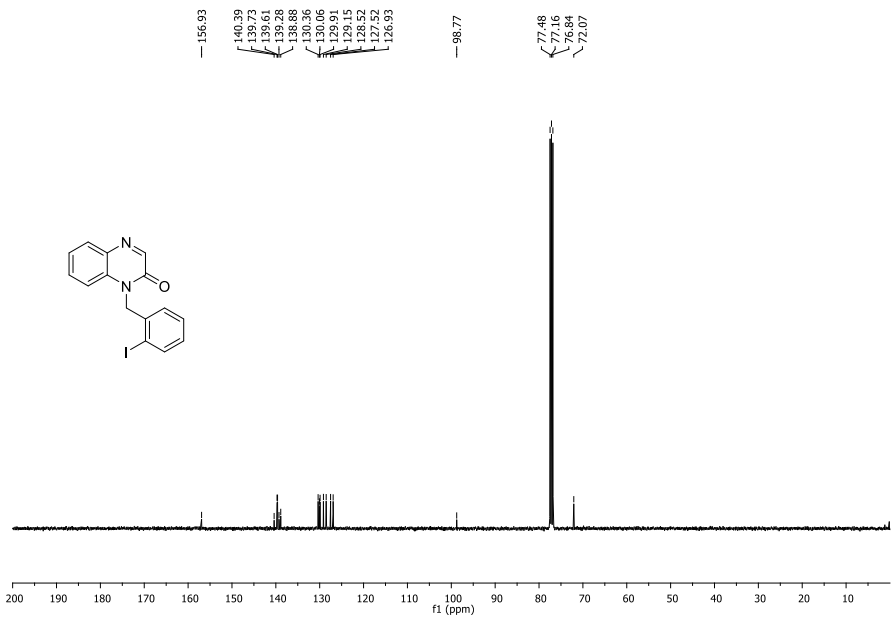

Figure S42. $^{13}C\{^{1}H\}$ NMR (100 MHz, $CDCl_3$) of 1-(2-Iodobenzyl)quinoxalin-2(1*H*)-one (**1p**)

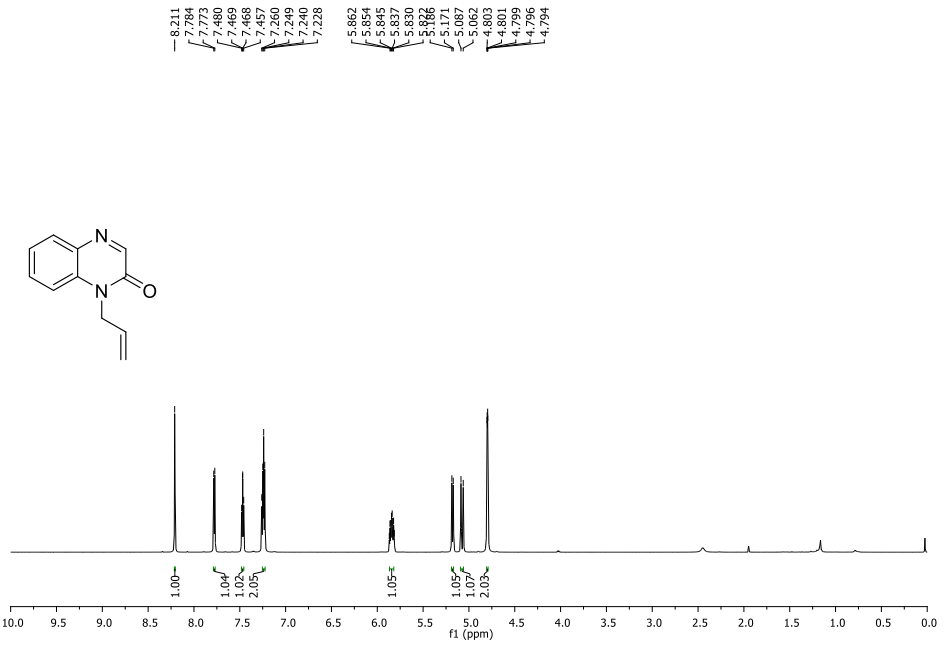

Figure S43. ^{1}H NMR (700 MHz, $CDCl_3$) of 1-Allylquinoxalin-2(1*H*)-one (**1q**)

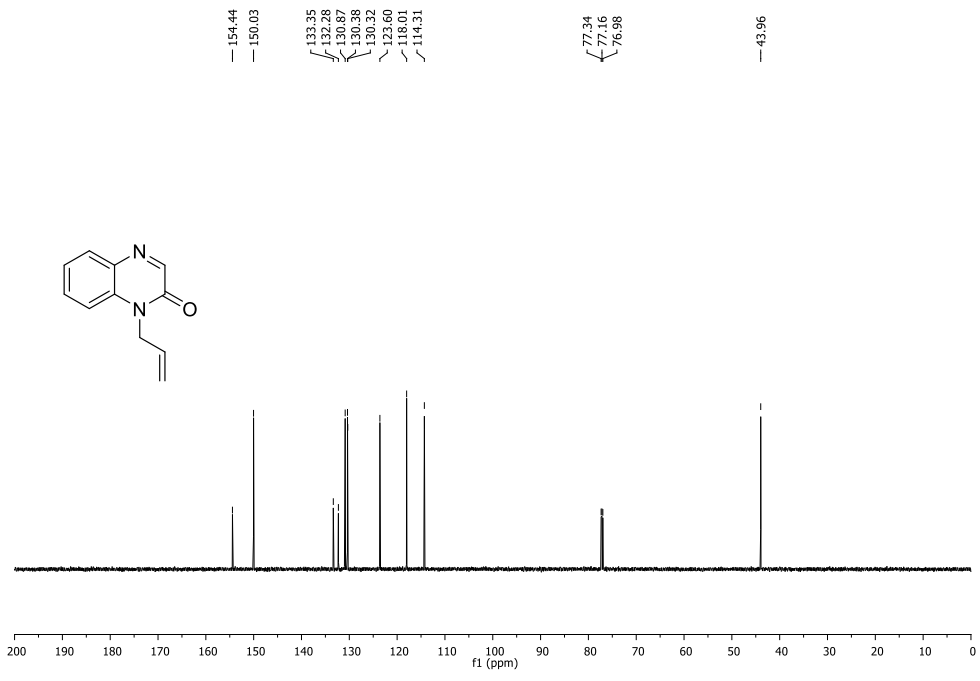

Figure S44. ^{13}C{^{1}H} NMR (175 MHz, $CDCl_3$) of 1-Allylquinoxalin-2(1*H*)-one (**1q**)

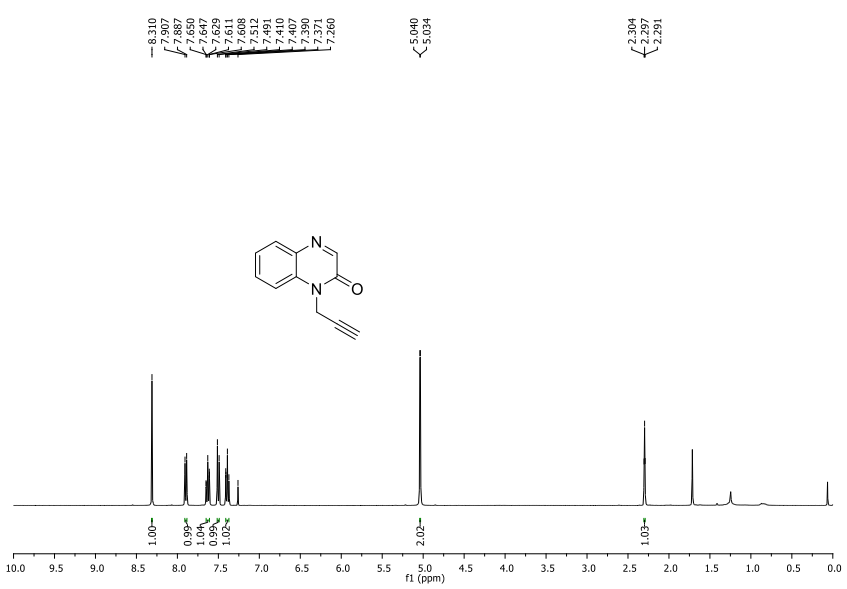

Figure S45. ^{1}H NMR (400 MHz, $CDCl_3$) of 1-(Prop-2-yn-1-yl)quinoxalin-2(1*H*)-one (**1r**)

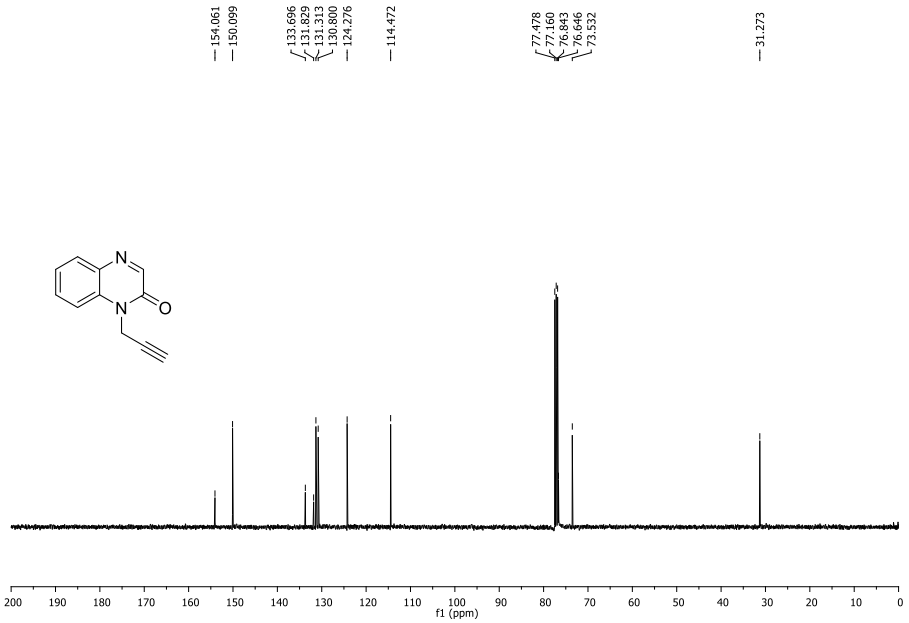

Figure S46. $^{13}C\{^{1}H\}$ NMR (100 MHz, $CDCl_3$) of 1-(Prop-2-yn-1-yl)quinoxalin-2(1*H*)-one (**1r**)

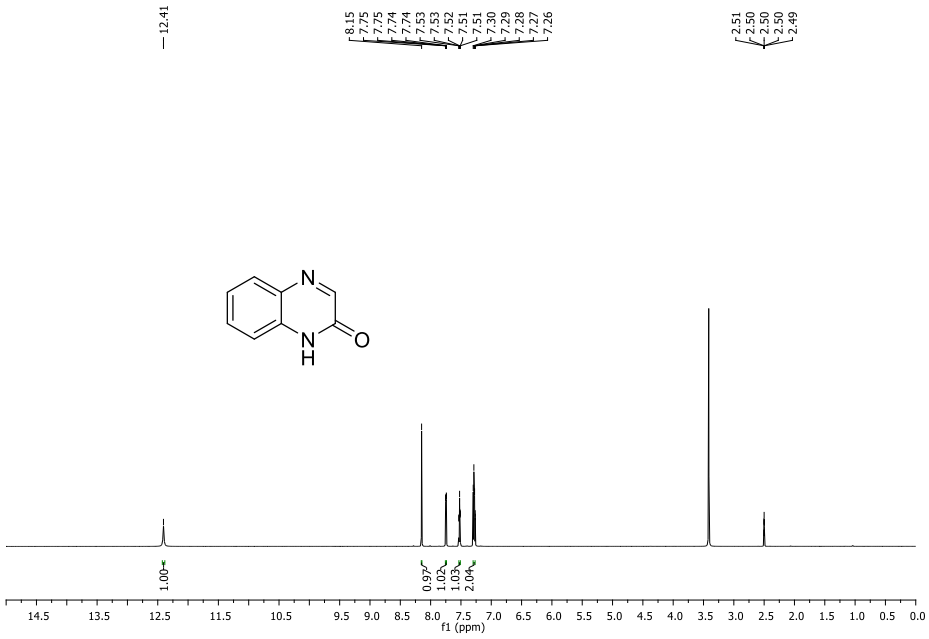

Figure S47. ^{1}H NMR (700 MHz, DMSO-d_6) of Quinoxalin-2(1*H*)-one (**1s**)

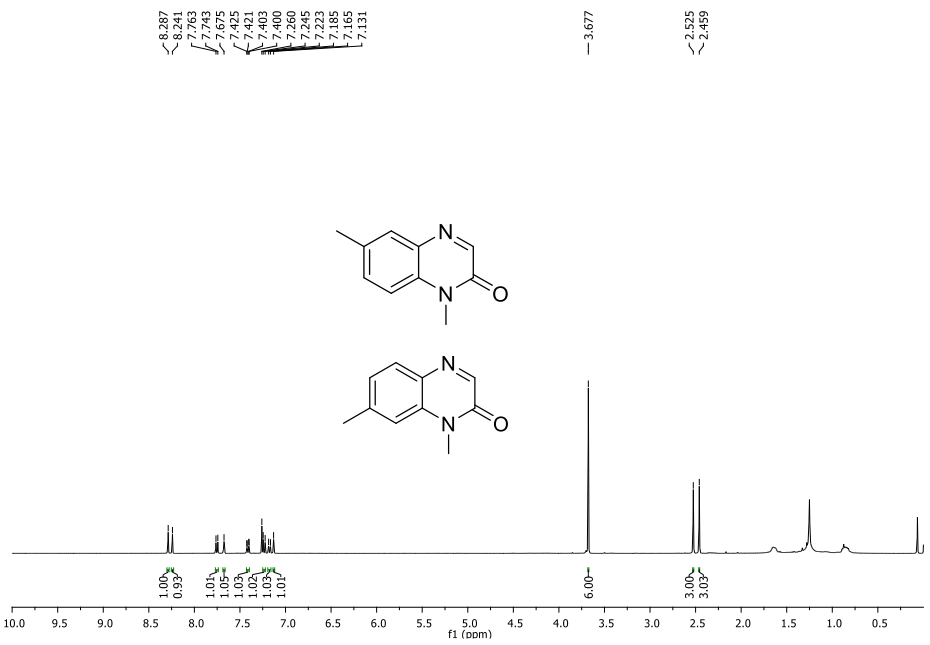

Figure S48. ^{1}H NMR (400 MHz, $CDCl_3$) of 1,6-dimethylquinoxalin-2(1*H*)-one **(1t)**

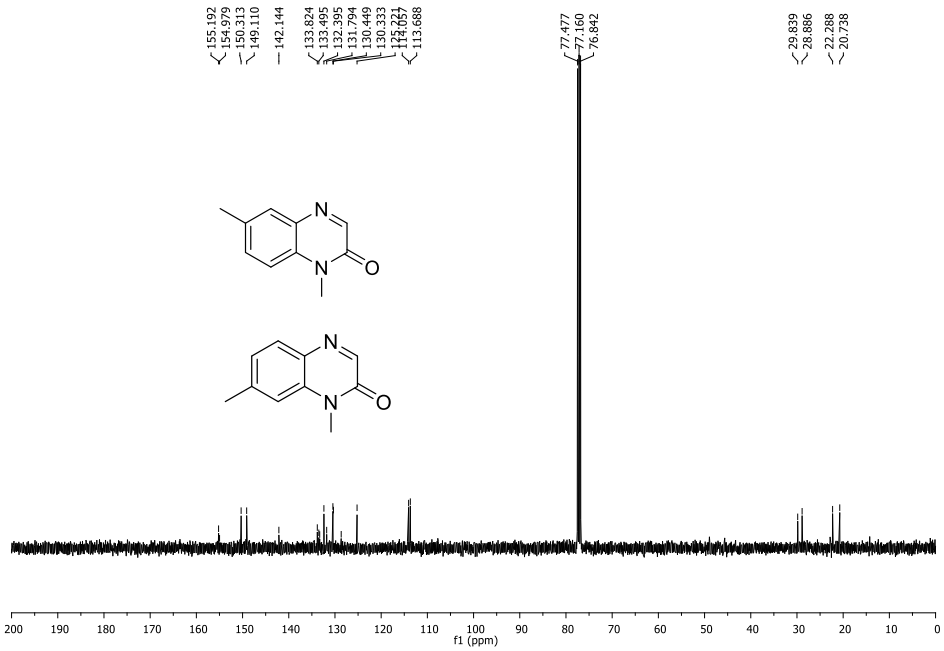

Figure 49. ^{13}C{^{1}H} NMR (100 MHz, $CDCl_3$) of 1,6-dimethylquinoxalin-2(1*H*)-one **(1t)**

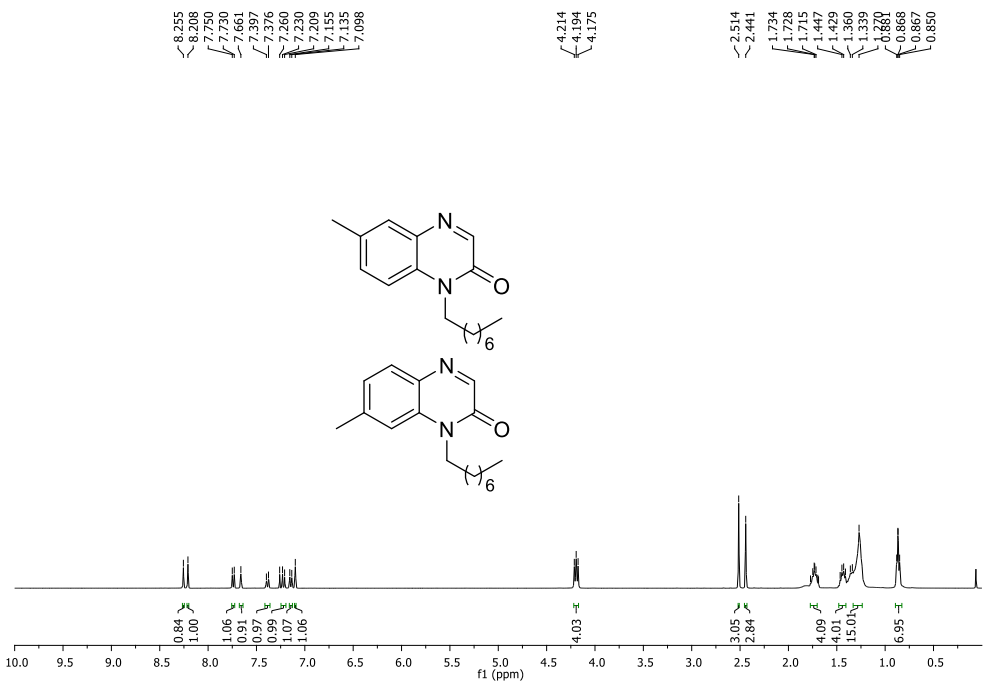

Figure S50. ^{1}H NMR (400 MHz, $CDCl_3$) of 6-methyl-1-octylquinoxalin-2(1*H*)-one **(1u)**

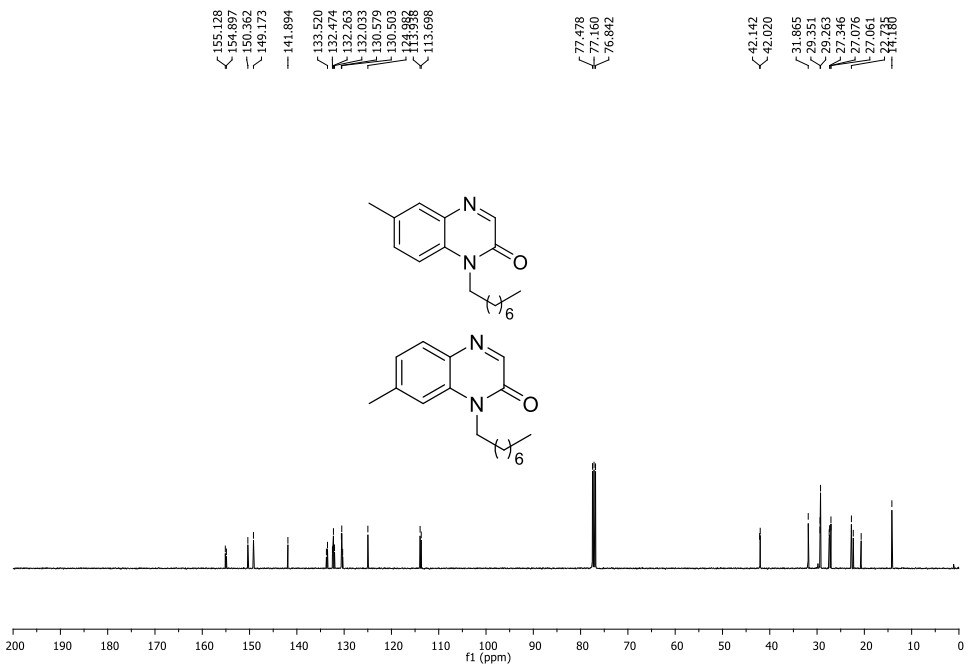

Figure S51. ^{13}C{^{1}H} NMR (100 MHz, $CDCl_3$) of 6-methyl-1-octylquinoxalin-2(1*H*)-one **(1u)**

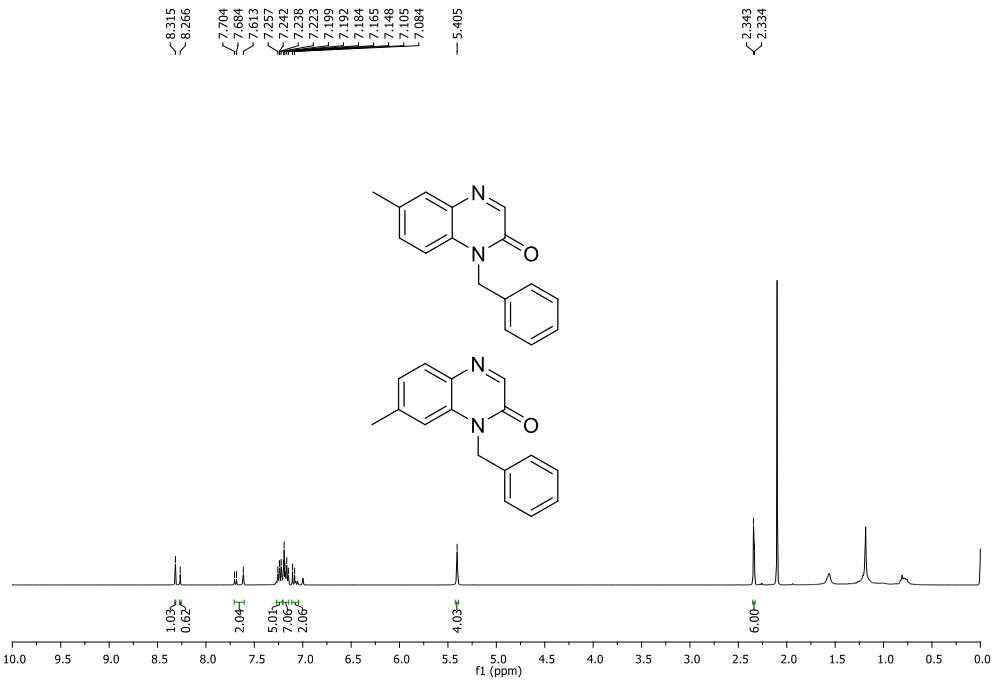

Figure S52. ^{1}H NMR (400 MHz, $CDCl_3$) of 1-benzyl-6-methylquinoxalin-2(1*H*)-one **(1v)**

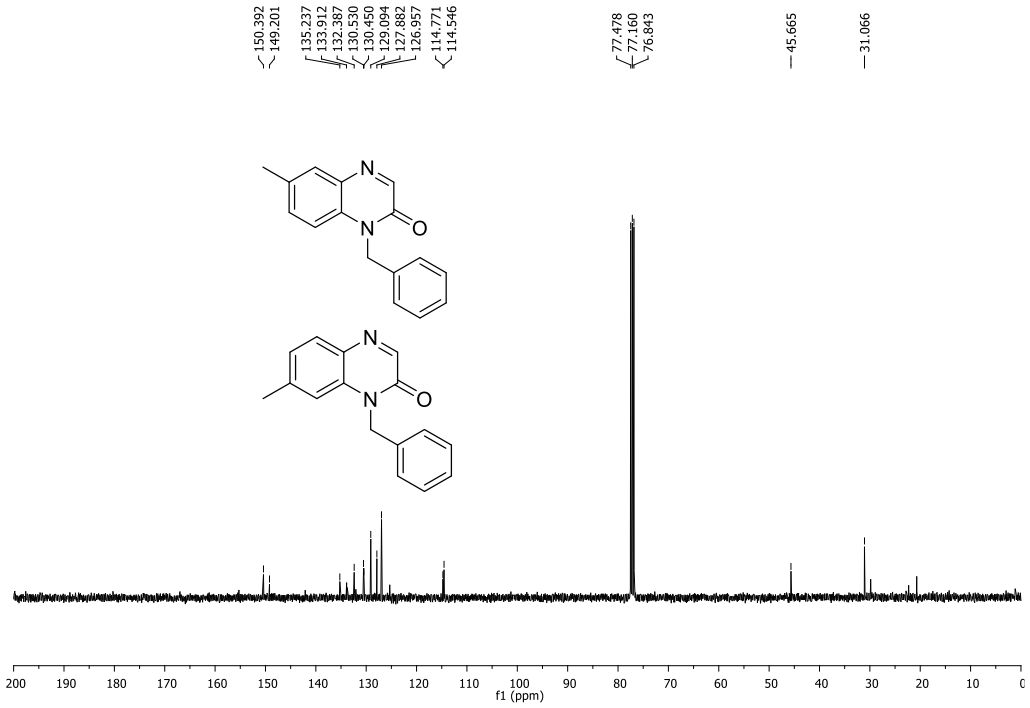

Figure S53. ^{13}C{^{1}H} NMR (100 MHz, $CDCl_3$) of 1-benzyl-6-methylquinoxalin-2(1*H*)-one **(1v)**

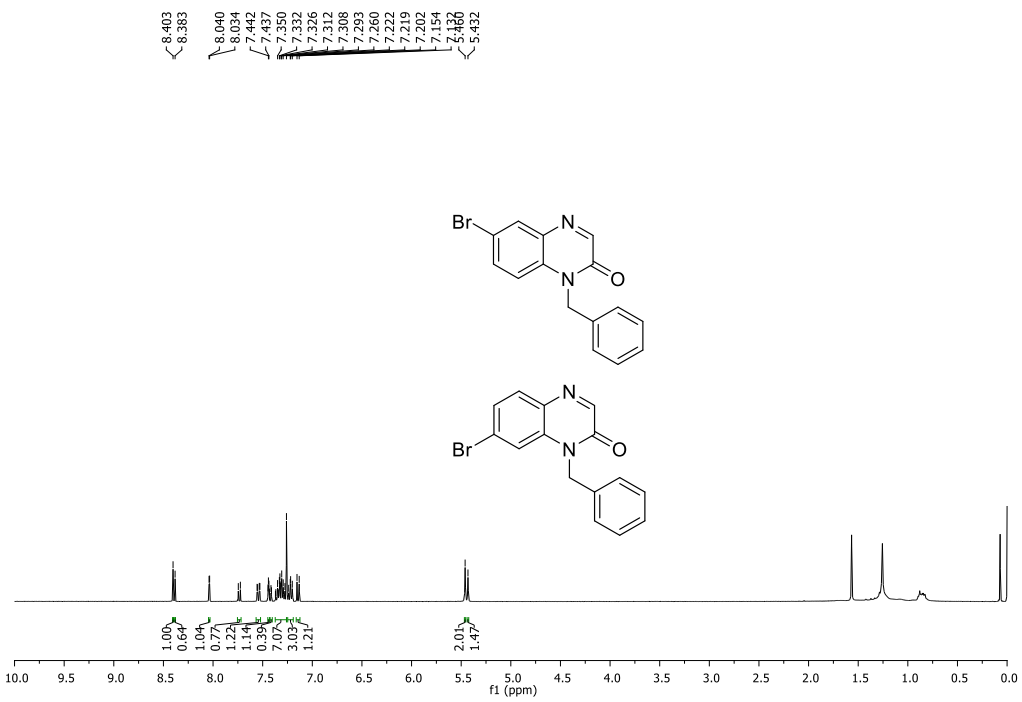

Figure S54. ^{1}H NMR (700 MHz, $CDCl_3$) of 1-benzyl-6-bromoquinoxalin-2(1*H*)-one **(1w)**

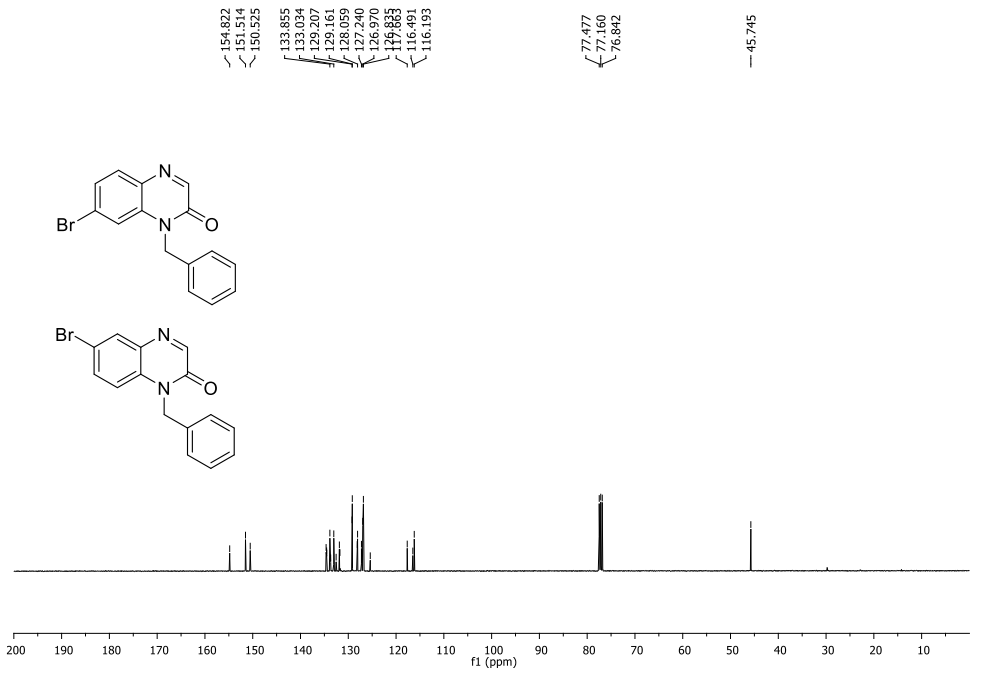

Figure S55. ^{13}C{^{1}H} NMR (100 MHz, $CDCl_3$) of 1-benzyl-6-bromoquinoxalin-2(1*H*)-one **(1w)**

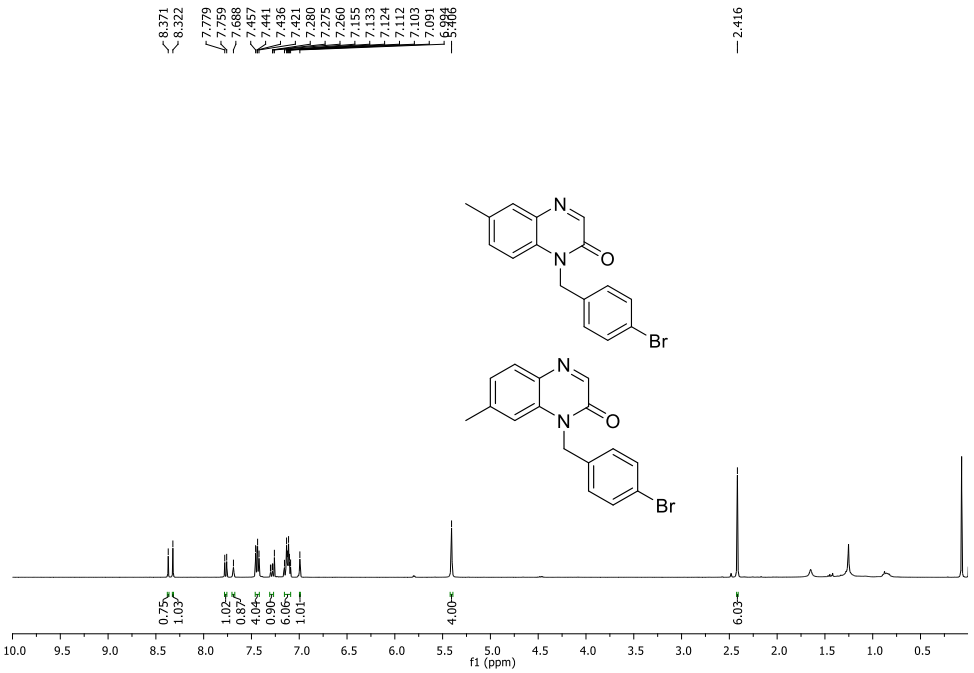

Figure S56. ^{1}H NMR (400 MHz, $CDCl_3$) of 1-(4-bromobenzyl)-6-methylquinoxalin-2(1*H*)-one **(1x)**

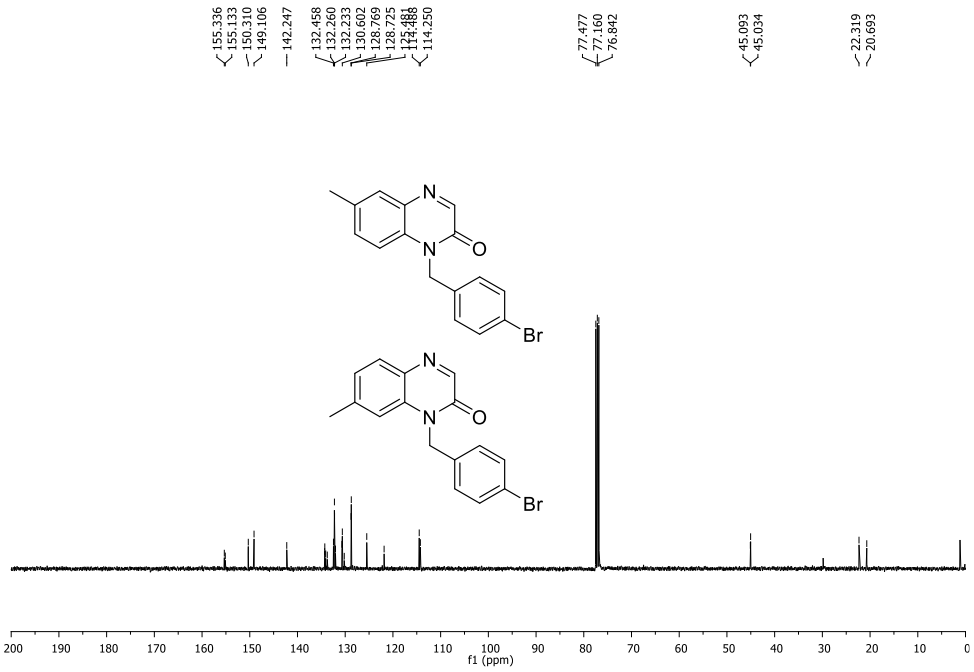

Figure S57. ^{13}C{^{1}H} NMR (100 MHz, $CDCl_3$) of 1-(4-bromobenzyl)-6-methylquinoxalin-2(1*H*)-one **(1x)**

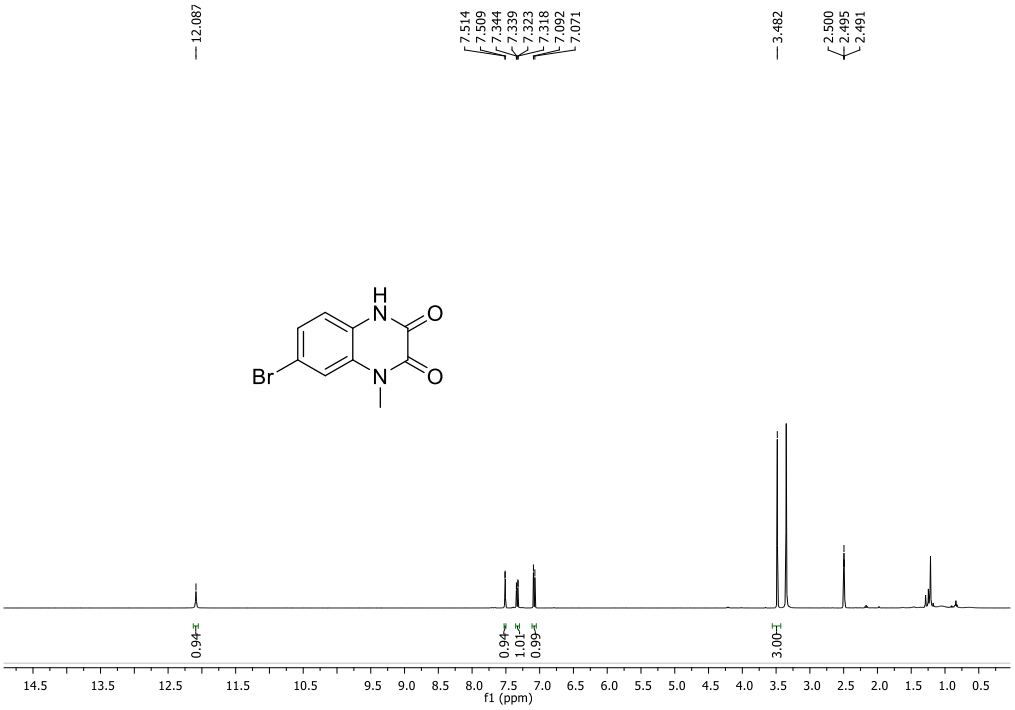

Figure S58. ^{1}H NMR (400 MHz, DMSO-d_6) of 7-bromo-1-methyl-1,4-dihydroquinoxaline-2,3-dione **(2a)**

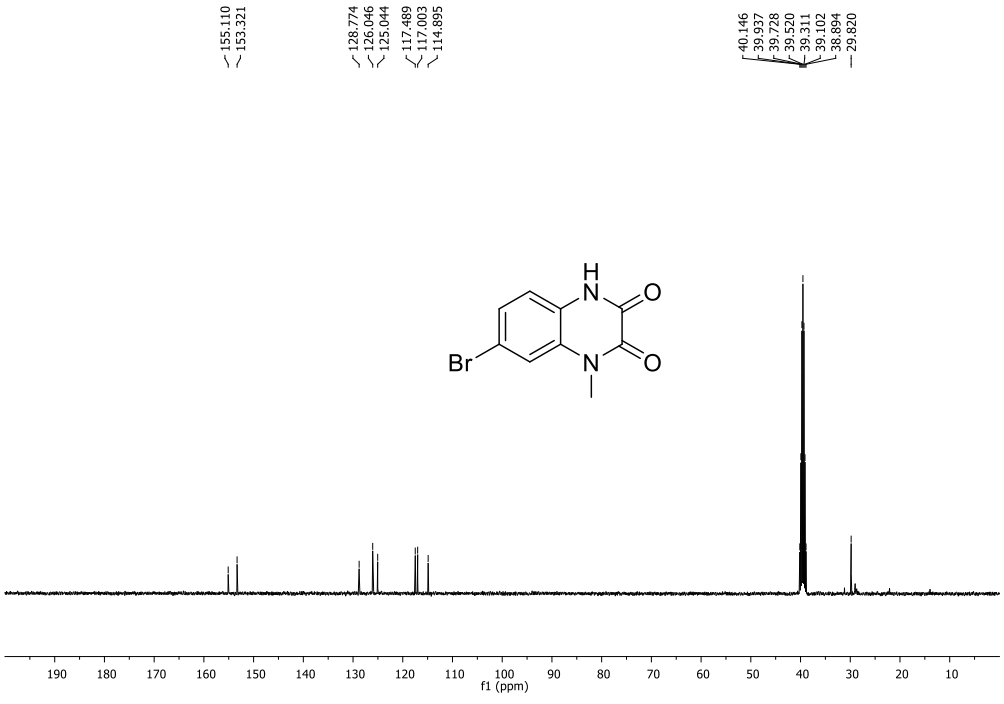

Figure S59. ^{13}C{^{1}H} NMR (100 MHz, DMSO-d_6) of 7-bromo-1-methyl-1,4-dihydroquinoxaline-2,3-dione **(2a)**

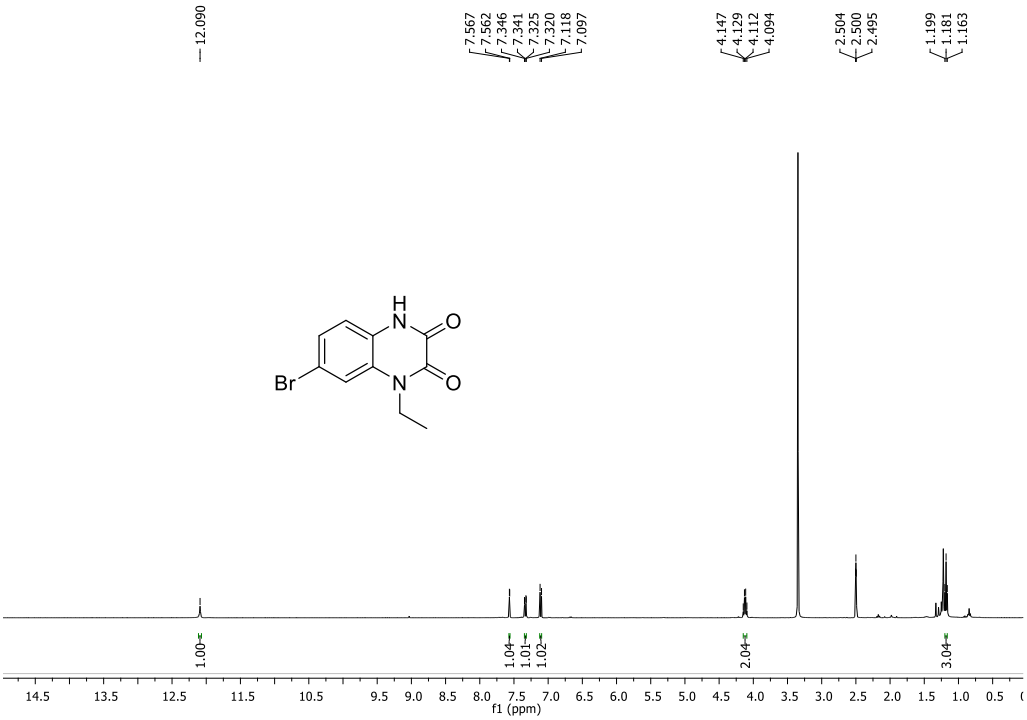

Figure S60. ^{1}H NMR (400 MHz, DMSO-d_6) of 7-bromo-1-ethyl-1,4-dihydroquinoxaline-2,3-dione **(2b)**

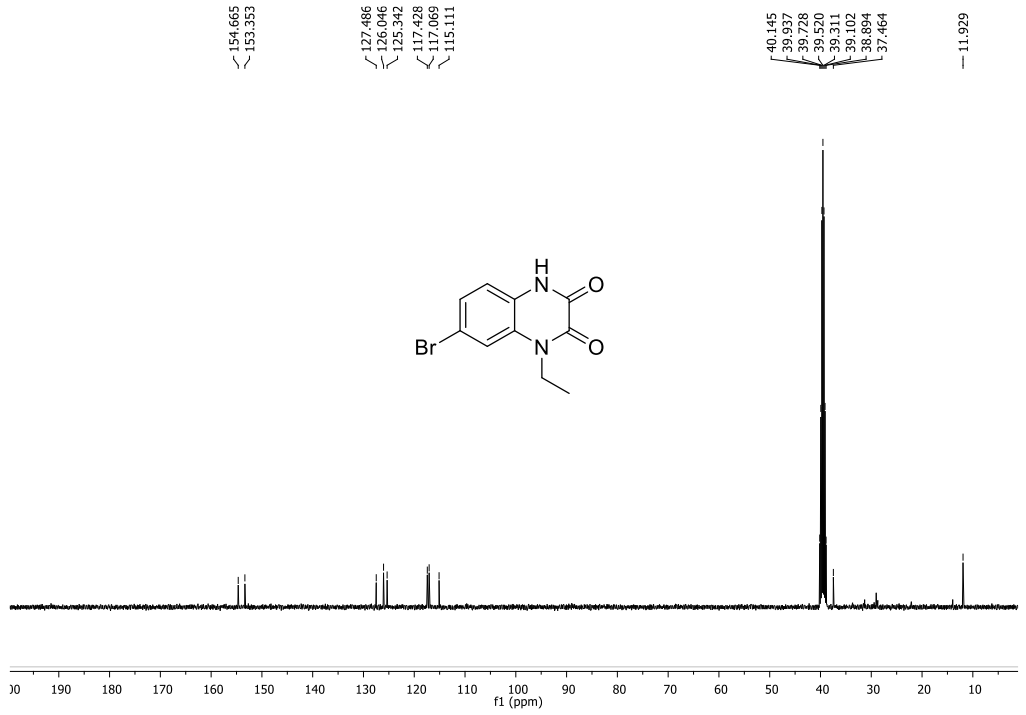

Figure S61. ^{13}C{^{1}H} NMR (100 MHz, DMSO-d_6) of 7-bromo-1-ethyl-1,4-dihydroquinoxaline-2,3-dione **(2b)**

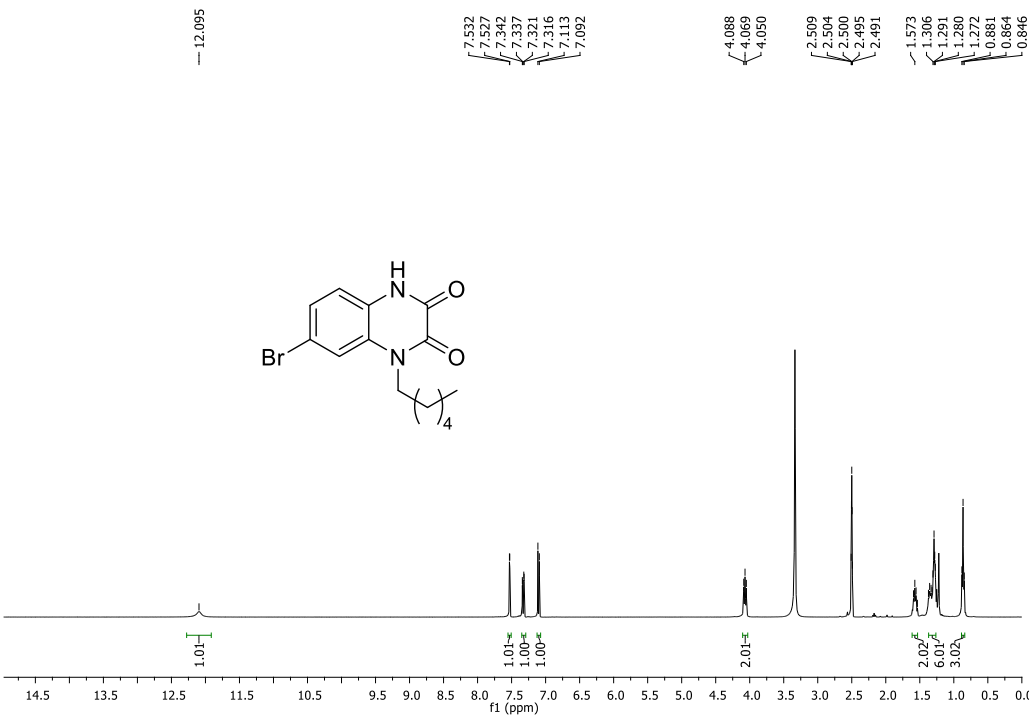

Figure S62. ^{1}H NMR (400 MHz, DMSO-d_6) of 7-bromo-1-hexyl-1,4-dihydroquinoxaline-2,3-dione **(2c)**

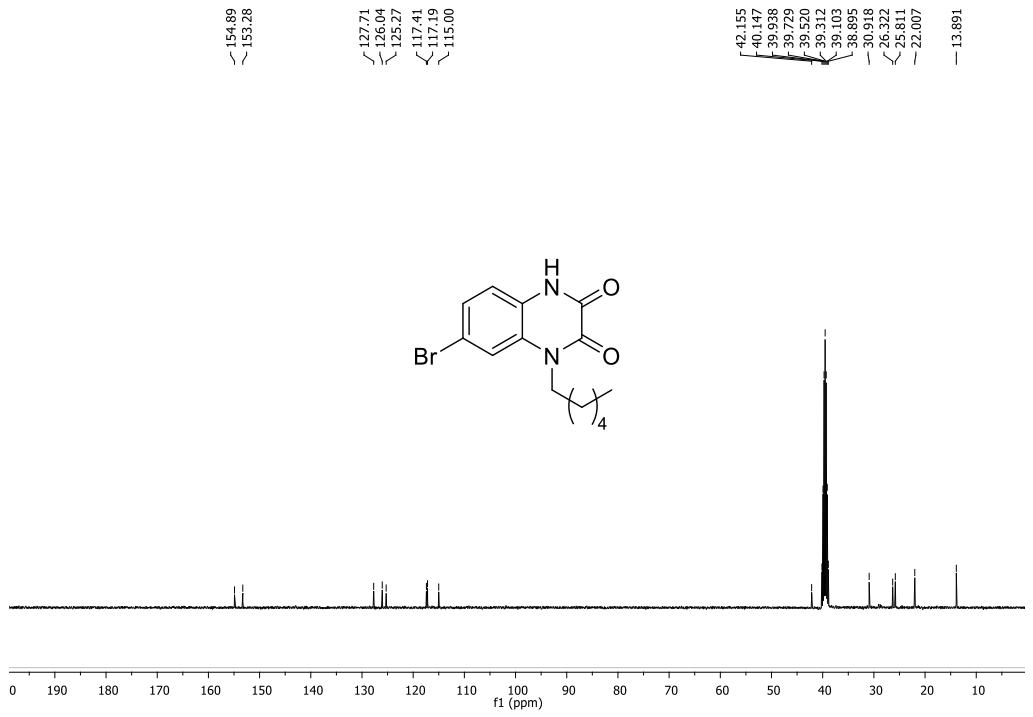

Figure S63. ^{13}C{^{1}H} NMR (100 MHz, DMSO-d_6) of 7-bromo-1-hexyl-1,4-dihydroquinoxaline-2,3-dione **(2c)**

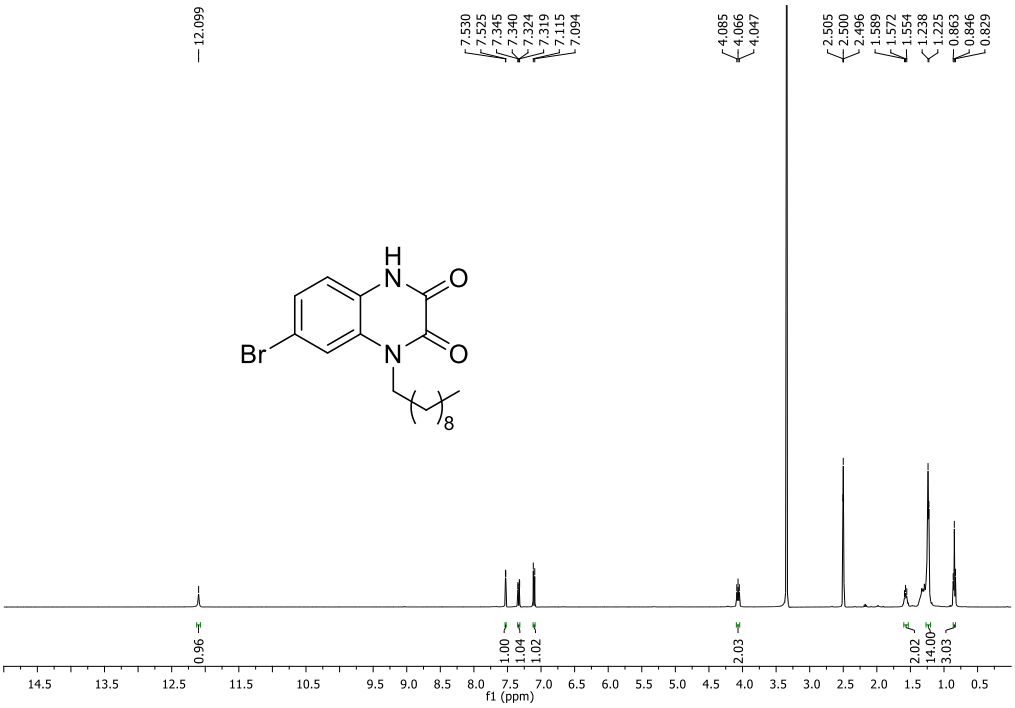

Figure S64. ^{1}H NMR (400 MHz, DMSO-d_6) of 7-bromo-1-decyl-1,4-dihydroquinoxaline-2,3-dione **(2d)**

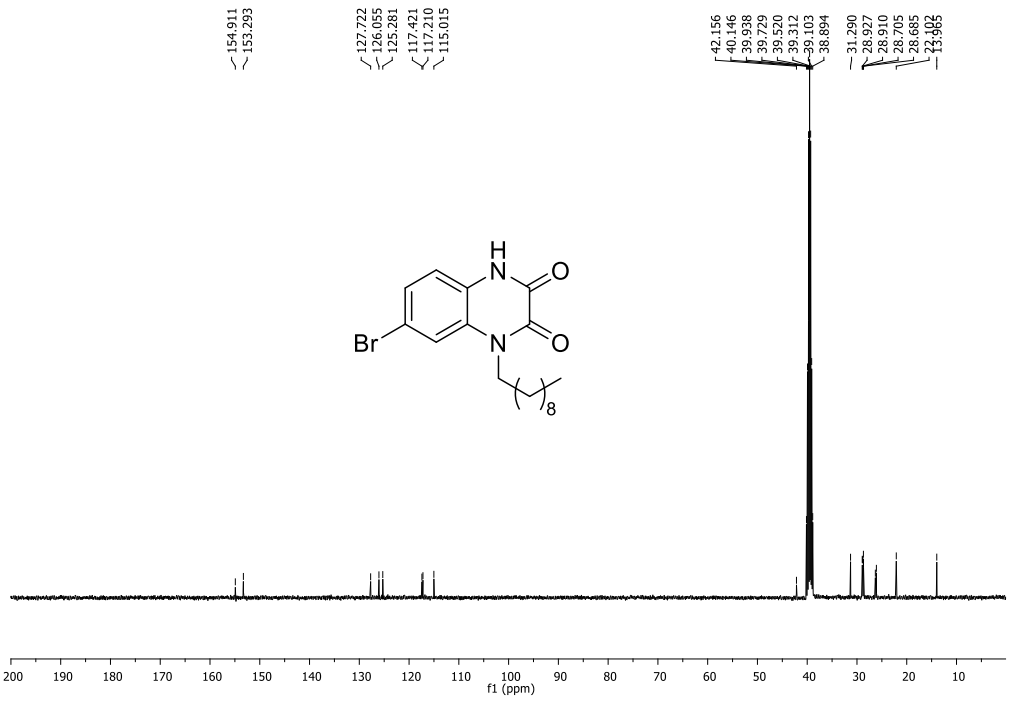

Figure S65. ^{13}C{^{1}H} NMR (100 MHz, DMSO-d_6) of 7-bromo-1-decyl-1,4-dihydroquinoxaline-2,3-dione **(2d)**

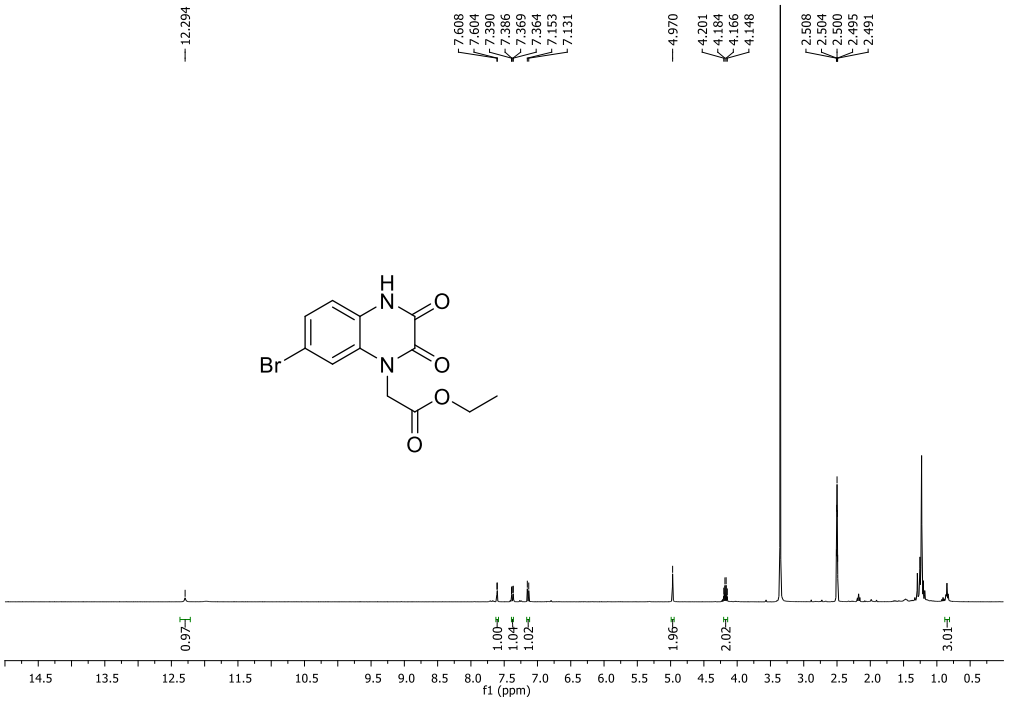

Figure S66. ^{1}H NMR (400 MHz, DMSO-d_6) of ethyl 2-(7-bromo-2,3-dioxo-3,4-dihydroquinoxalin-1(2H)-yl)acetate **(2e)**

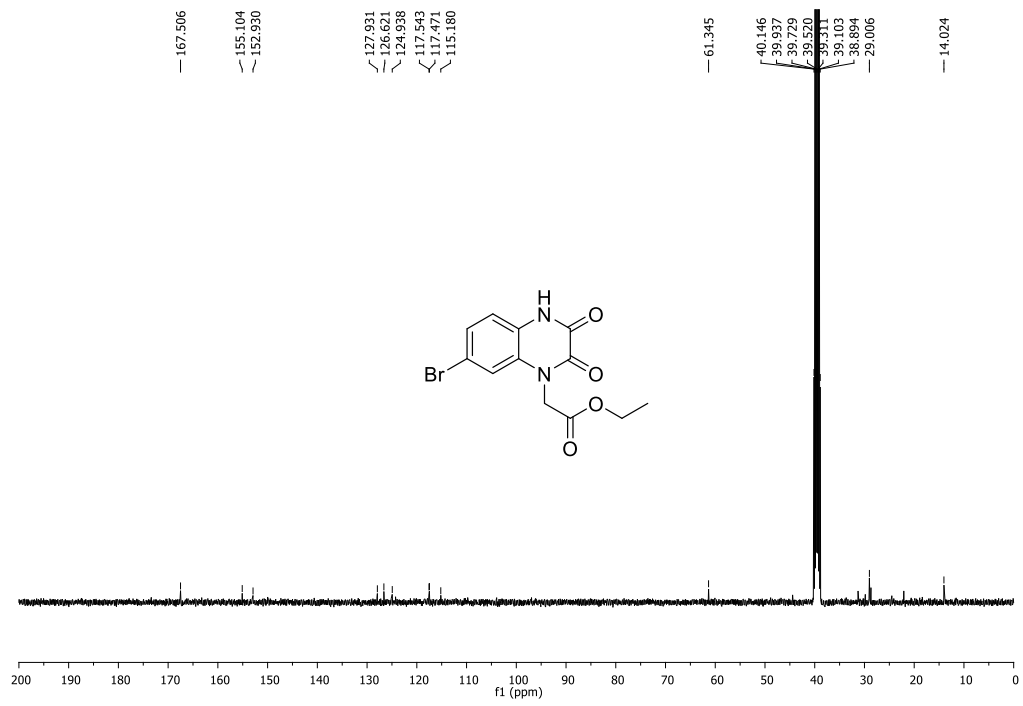

Figure S67. ^{13}C{^{1}H} NMR (100 MHz, DMSO-d_6) of ethyl 2-(7-bromo-2,3-dioxo-3,4-dihydroquinoxalin-1(2H)-yl)acetate **(2e)**

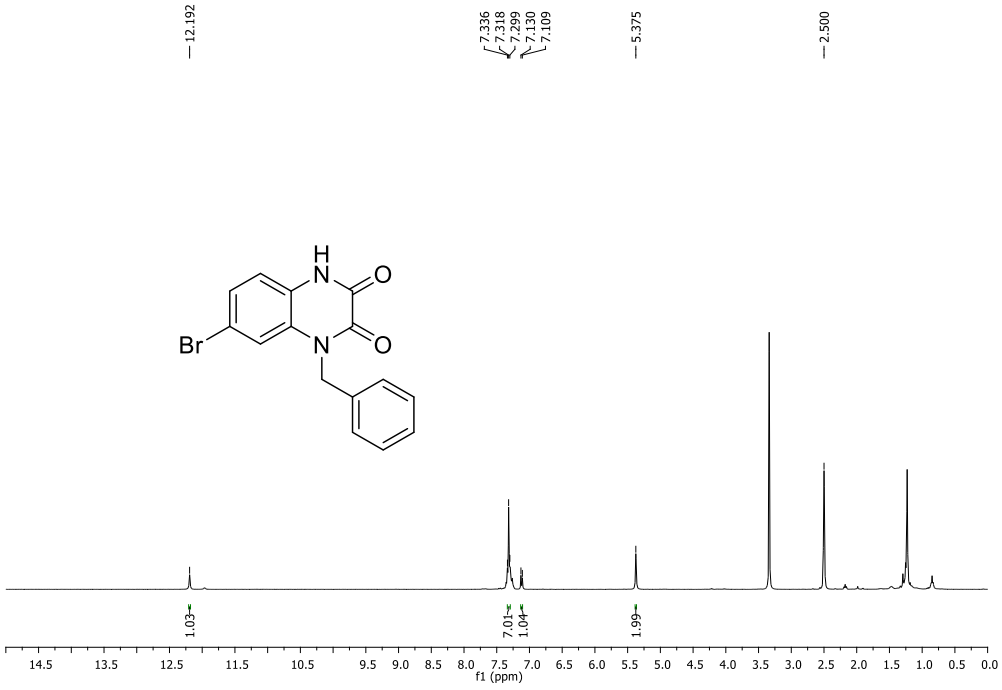

Figure S68. ^{1}H NMR (400 MHz, DMSO-d_6) of 1-benzyl-7-bromo-1,4-dihydroquinoxaline-2,3-dione **(2f)**

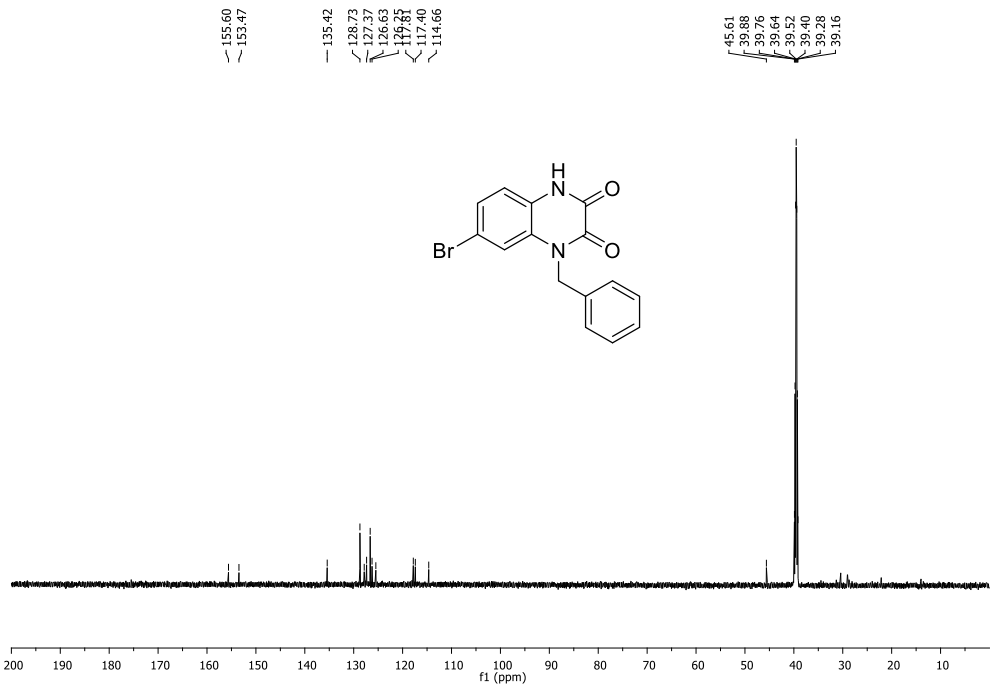

Figure S69. ^{13}C{^{1}H} NMR (175 MHz, DMSO-d_6) of 1-benzyl-7-bromo-1,4-dihydroquinoxaline-2,3-dione **(2f)**

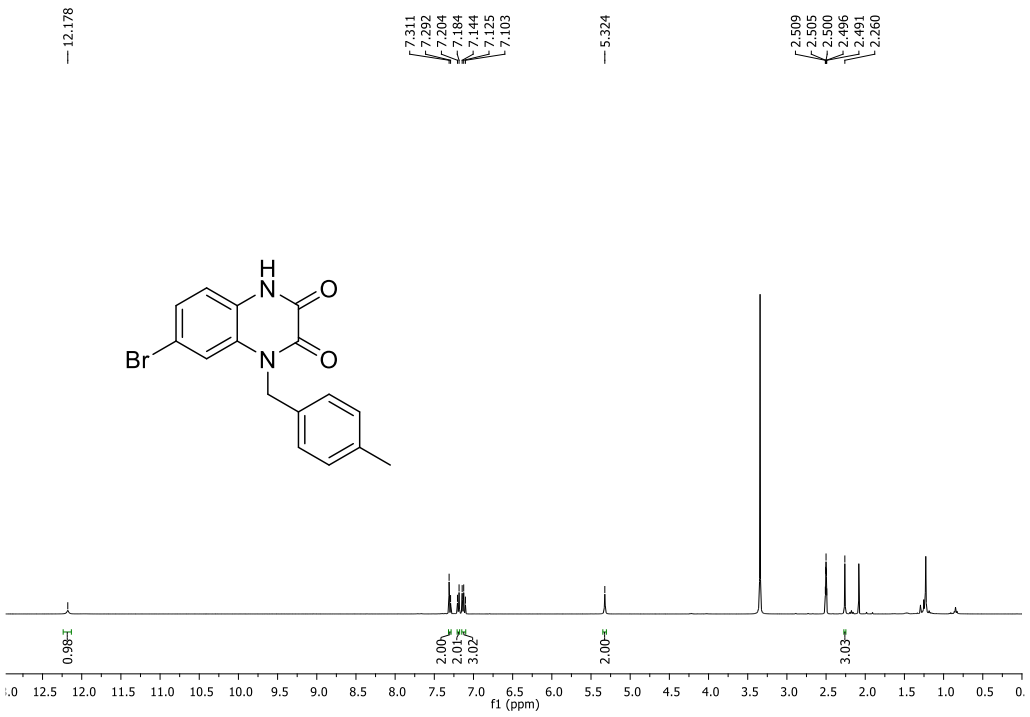

Figure S70. ^{1}H NMR (400 MHz, DMSO-d_6) of 7-bromo-1-(4-methylbenzyl)-1,4-dihydroquinoxaline-2,3-dione **(2g)**

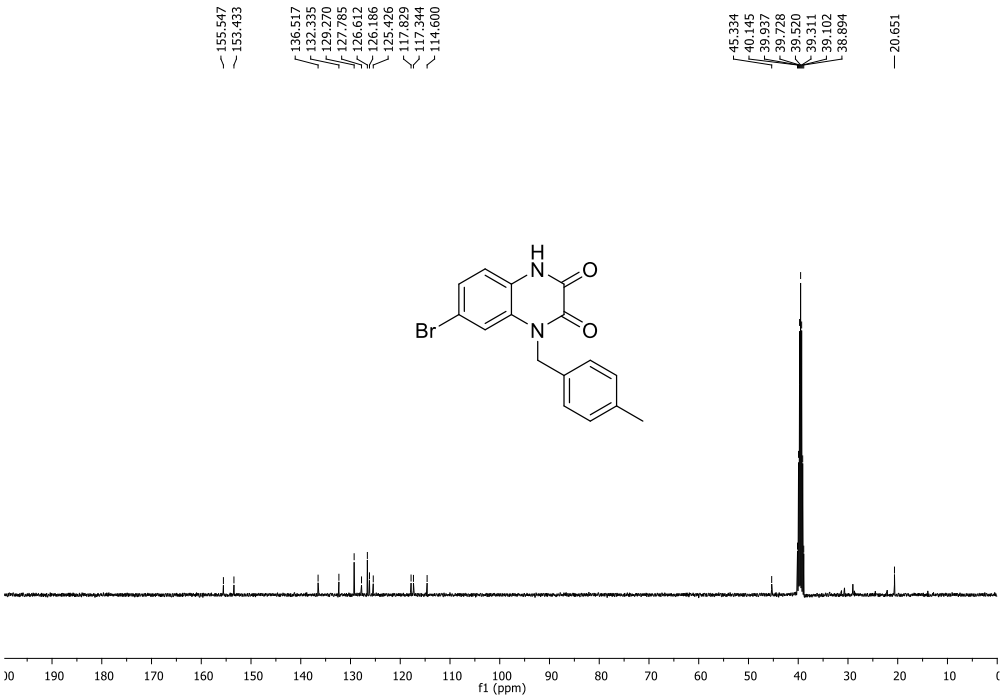

Figure S71. ^{13}C{^{1}H} NMR (100 MHz, DMSO-d_6) of 7-bromo-1-(4-methylbenzyl)-1,4-dihydroquinoxaline-2,3-dione **(2g)**

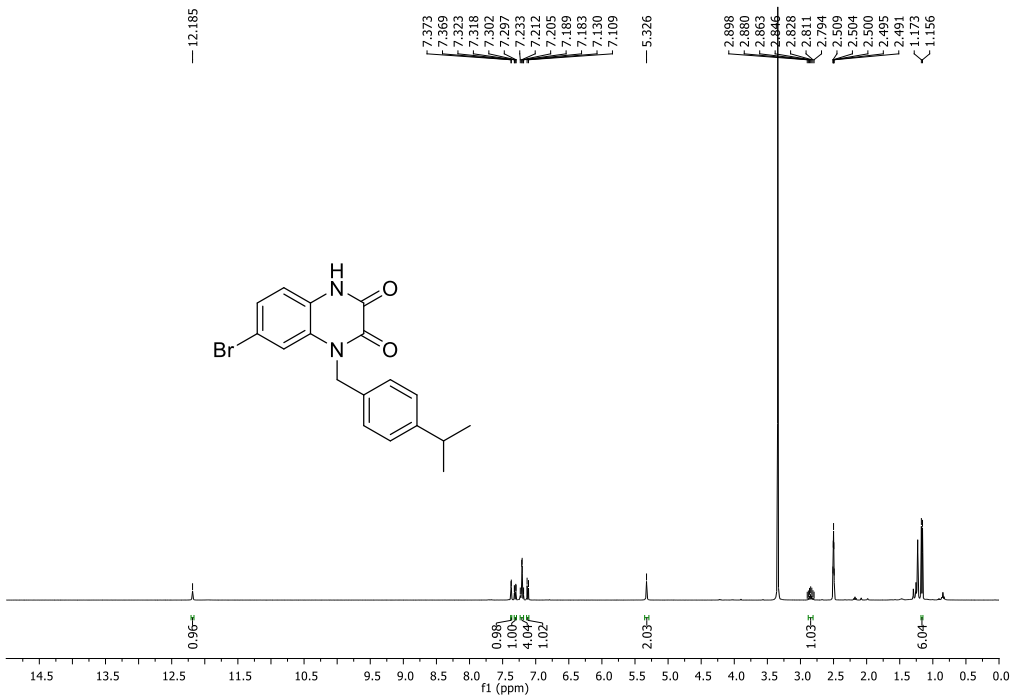

Figure S72. ^{1}H NMR (400 MHz, DMSO-d_6) of 7-bromo-1-(4-isopropylbenzyl)-1,4-dihydroquinoxaline-2,3-dione **(2h)**

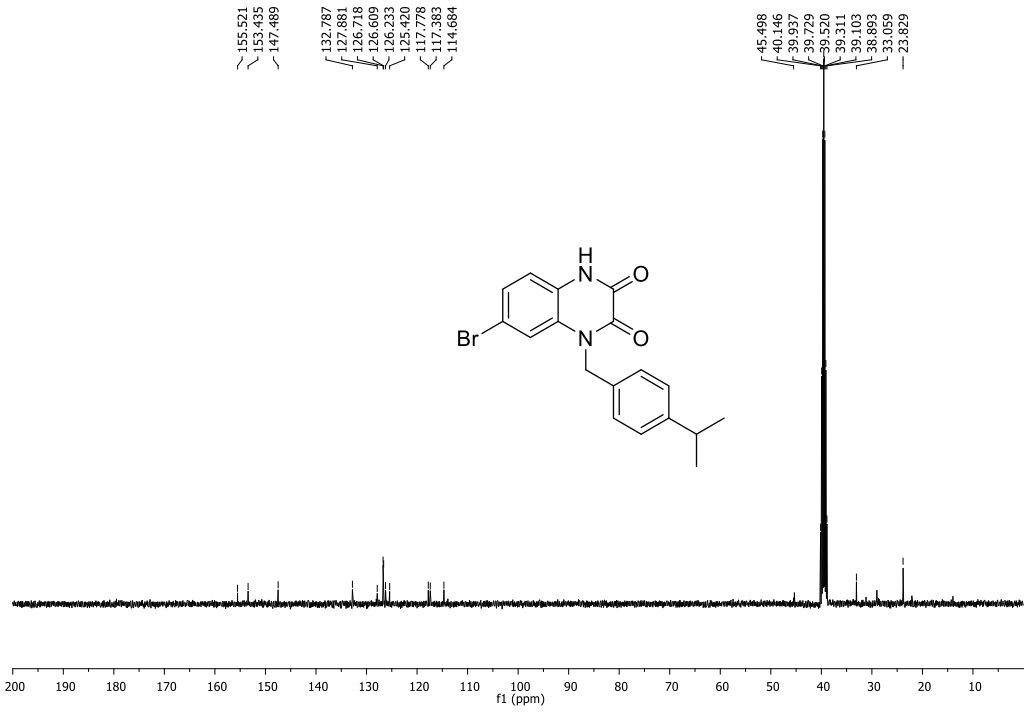

Figure S73. ^{13}C{^{1}H} NMR (100 MHz, DMSO-d_6) of 7-bromo-1-(4-isopropylbenzyl)-1,4-dihydroquinoxaline-2,3-dione **(2h)**

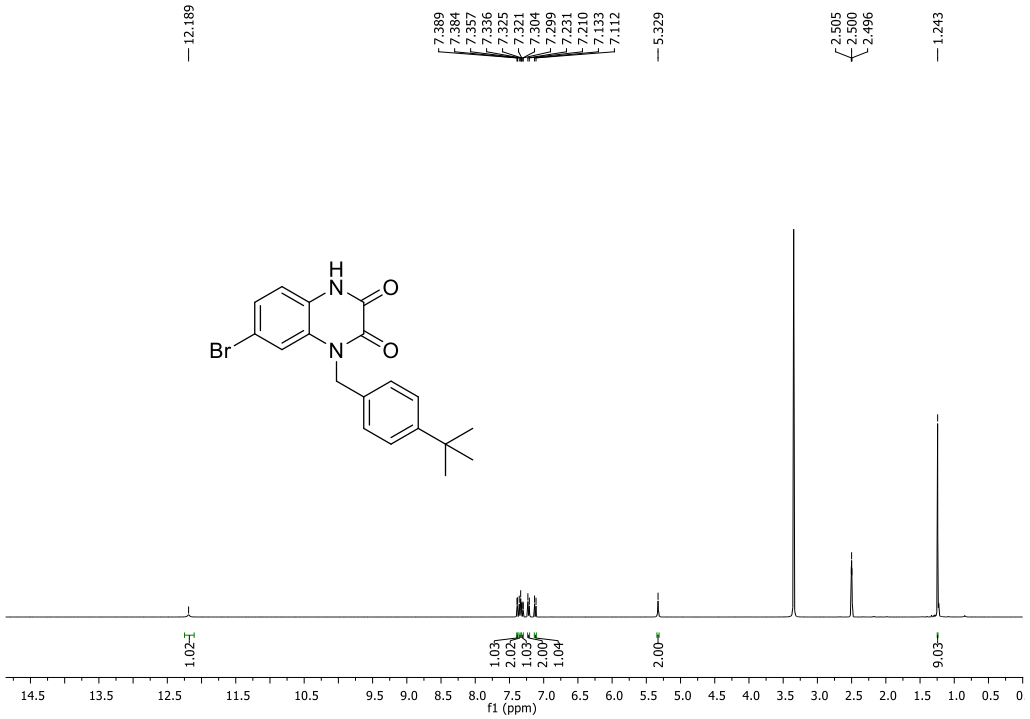

Figure S74. ^{1}H NMR (400 MHz, DMSO-d_6) of 7-bromo-1-(4-(tert-butyl)benzyl)-1,4-dihydroquinoxaline-2,3-dione **(2i)**

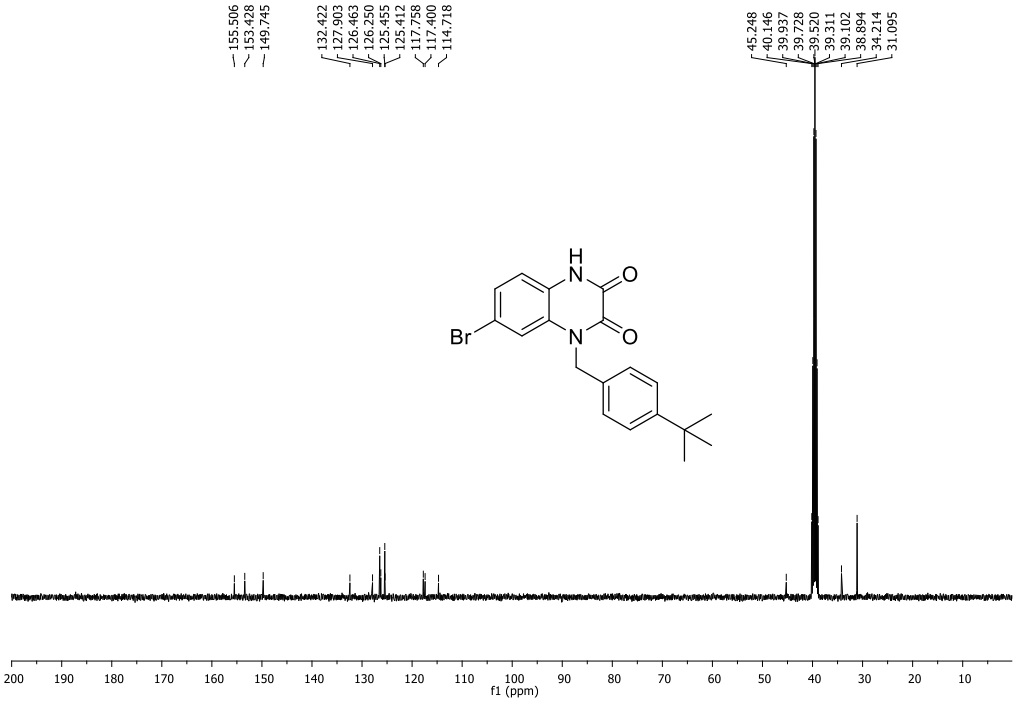

Figure S75. ^{13}C{^{1}H} NMR (100 MHz, DMSO-d_6) of 7-bromo-1-(4-(tert-butyl)benzyl)-1,4-dihydroquinoxaline-2,3-dione **(2i)**

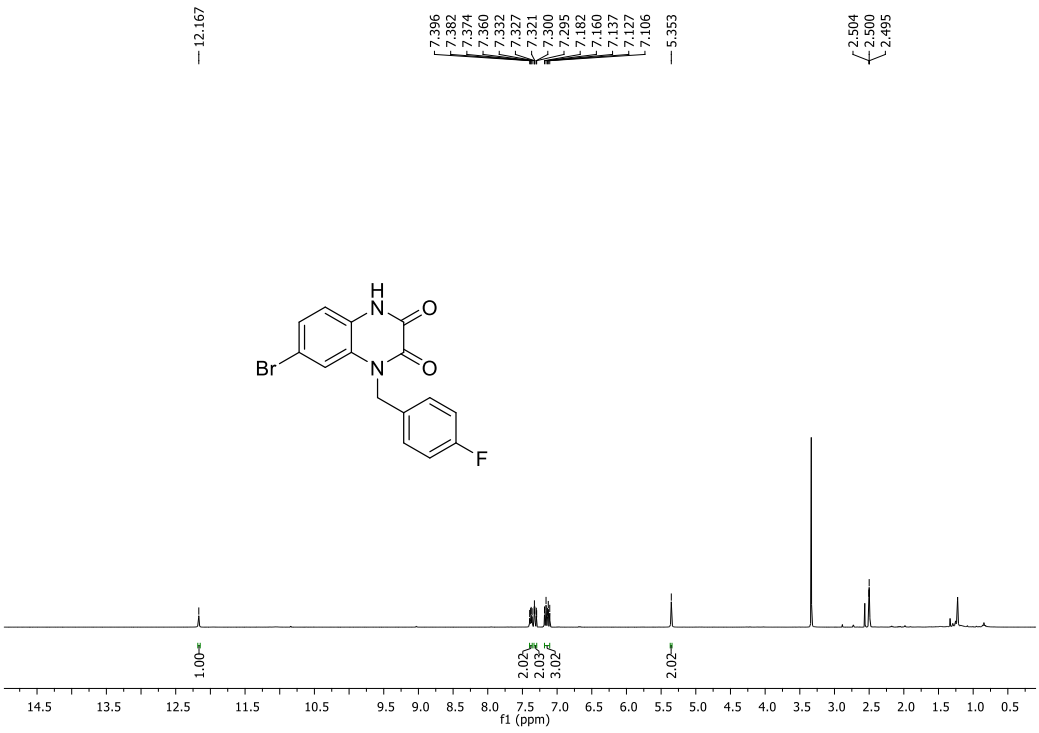

Figure S76. ^{1}H NMR (400 MHz, DMSO-d_6) of 7-bromo-1-(4-fluorobenzyl)-1,4-dihydroquinoxaline-2,3-dione **(2j)**

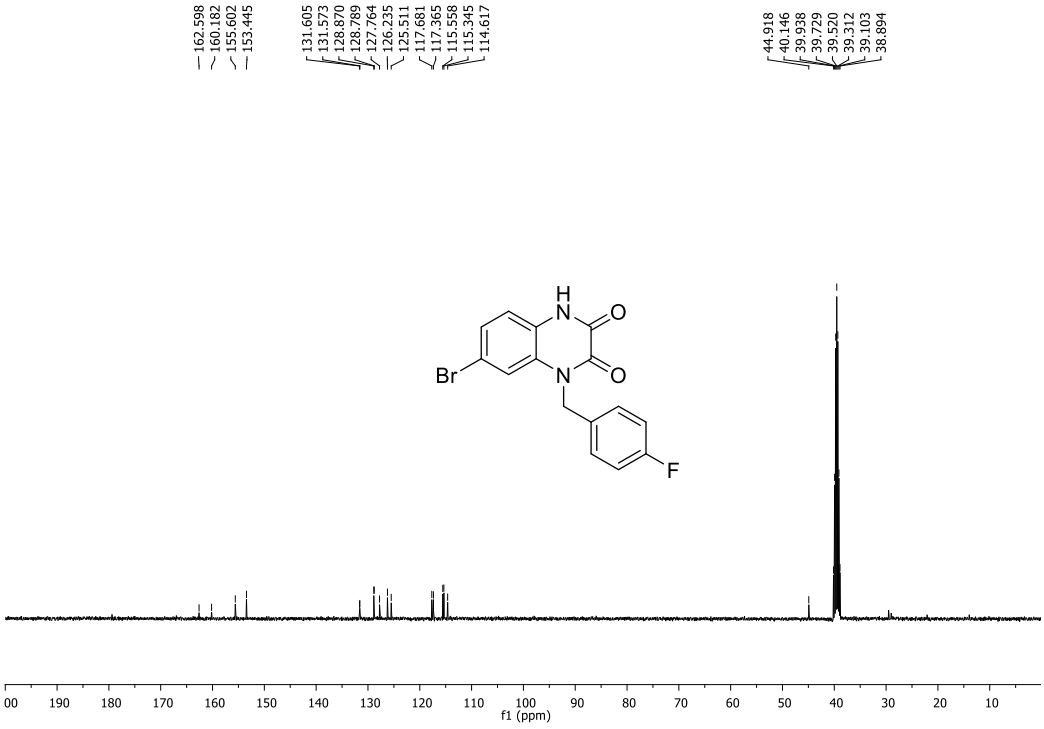

Figure S77. ^{13}C{^{1}H} NMR (100 MHz, DMSO-d_6) of 7-bromo-1-(4-fluorobenzyl)-1,4-dihydroquinoxaline-2,3-dione **(2j)**

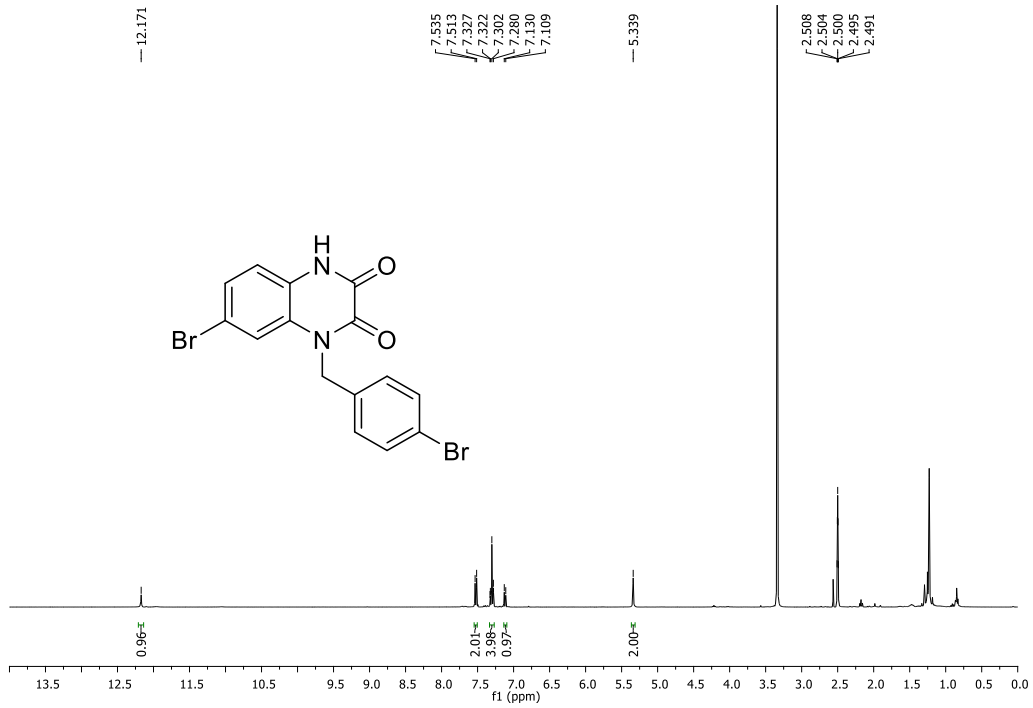

Figure S78. ^{1}H NMR (400 MHz, DMSO-d_6) of 7-bromo-1-(4-bromobenzyl)-1,4-dihydroquinoxaline-2,3-dione **(2k)**

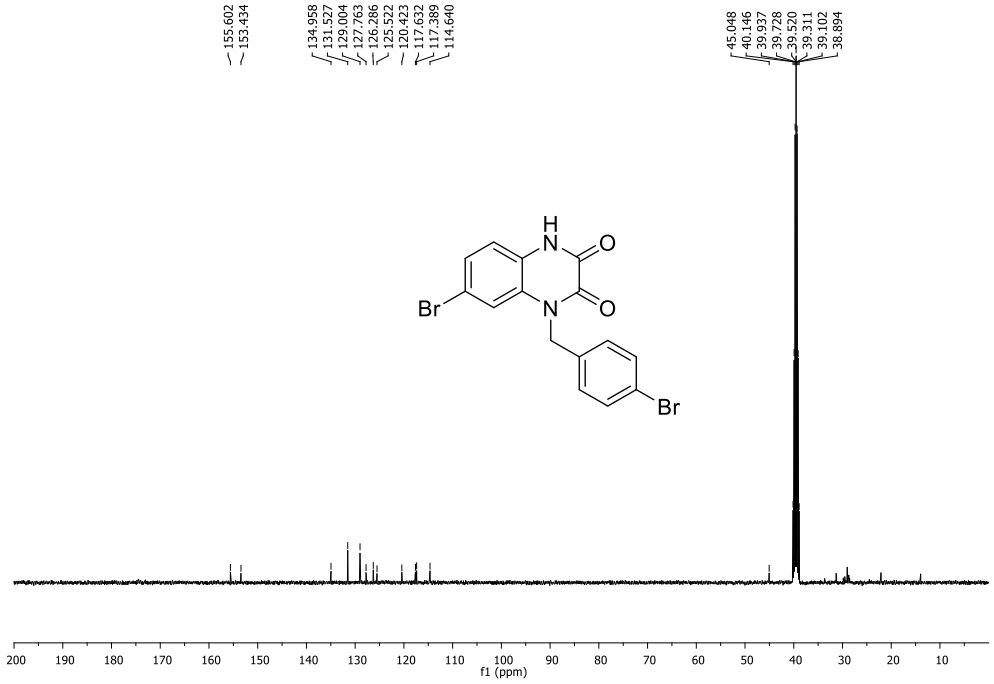

Figure S79. ^{13}C{^{1}H} NMR (100 MHz, DMSO-d_6) of 7-bromo-1-(4-bromobenzyl)-1,4-dihydroquinoxaline-2,3-dione **(2k)**

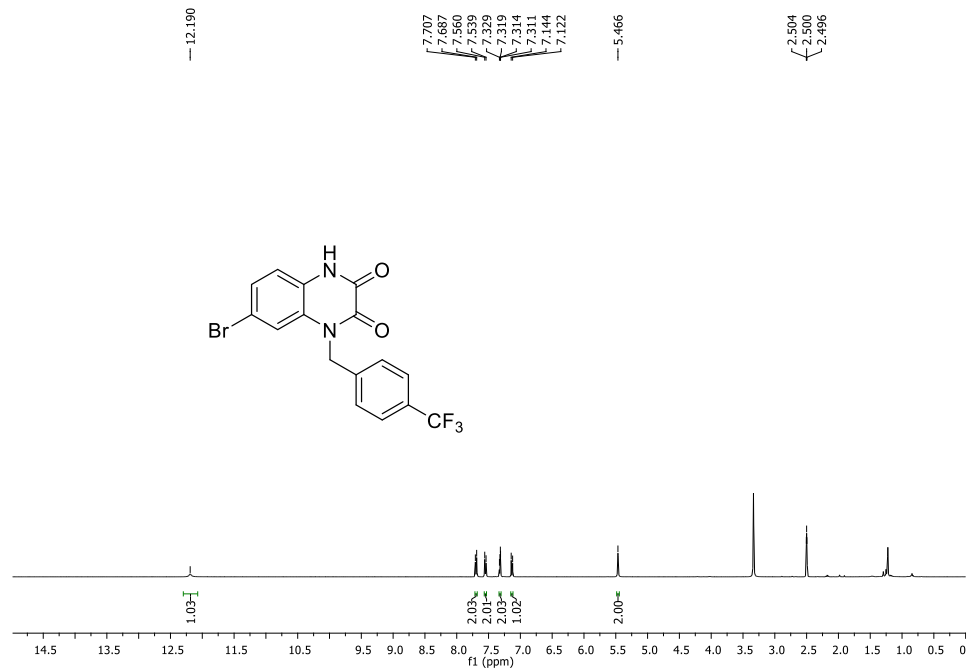

Figure S80. ^{1}H NMR (400 MHz, DMSO-d_6) of 7-bromo-1-(4-(trifluoromethyl)benzyl)-1,4-dihydroquinoxaline-2,3-dione **(2l)**

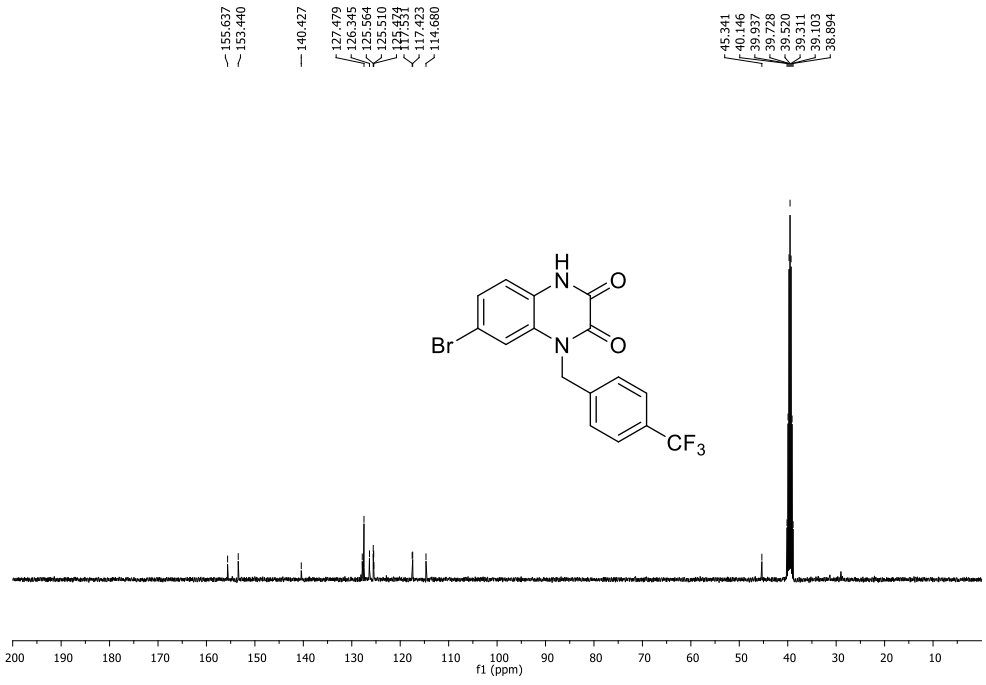

Figure S81. ^{13}C{^{1}H} NMR (100 MHz, DMSO-d_6) of 7-bromo-1-(4-(trifluoromethyl)benzyl)-1,4-dihydroquinoxaline-2,3-dione **(2l)**

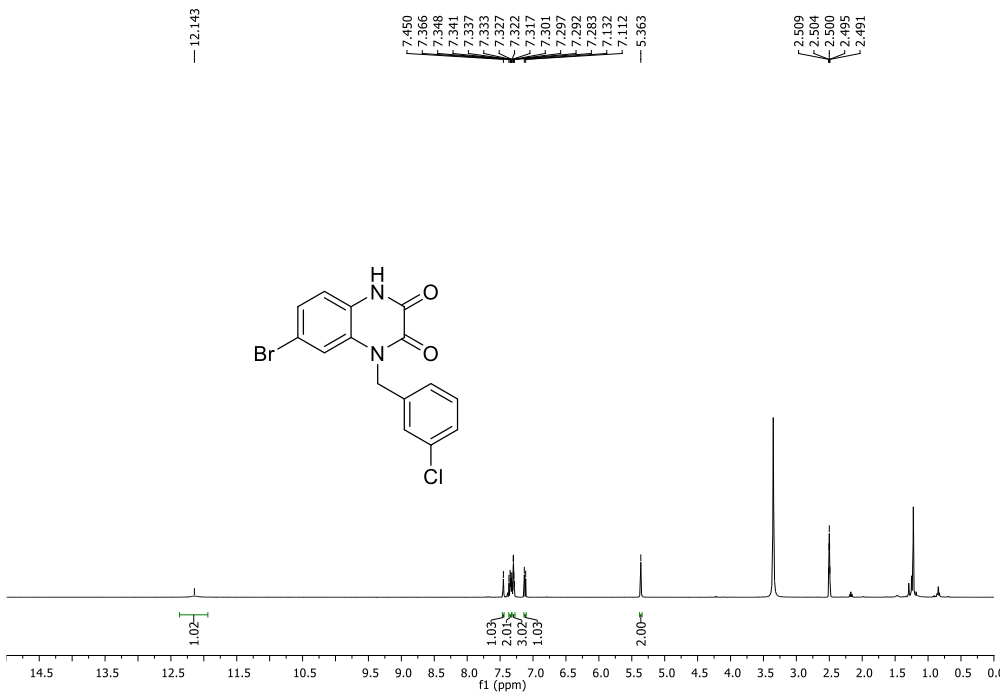

Figure S82. ^{1}H NMR (400 MHz, DMSO-d_6) of 7-bromo-1-(3-chlorobenzyl)-1,4-dihydroquinoxaline-2,3-dione **(2m)**

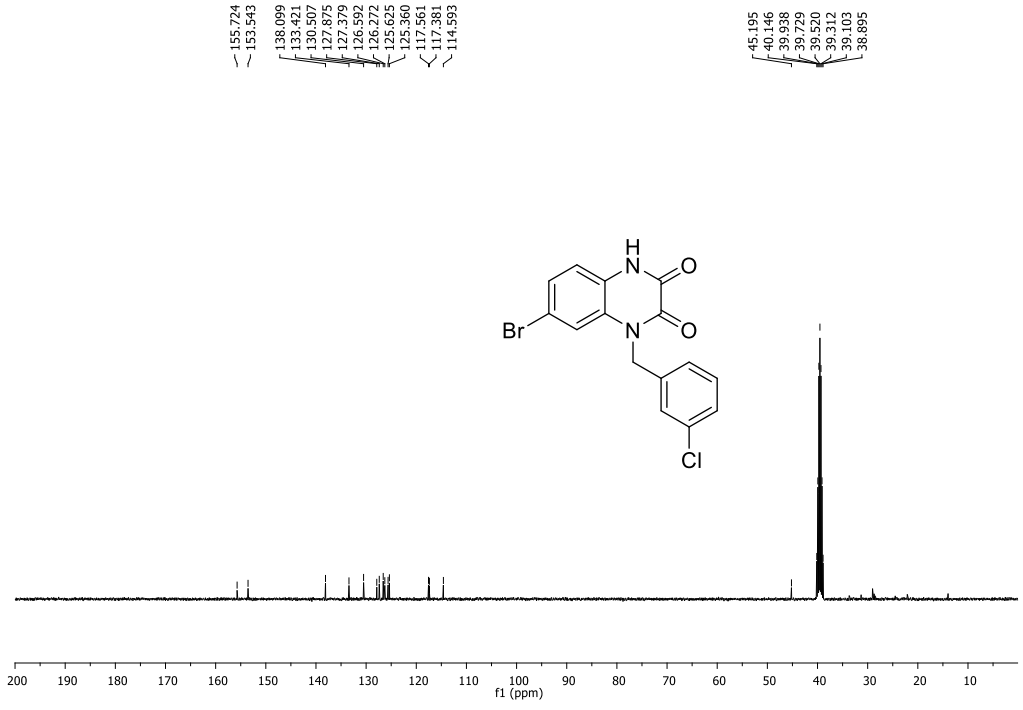

Figure S83. ^{13}C{^{1}H} NMR (100 MHz, DMSO-d_6) of 7-bromo-1-(3-chlorobenzyl)-1,4-dihydroquinoxaline-2,3-dione **(2m)**

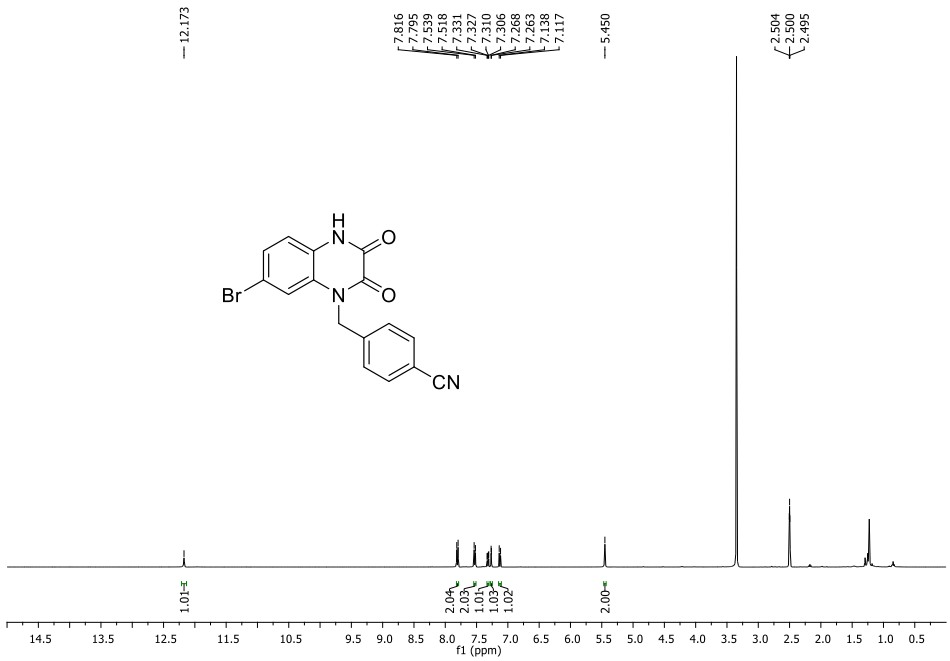

Figure S84. ^{1}H NMR (400 MHz, DMSO-d_6) of 4-((7-bromo-2,3-dioxo-3,4-dihydroquinoxalin-1(2H)-yl)methyl)benzonitrile **(2n)**

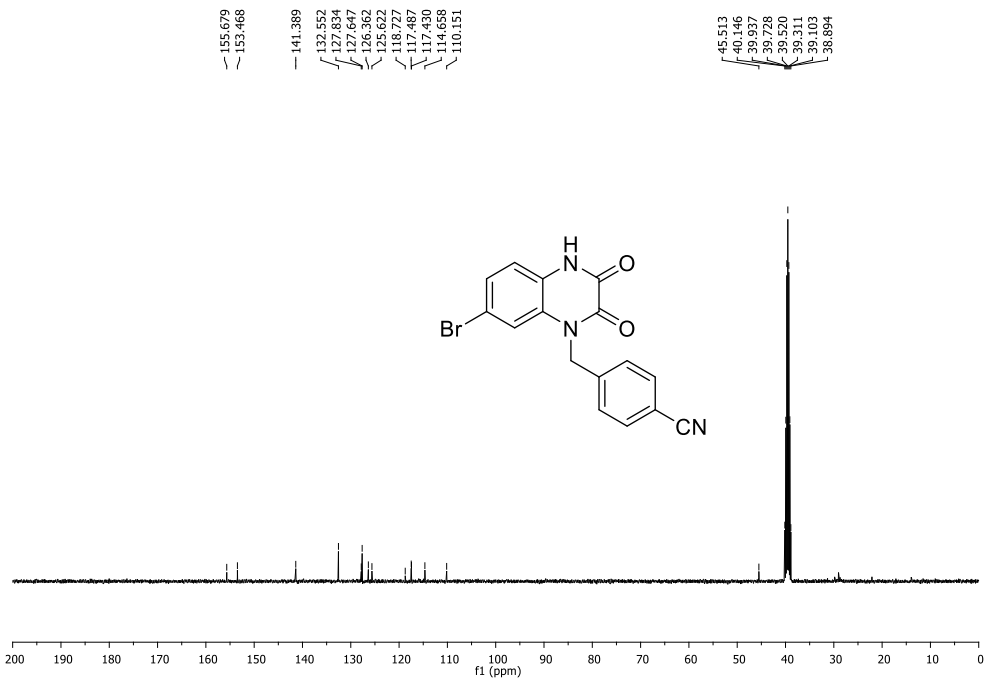

Figure S85. ^{13}C NMR {^{1}H} (100 MHz, DMSO-d_6) of 4-((7-bromo-2,3-dioxo-3,4-dihydroquinoxalin-1(2H)-yl)methyl)benzonitrile **(2n)**

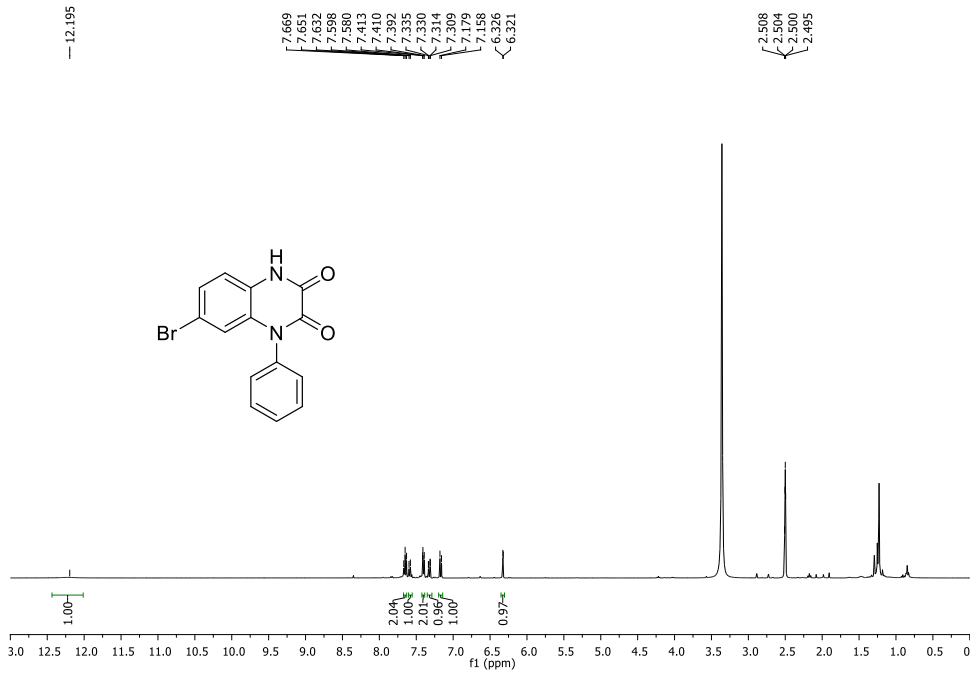

Figure S86. ^{1}H NMR (400 MHz, DMSO-d_6) of 7-bromo-1-phenyl-1,4-dihydroquinoxaline-2,3-dione **(2o)**

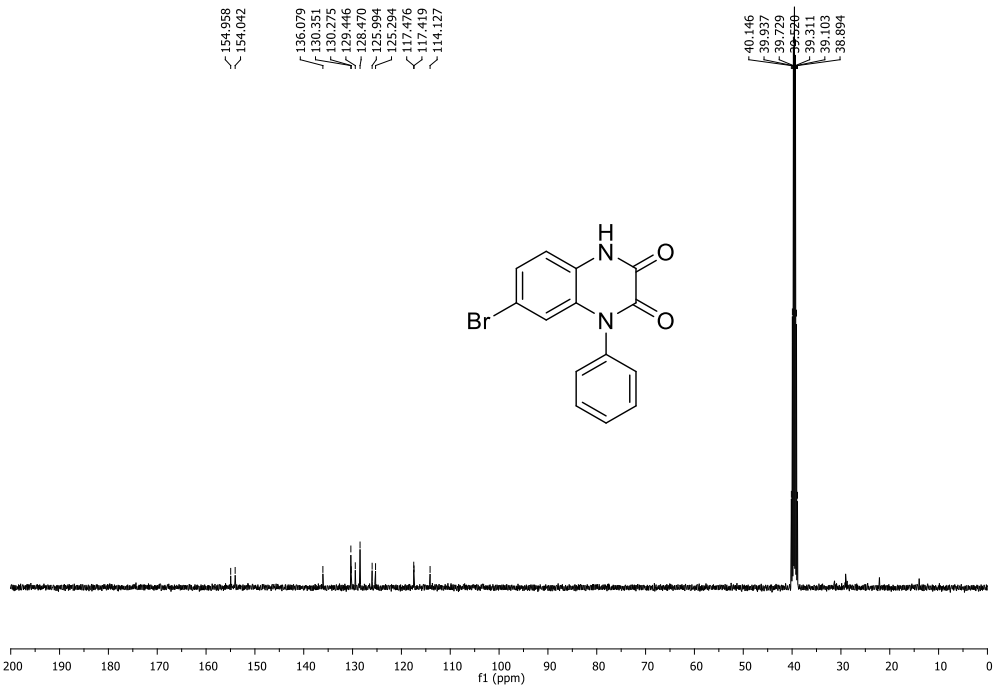

Figure S87. ^{13}C{^{1}H} NMR (100 MHz, DMSO-d_6) of 7-bromo-1-phenyl-1,4-dihydroquinoxaline-2,3-dione **(2o)**

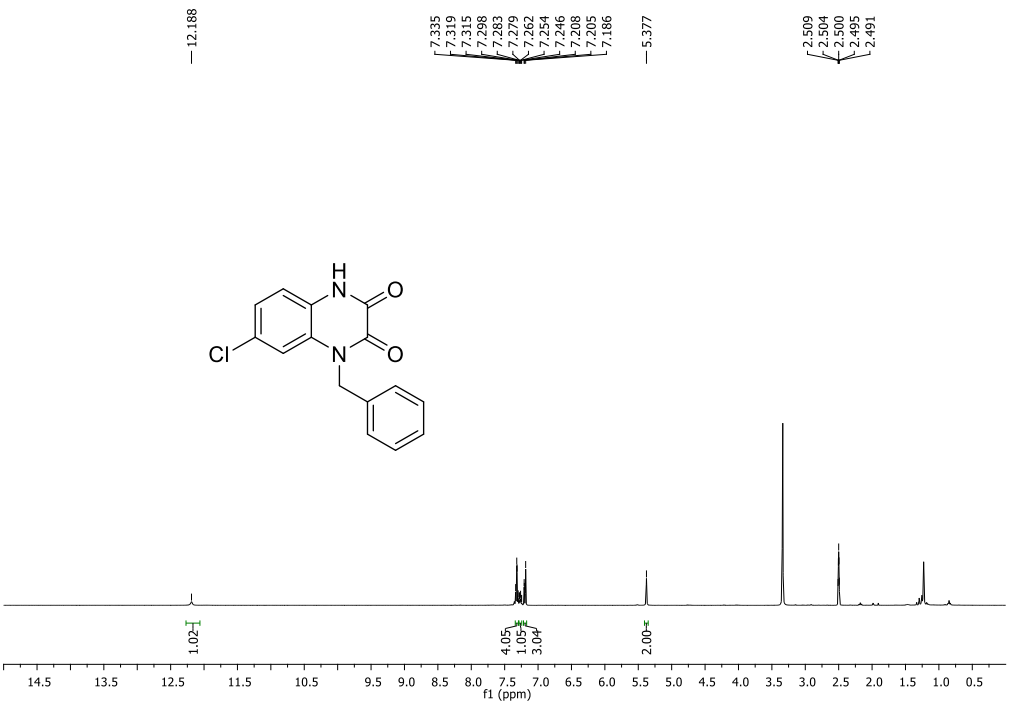

Figure S88. ^{1}H NMR (400 MHz, DMSO-d_6) of 1-benzyl-7-chloro-1,4-dihydroquinoxaline-2,3-dione **(2a')**

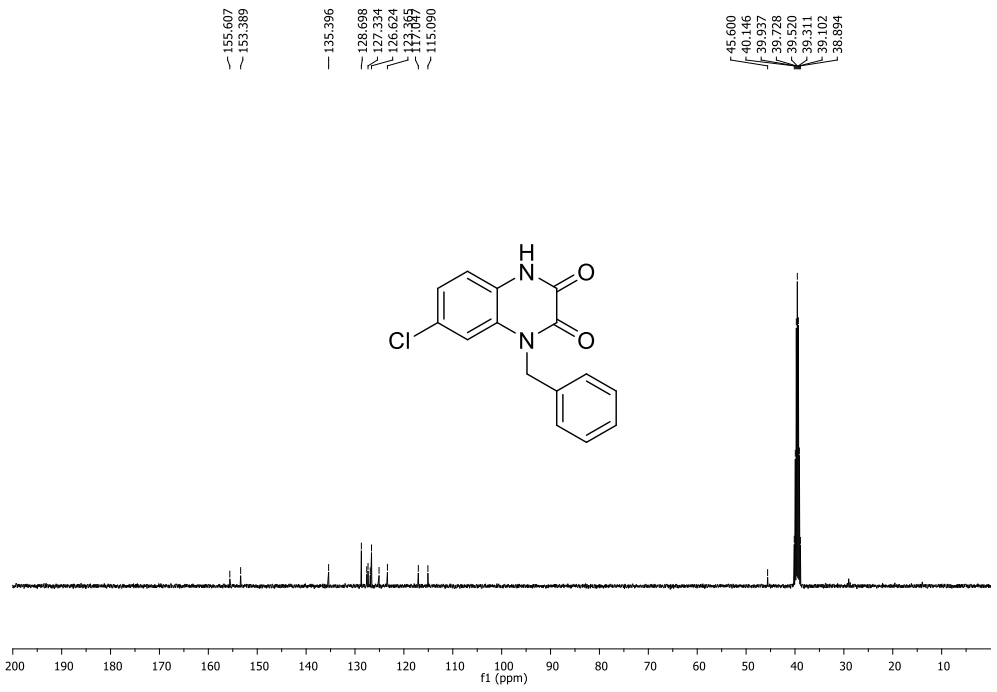

Figure S89. ^{13}C{^{1}H} NMR (100 MHz, DMSO-d_6) of 1-benzyl-7-chloro-1,4-dihydroquinoxaline-2,3-dione **(2a')**

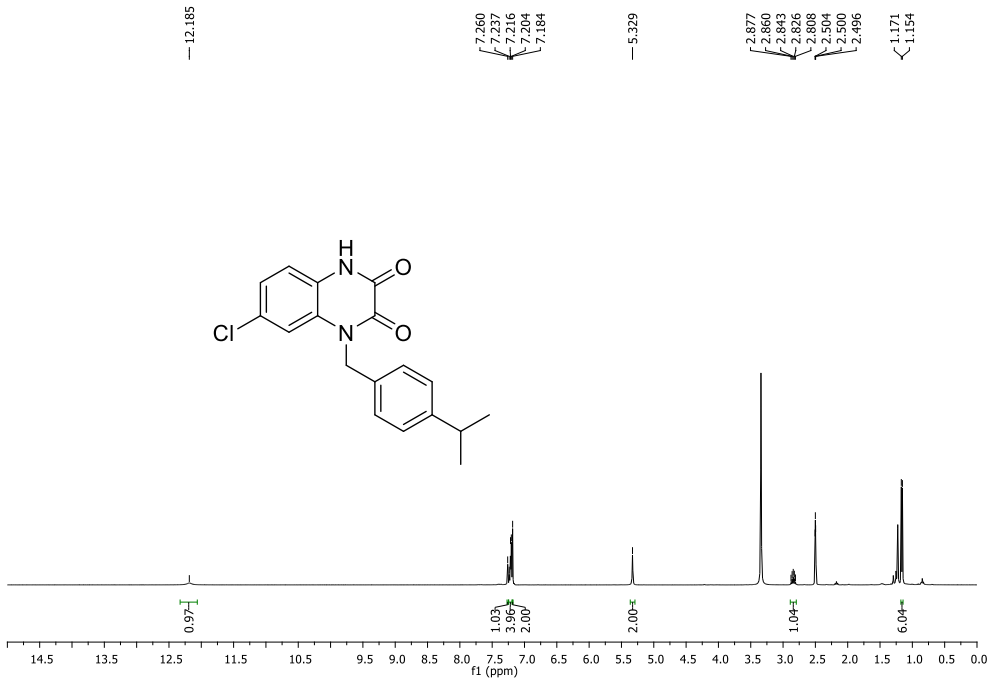

Figure S90. ^{1}H NMR (400 MHz, DMSO-d_6) of 7-chloro-1-(4-isopropylbenzyl)-1,4-dihydroquinoxaline-2,3-dione **(2b')**

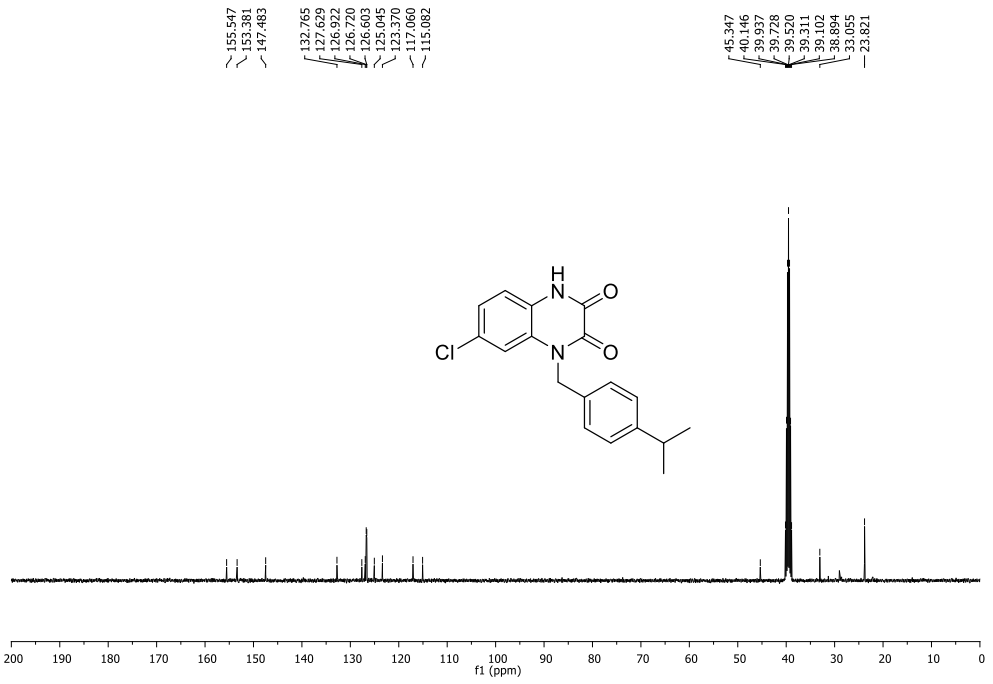

Figure S91. ^{13}C{^{1}H} NMR (100 MHz, DMSO-d_6) of 7-chloro-1-(4-isopropylbenzyl)-1,4-dihydroquinoxaline-2,3-dione **(2b')**

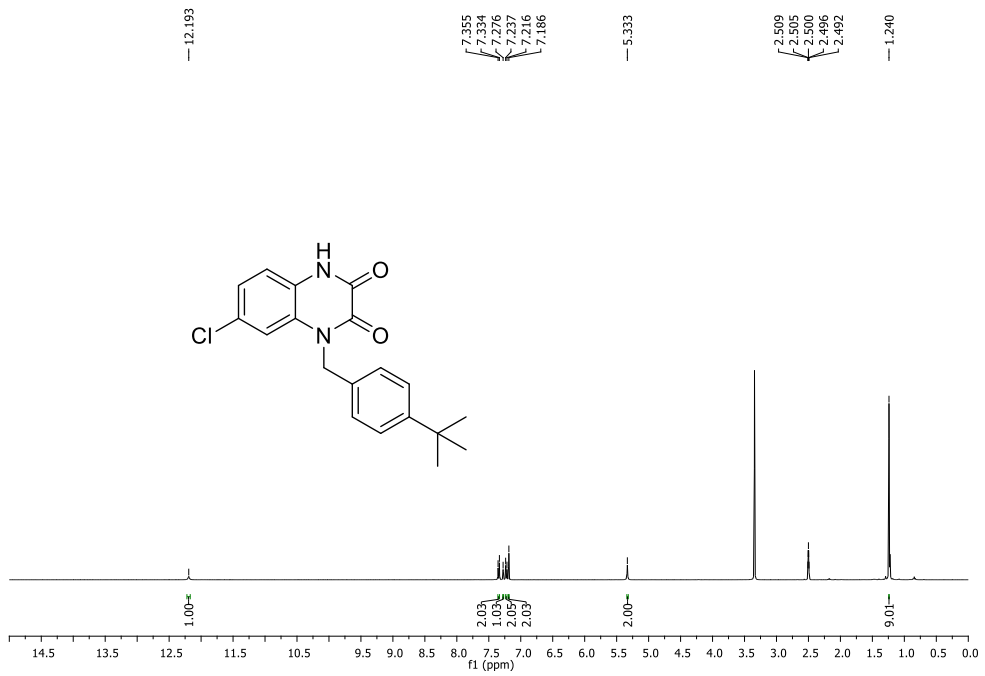

Figure S92. ^{1}H NMR (400 MHz, DMSO-d_6) of 1-(4-(tert-butyl)benzyl)-7-chloro-1,4-dihydroquinoxaline-2,3-dione **(2c')**

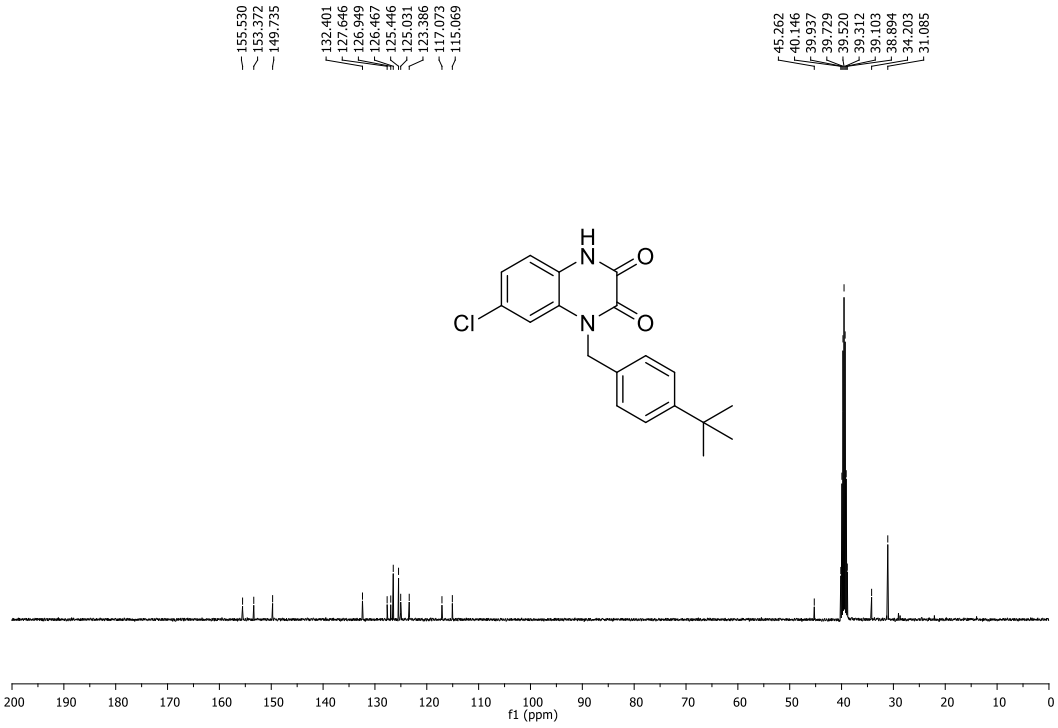

Figure S93. ^{13}C{^{1}H} NMR (100 MHz, DMSO-d_6) of 1-(4-(tert-butyl)benzyl)-7-chloro-1,4-dihydroquinoxaline-2,3-dione **(2c')**

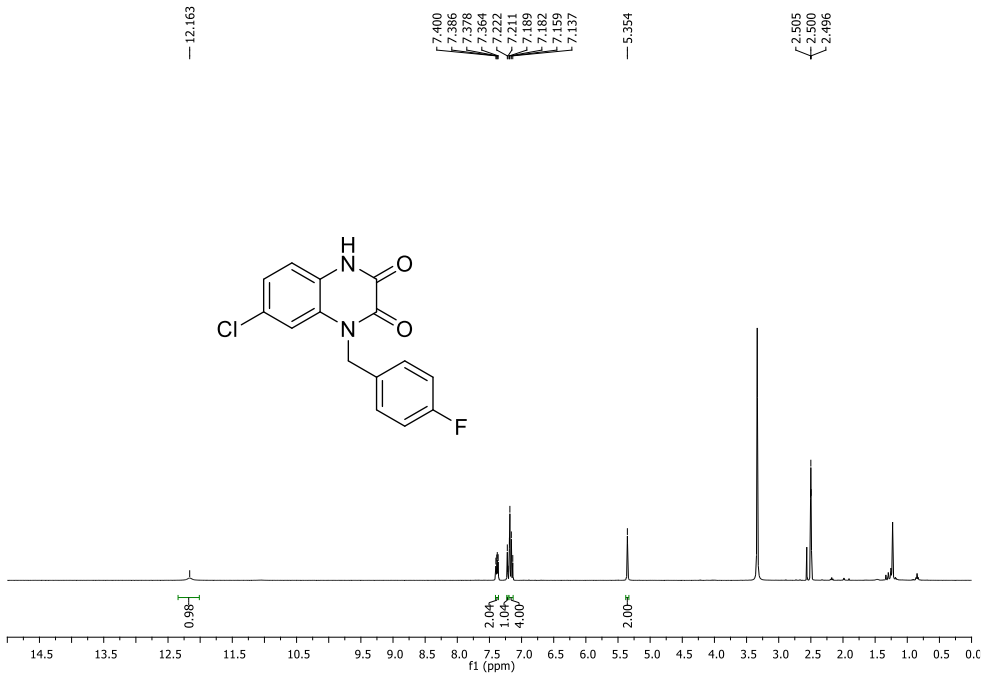

Figure S94. ^{1}H NMR (400 MHz, DMSO-d_6) of 7-chloro-1-(4-fluorobenzyl)-1,4-dihydroquinoxaline-2,3-dione **(2d')**

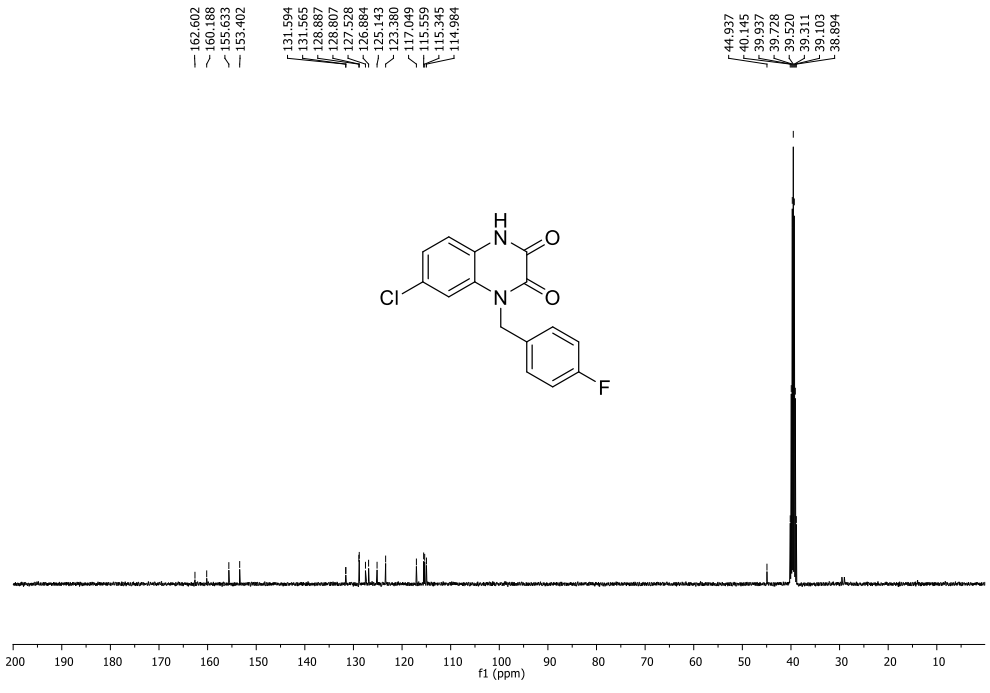

Figure S95. ^{13}C{^{1}H} NMR (100 MHz, DMSO-d_6) of 7-chloro-1-(4-fluorobenzyl)-1,4-dihydroquinoxaline-2,3-dione **(2d')**

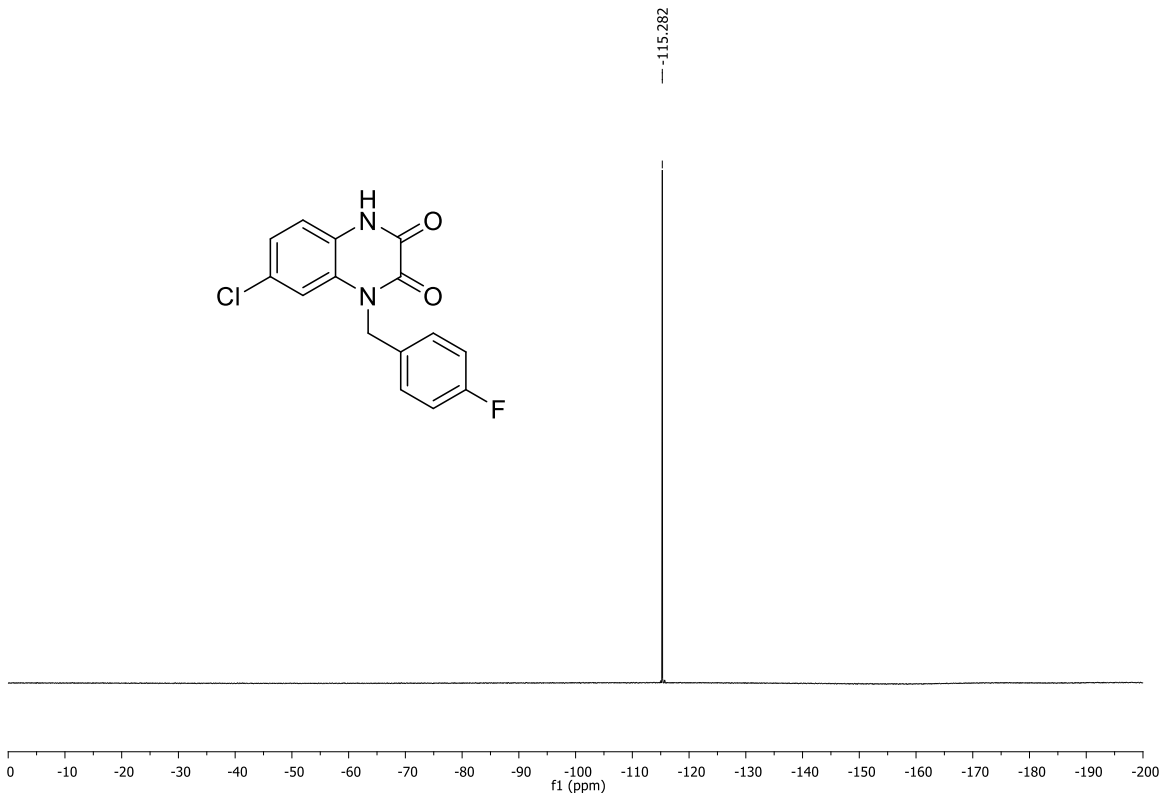

Figure S96. ^{19}F NMR (375 MHz, DMSO-d_6) of 7-chloro-1-(4-fluorobenzyl)-1,4-dihydroquinoxaline-2,3-dione **(2d')**

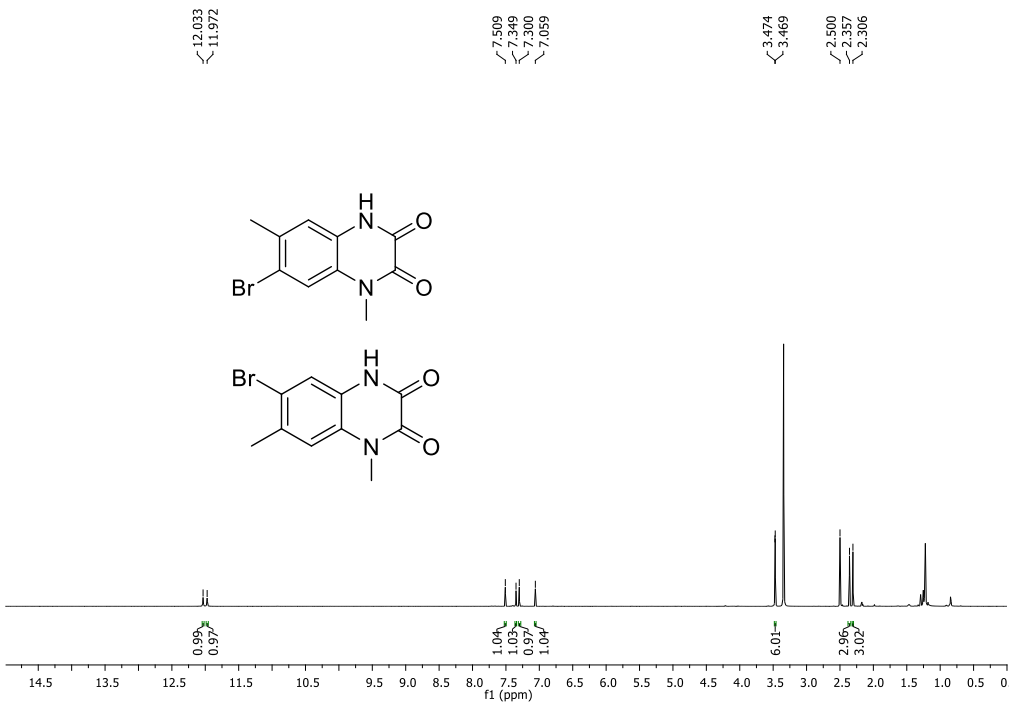

Figure S97. ^{1}H NMR (700 MHz, DMSO-d_6) of 7-bromo-1,6-dimethyl-1,4-dihydroquinoxaline-2,3-dione **(2t)**

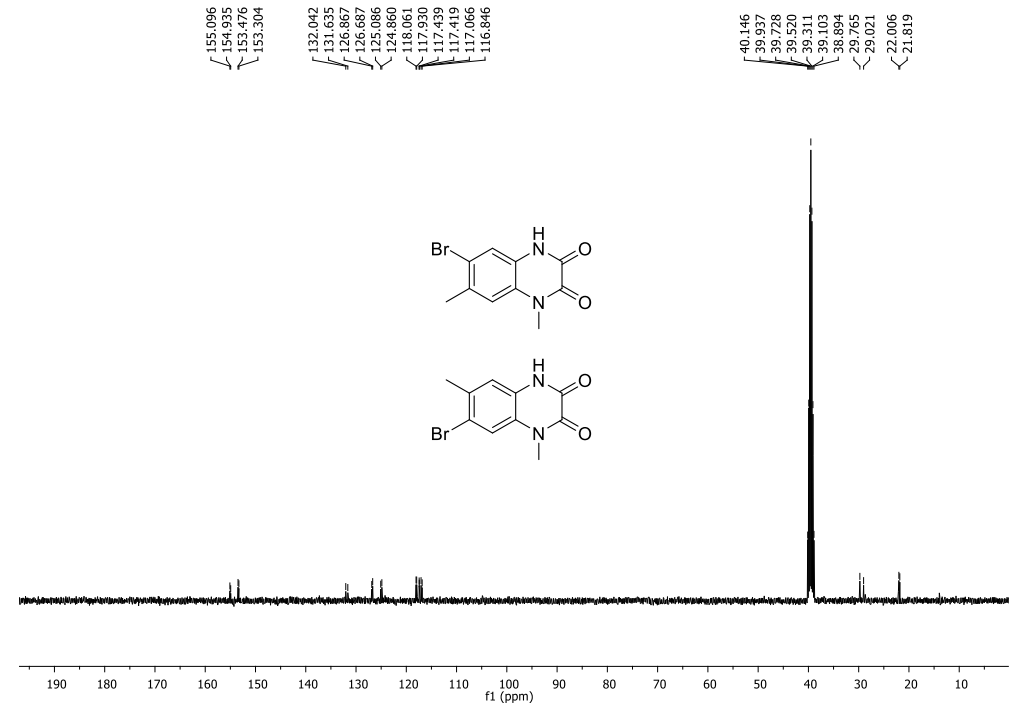

Figure S98. ^{13}C{^{1}H} NMR (100 MHz, DMSO-d_6) of 7-bromo-1,6-dimethyl-1,4-dihydroquinoxaline-2,3-dione **(2t)**

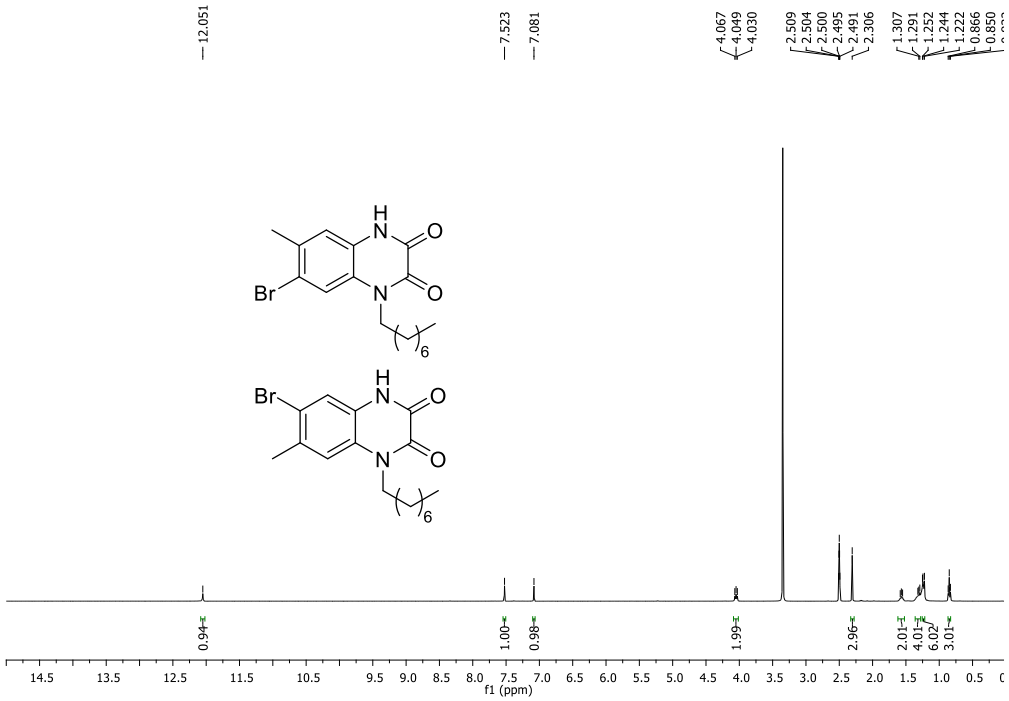

Figure S99. ^{1}H NMR (400 MHz, DMSO-d_6) of 7-bromo-6-methyl-1-octyl-1,4-dihydroquinoxaline-2,3-dione **(2u)**

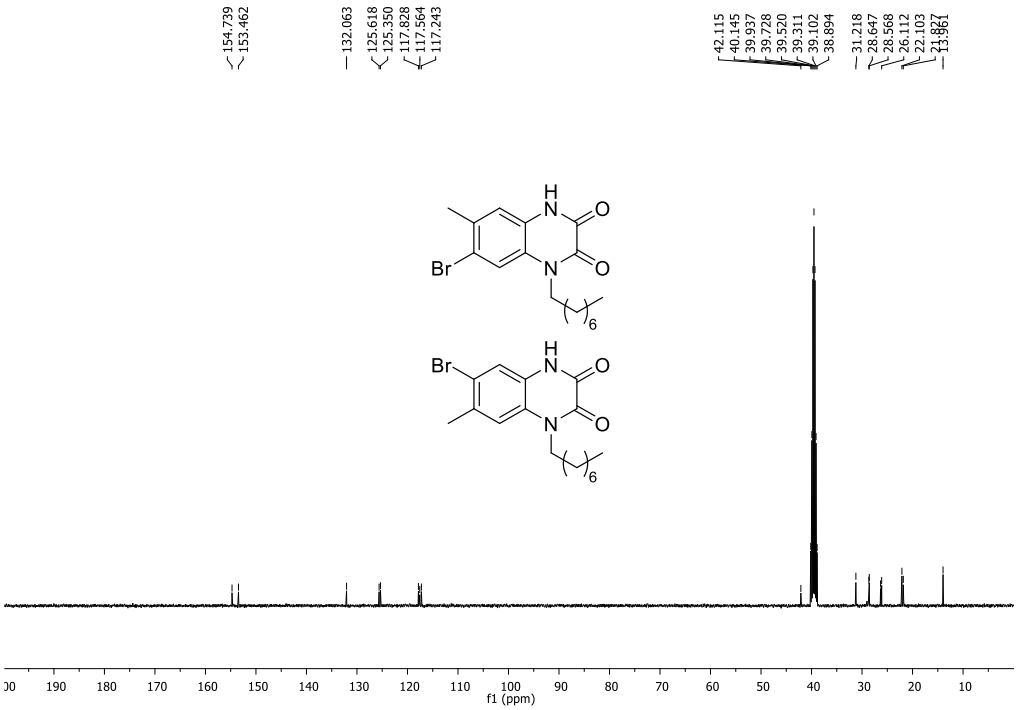

Figure S100. ^{13}C{^{1}H} NMR (100 MHz, DMSO-d_6) of 7-bromo-6-methyl-1-octyl-1,4-dihydroquinoxaline-2,3-dione **(2u)**

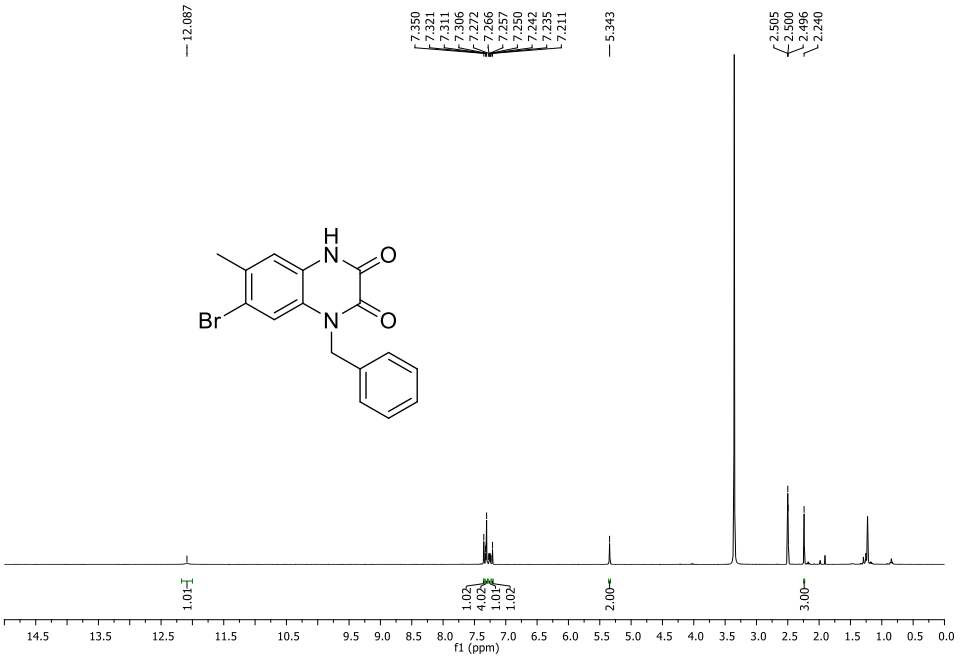

Figure S101. ^{1}H NMR (400 MHz, DMSO-d_6) of 1-benzyl-7-bromo-6-methyl-1,4-dihydroquinoxaline-2,3-dione **(2v)**

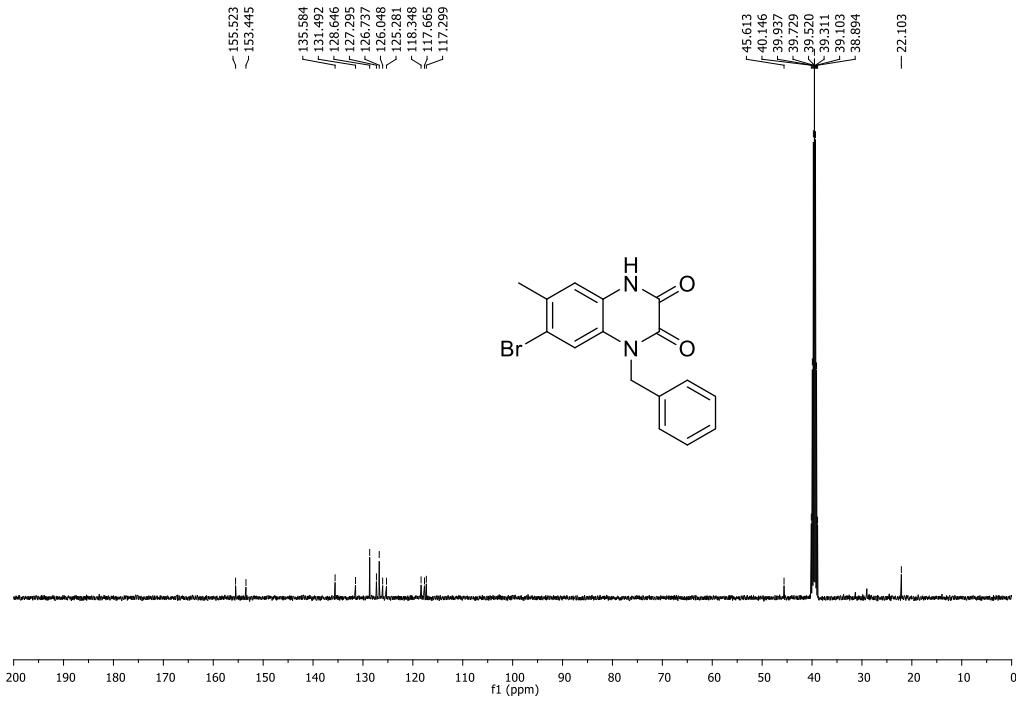

Figure S102. ^{13}C{^{1}H} NMR (100 MHz, DMSO-d_6) of 1-benzyl-7-bromo-6-methyl-1,4-dihydroquinoxaline-2,3-dione **(2v)**

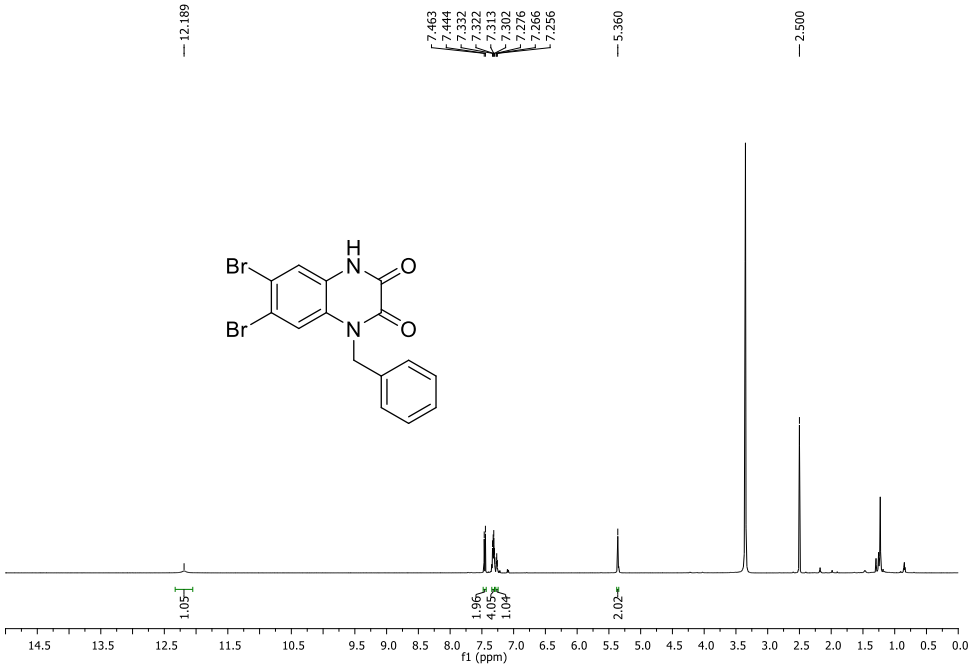

Figure S103. ^{1}H NMR (700 MHz, DMSO-d_6) of 1-benzyl-6,7-dibromo-1,4-dihydroquinoxaline-2,3-dione **(2w)**

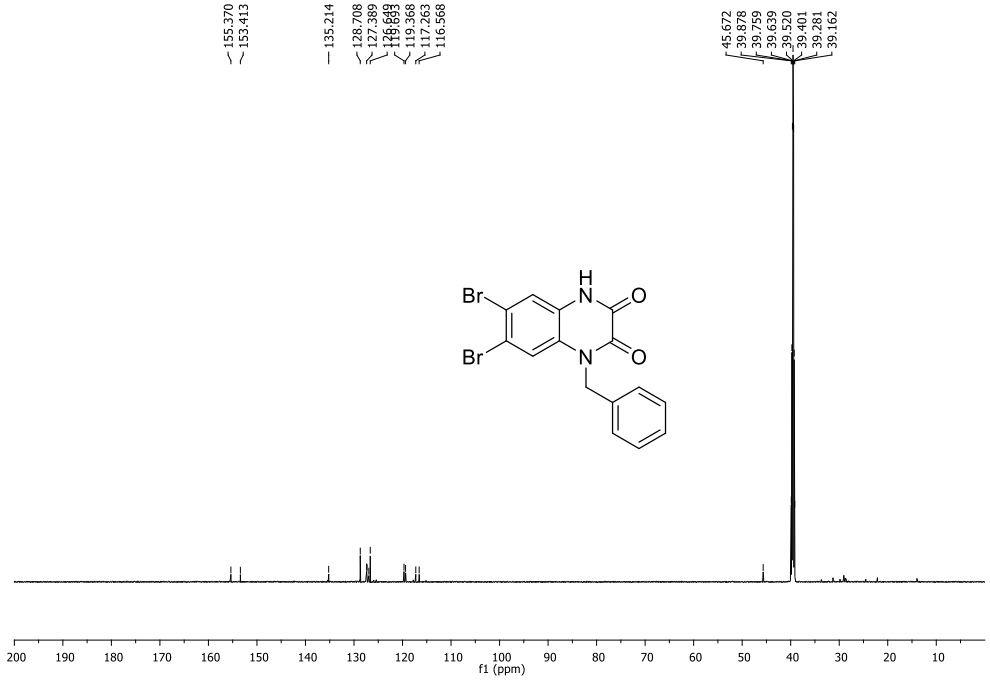

Figure S104. ^{13}C{^{1}H} NMR (175 MHz, DMSO-d_6) of 1-benzyl-6,7-dibromo-1,4-dihydroquinoxaline-2,3-dione **(2w)**

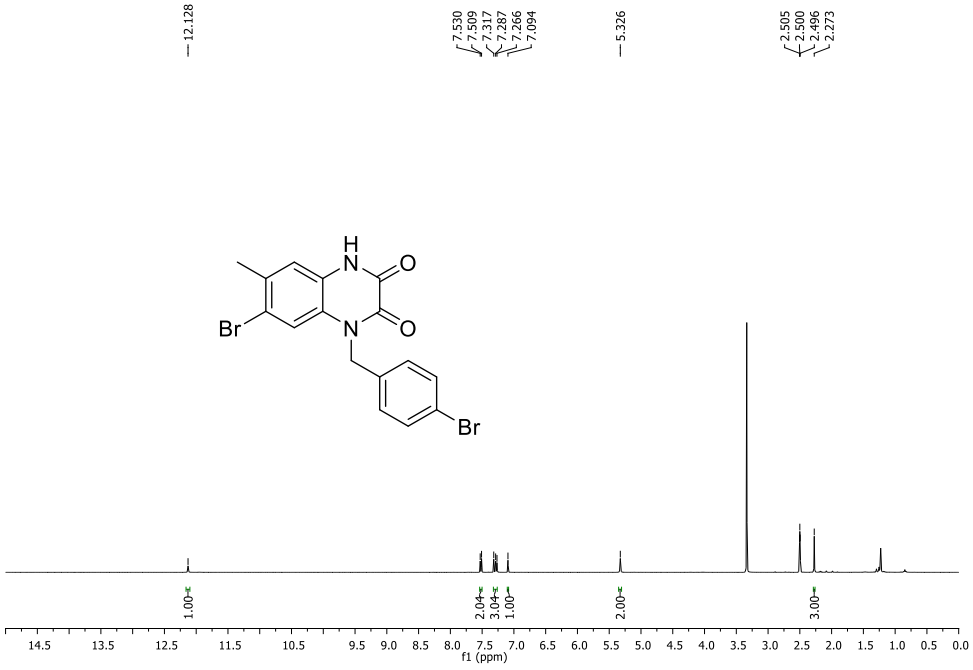

Figure S105. ^{1}H NMR (400 MHz, DMSO-d_6) of 7-bromo-1-(4-bromobenzyl)-6-methyl-1,4-dihydroquinoxaline-2,3-dione **(2x)**

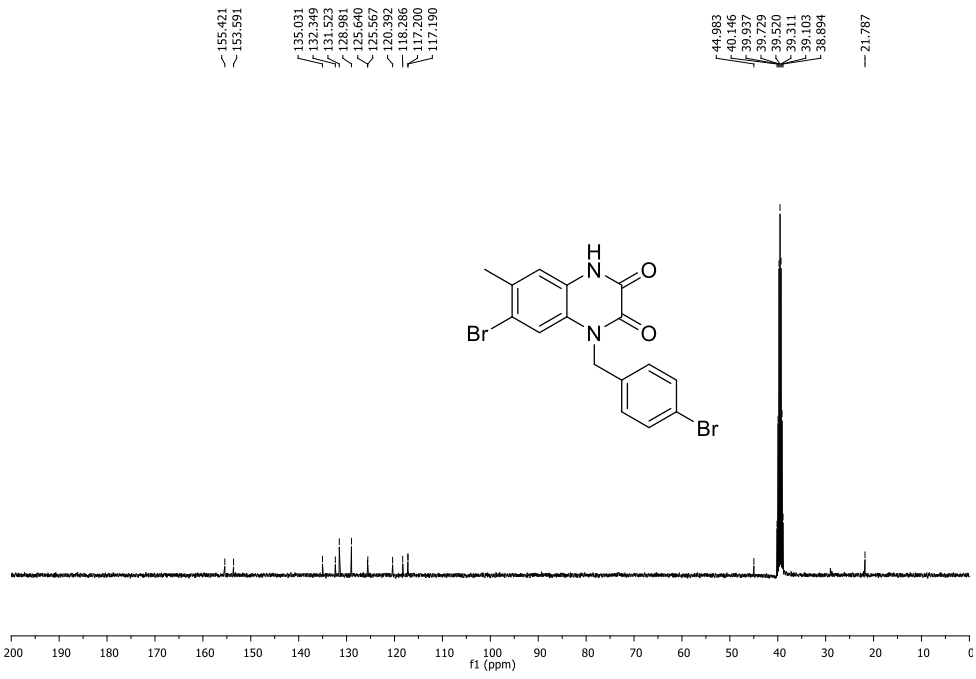

Figure S106. ^{13}C{^{1}H} NMR (100 MHz, DMSO-d_6) of 7-bromo-1-(4-bromobenzyl)-6-methyl-1,4-dihydroquinoxaline-2,3-dione **(2x)**

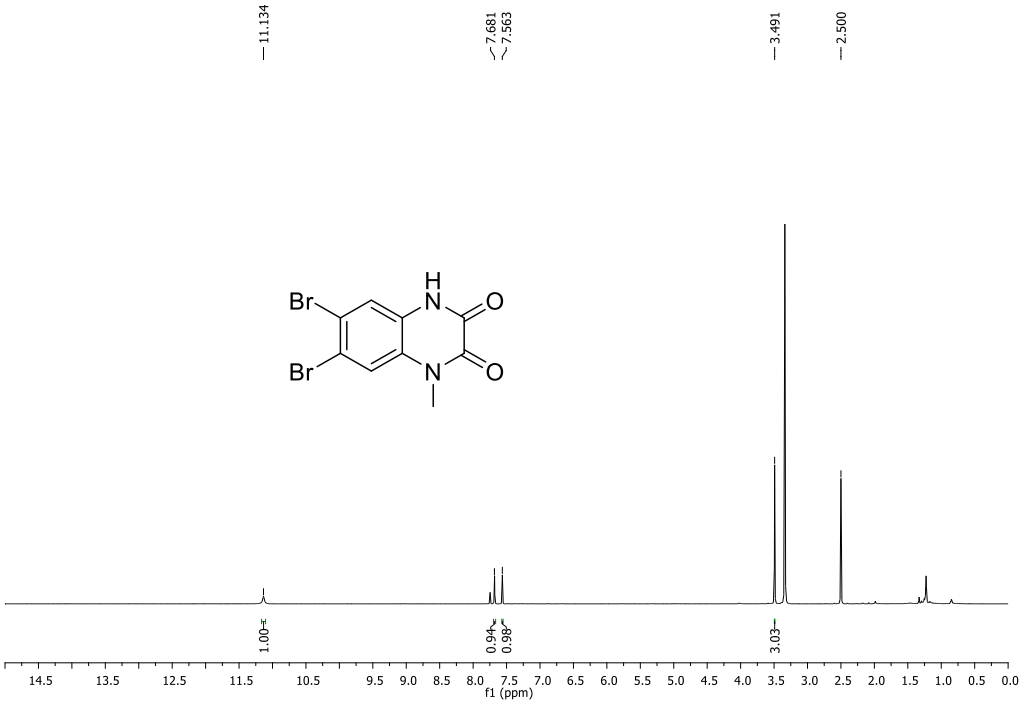

Figure S107. ^{1}H NMR (700 MHz, DMSO-d_6) of 6,7-dibromo-1-methyl-1,4-dihydroquinoxaline-2,3-dione **(3a)**

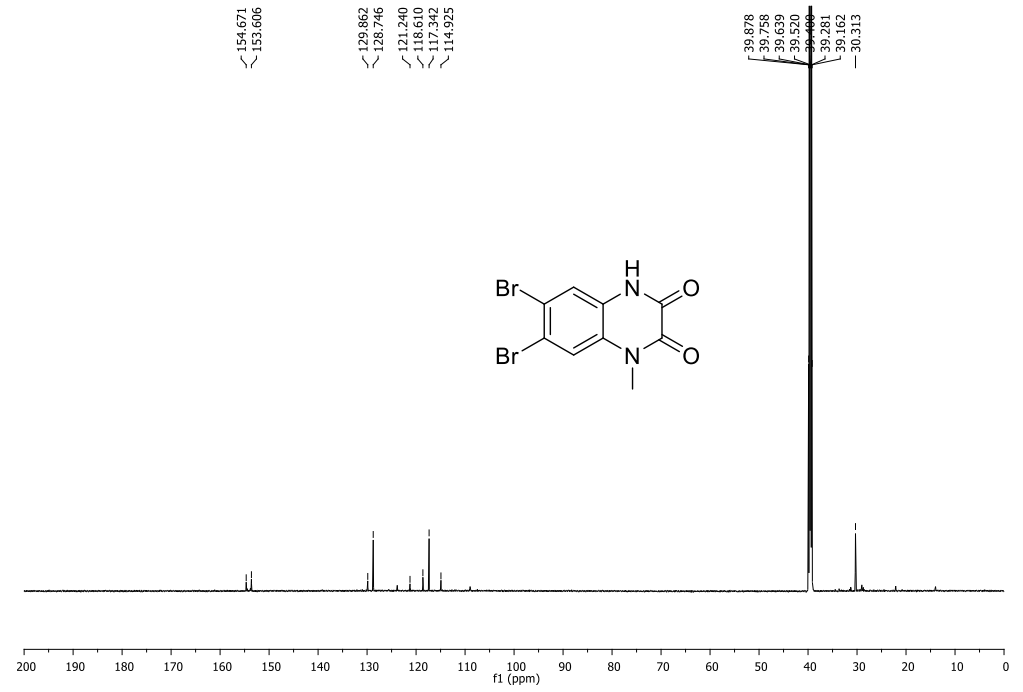

Figure S108. ^{13}C{^{1}H} NMR (175 MHz, DMSO-d_6) of 6,7-dibromo-1-methyl-1,4-dihydroquinoxaline-2,3-dione **(3a)**

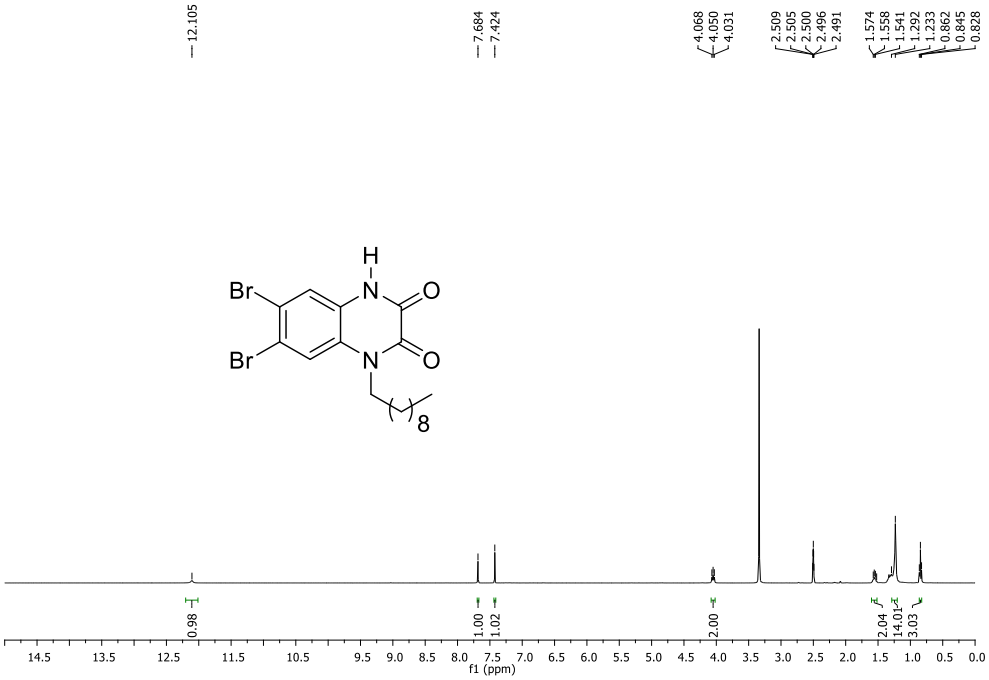

Figure S109. ^{1}H NMR (400 MHz, DMSO-d_6) of 6,7-dibromo-1-decyl-1,4-dihydroquinoxaline-2,3-dione **(3b)**

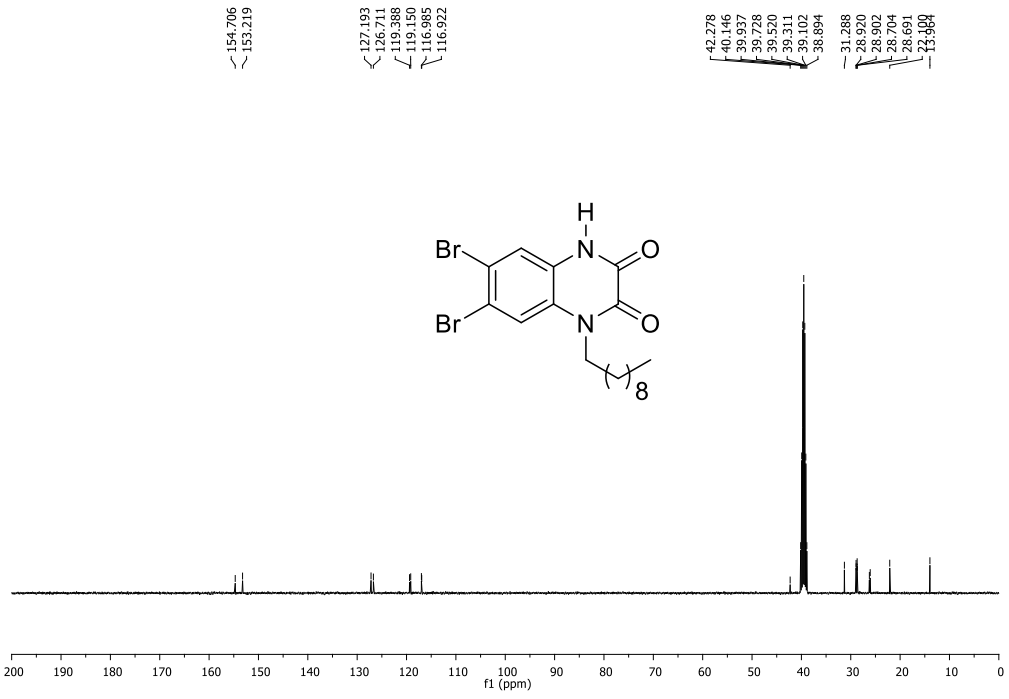

Figure S110. ^{13}C{^{1}H} NMR (100 MHz, DMSO-d_6) of 6,7-dibromo-1-decyl-1,4-dihydroquinoxaline-2,3-dione **(3b)**

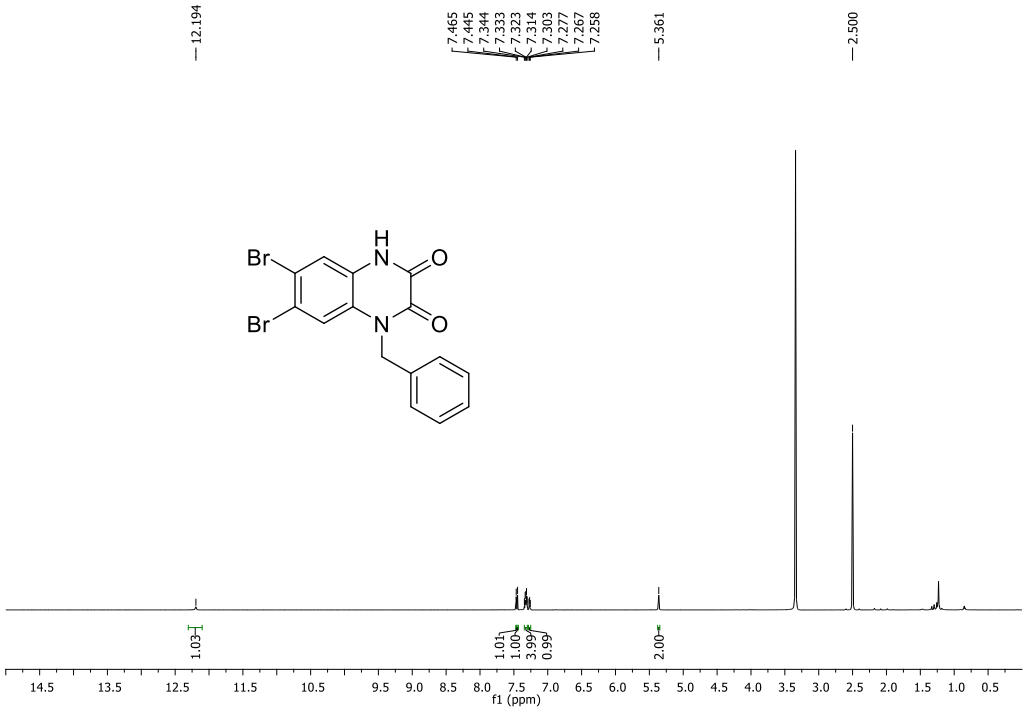

Figure S111. ^{1}H NMR (700 MHz, DMSO-d_6) of 1-benzyl-6,7-dibromo-1,4-dihydroquinoxaline-2,3-dione **(3c)**

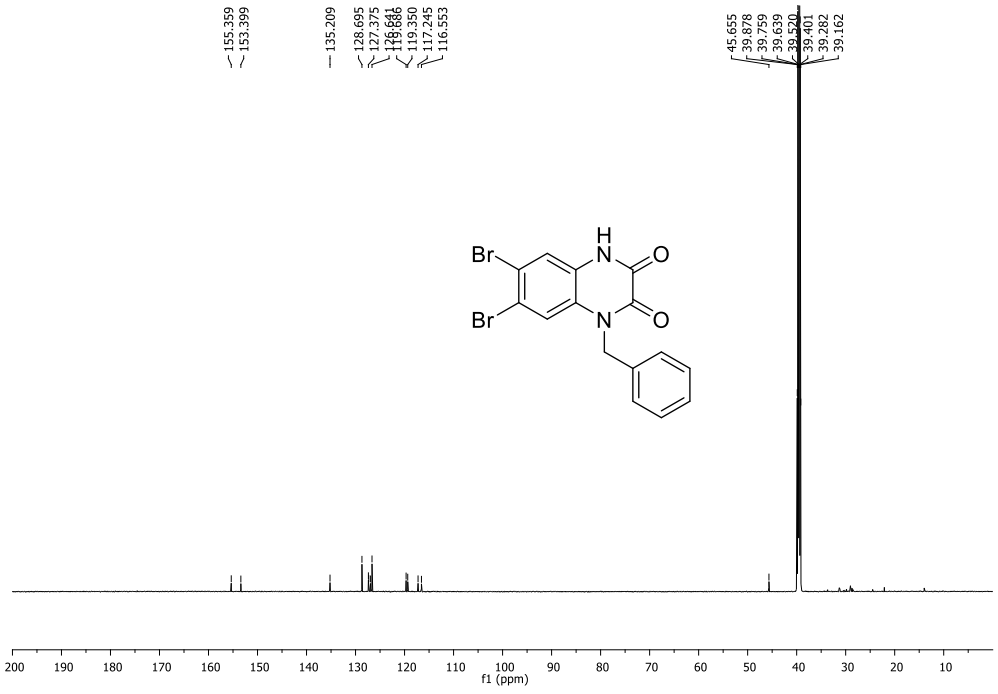

Figure S112. ^{13}C{^{1}H} NMR (175 MHz, DMSO-d_6) of 1-benzyl-6,7-dibromo-1,4-dihydroquinoxaline-2,3-dione **(3c)**

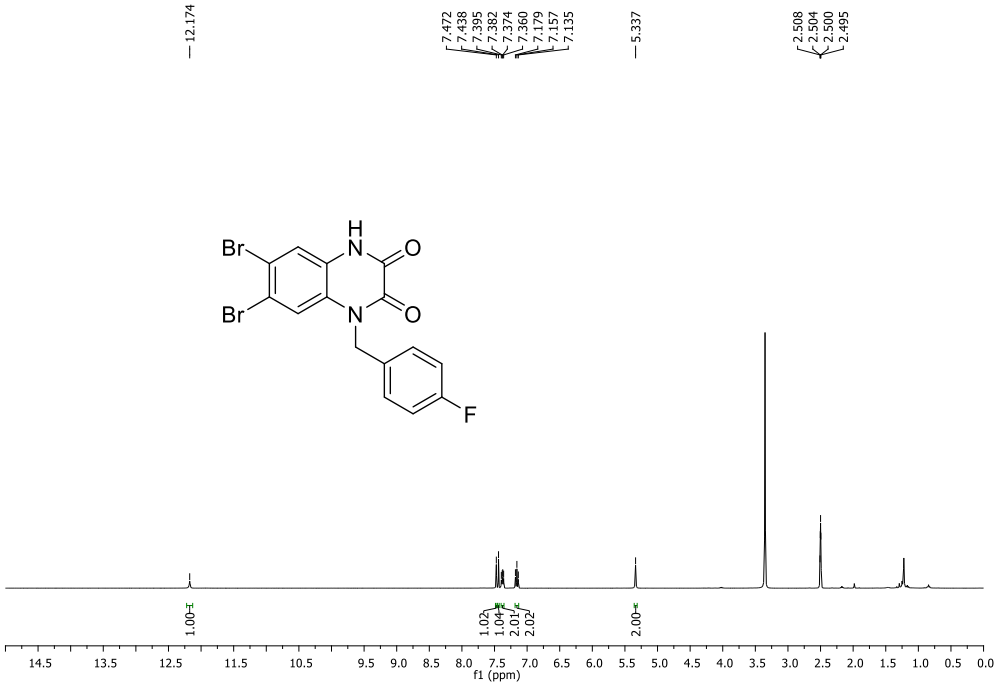

Figure S113. ^{1}H NMR (400 MHz, DMSO-d_6) of 6,7-dibromo-1-(4-fluorobenzyl)-1,4-dihydroquinoxaline-2,3-dione **(3d)**

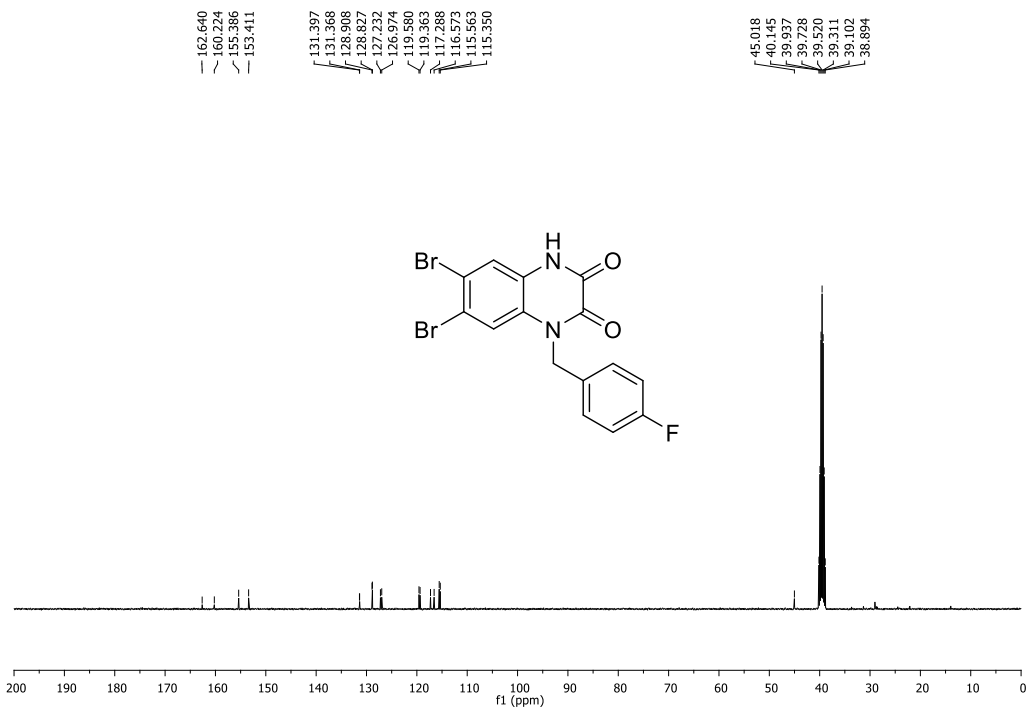

Figure S114. ^{13}C{^{1}H} NMR (100 MHz, DMSO-d_6) of 6,7-dibromo-1-(4-fluorobenzyl)-1,4-dihydroquinoxaline-2,3-dione **(3d)**

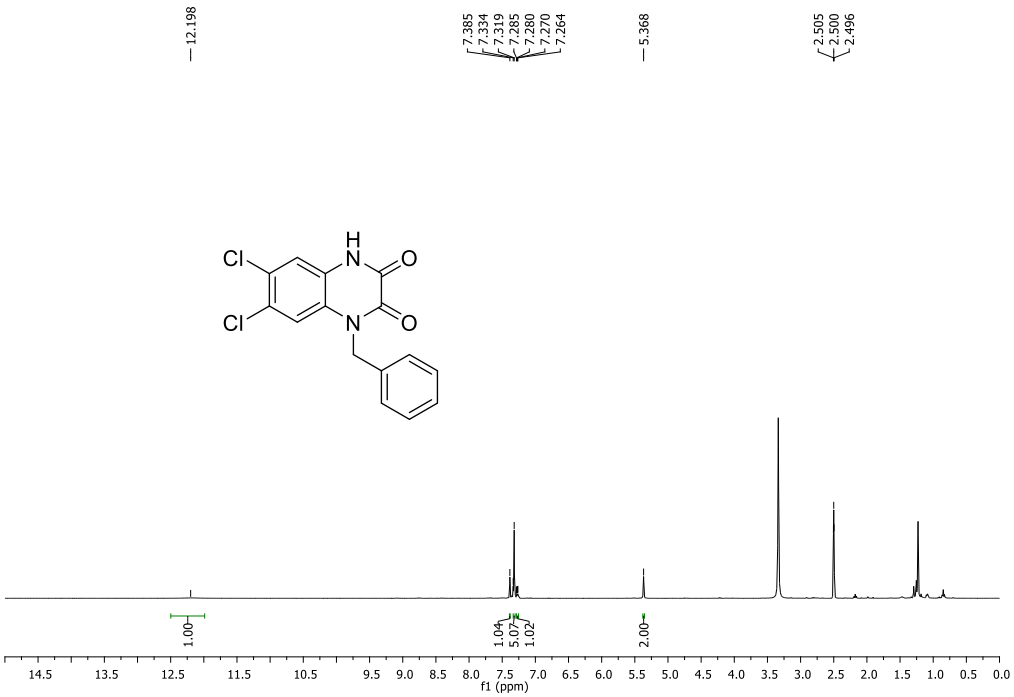

Figure S115. ^{1}H NMR (400 MHz, DMSO-d_6) of 1-benzyl-6,7-dichloro-1,4-dihydroquinoxaline-2,3-dione **(3a')**

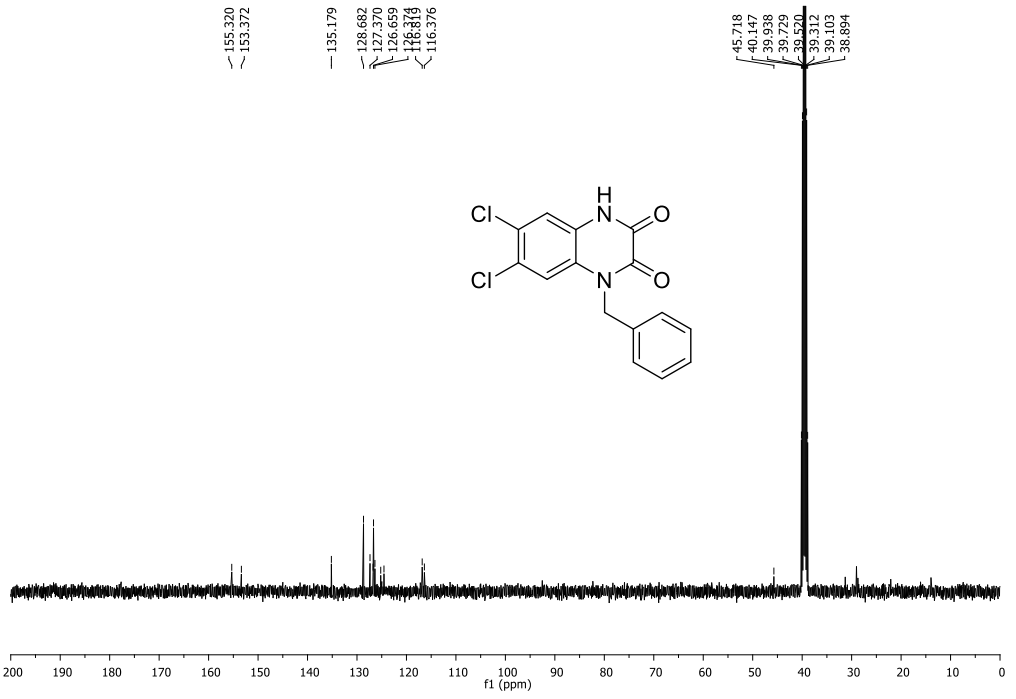

Figure S116. ^{13}C{^{1}H} NMR (100 MHz, DMSO-d_6) of 1-benzyl-6,7-dichloro-1,4-dihydroquinoxaline-2,3-dione **(3a')**

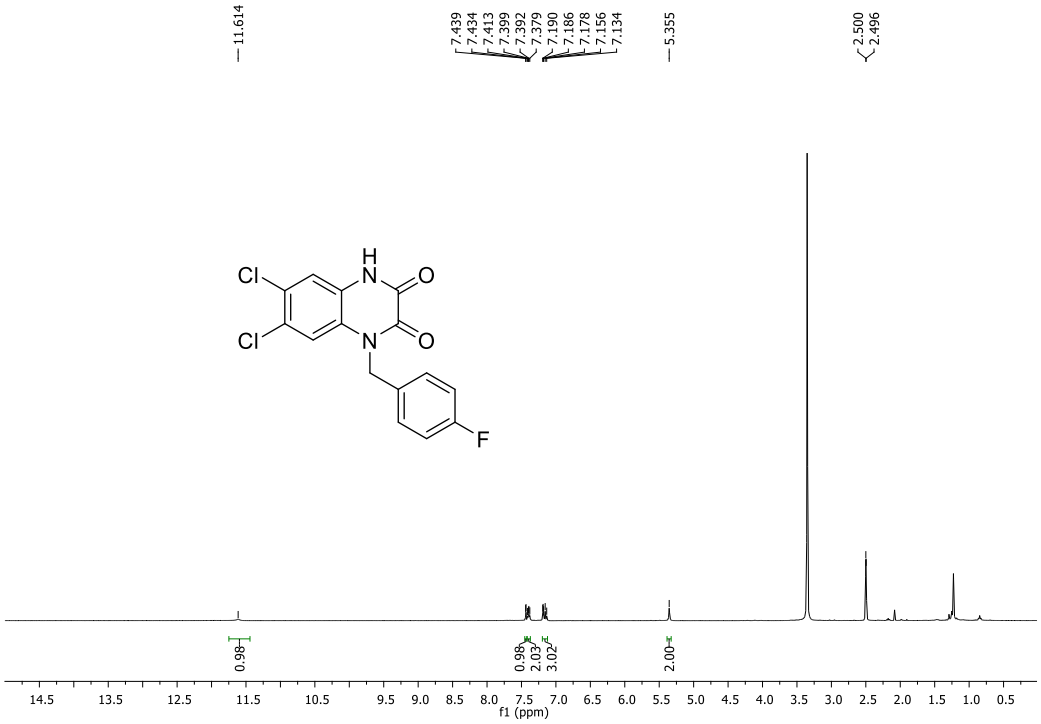

Figure S117. ^{1}H NMR (400 MHz, DMSO-d_6) of 6,7-dichloro-1-(4-fluorobenzyl)-1,4-dihydroquinoxaline-2,3-dione **(3b')**

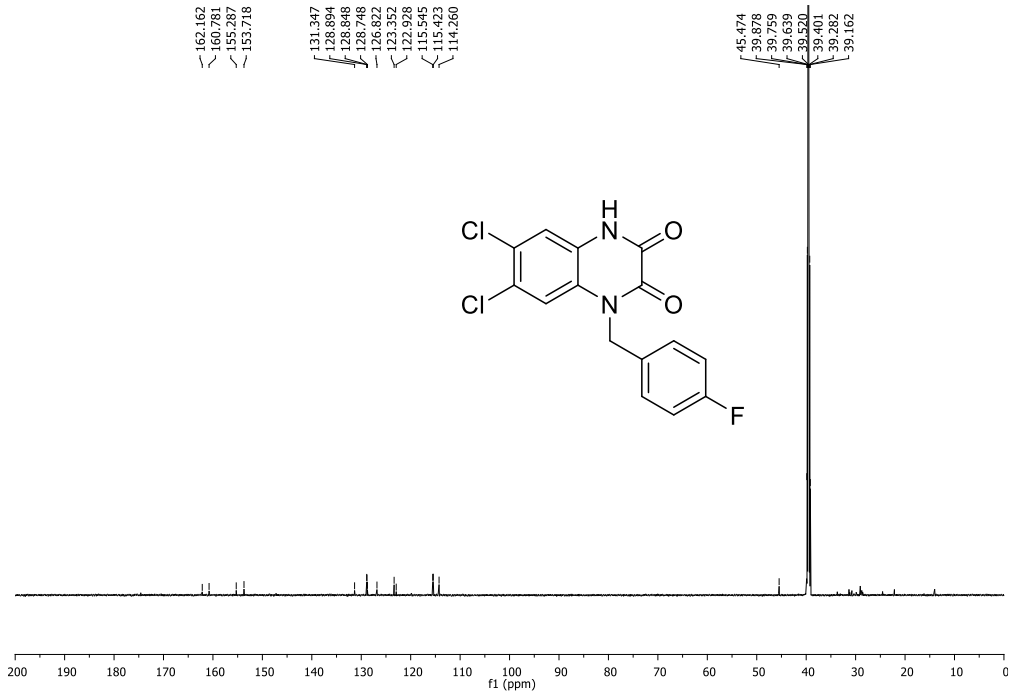

Figure S118. ^{13}C{^{1}H} NMR (100 MHz, DMSO-d_6) of 6,7-dichloro-1-(4-fluorobenzyl)-1,4-dihydroquinoxaline-2,3-dione **(3b')**

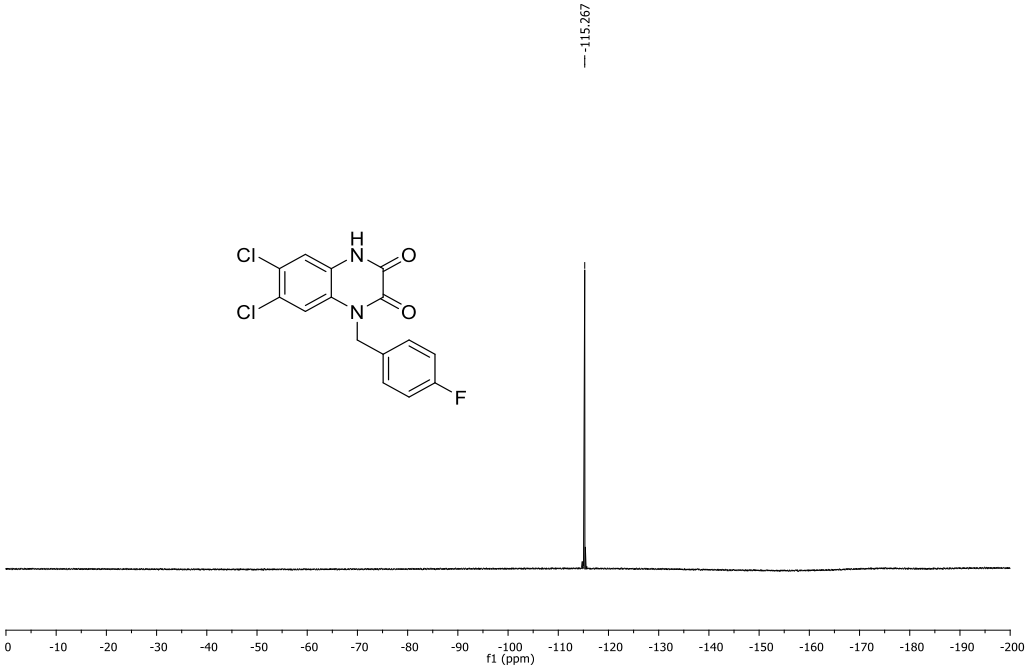

Figure S119. ^{19}F NMR (375 MHz, DMSO-d_6) of 6,7-dichloro-1-(4-fluorobenzyl)-1,4-dihydroquinoxaline-2,3-dione **(3b')**

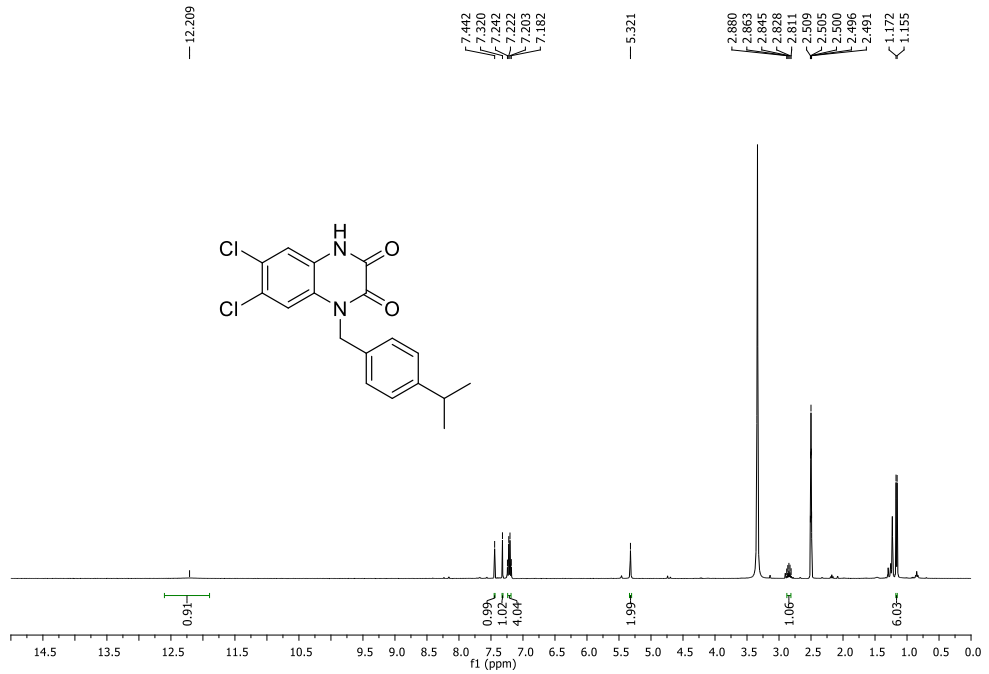

Figure S120. ^{1}H NMR (400 MHz, DMSO-d_6) of 6,7-dichloro-1-(4-isopropylbenzyl)-1,4-dihydroquinoxaline-2,3-dione**(3c')**

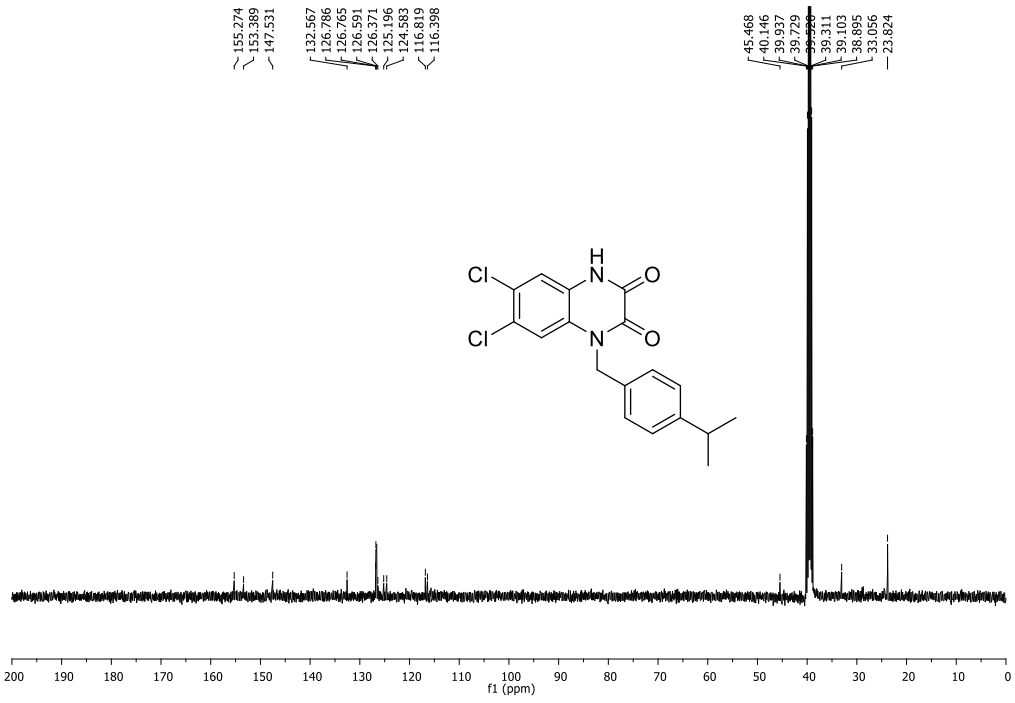

Figure S121. ^{13}C{^{1}H} NMR (100 MHz, DMSO-d_6) of 6,7-dichloro-1-(4-isopropylbenzyl)-1,4-dihydroquinoxaline-2,3-dione **(3c')**

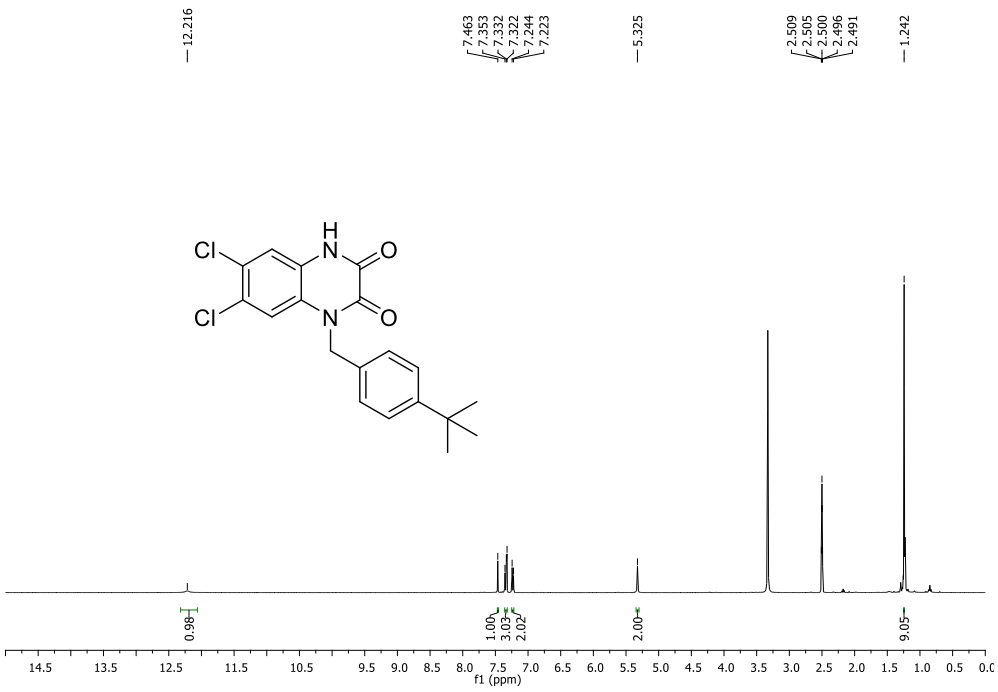

Figure S122. ^{1}H NMR (400 MHz, DMSO-d_6) of 1-(4-(*tert*-butyl)benzyl)-6,7-dichloro-1,4-dihydroquinoxaline-2,3-dione **(3d')**

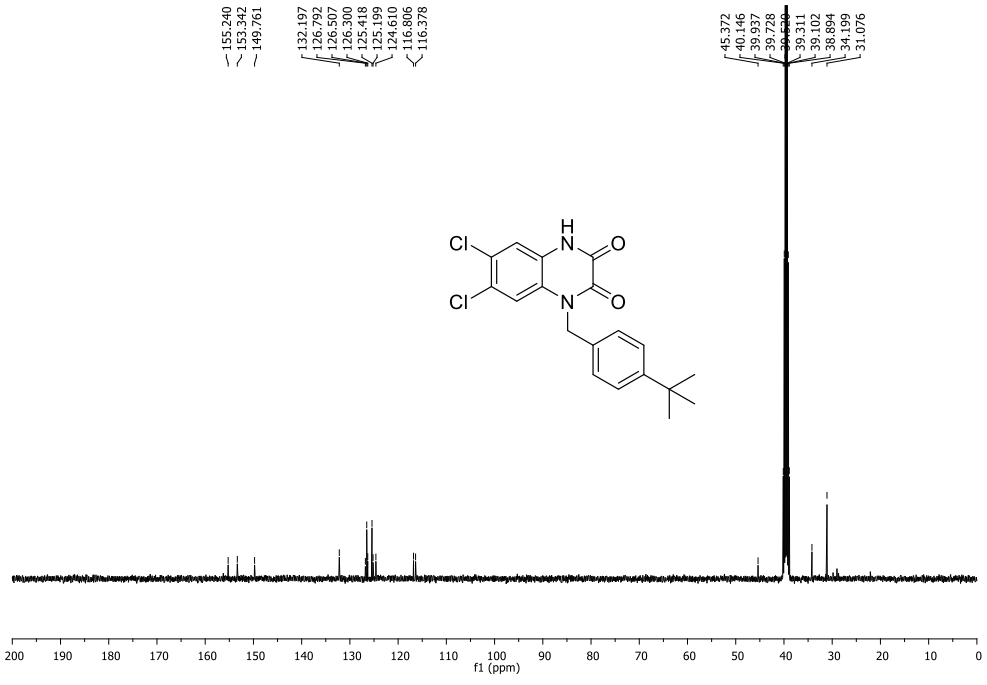

Figure S123. ^{13}C{^{1}H} NMR (100 MHz, DMSO-d_6) of 1-(4-(*tert*-butyl)benzyl)-6,7-dichloro-1,4-dihydroquinoxaline-2,3-dione **(3d')**

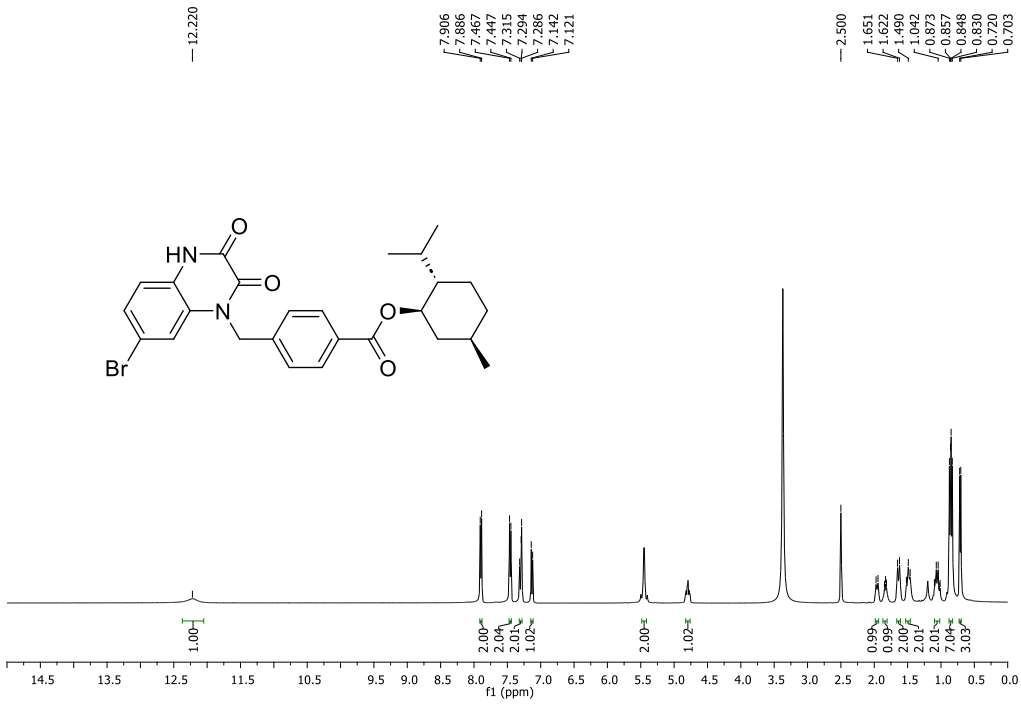

Figure S124. ^{1}H NMR (400 MHz, DMSO-d_6) of (1R,2S,5R)-2-isopropyl-5-methylcyclohexyl 4-((7-bromo-2,3-dioxo-3,4- dihydroquinoxalin-1(2*H*)-yl)methyl)benzoate **(2y)**

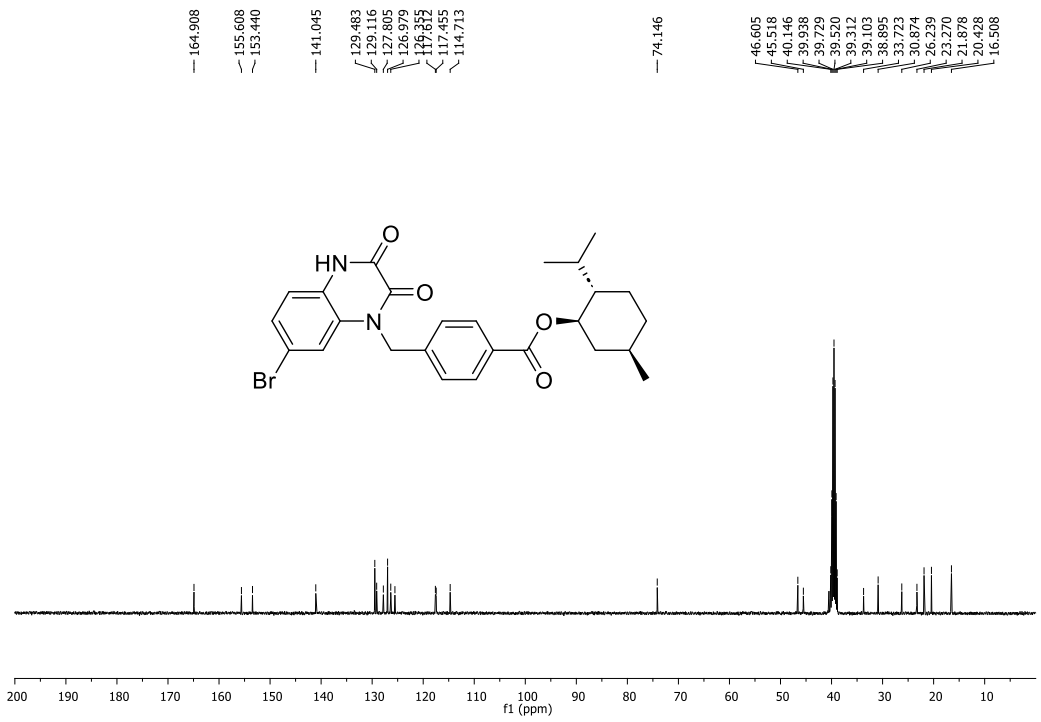

Figure S125. ^{13}C{^{1}H} NMR (100 MHz, DMSO-d_6) of (1R,2S,5R)-2-isopropyl-5-methylcyclohexyl 4-((7-bromo-2,3-dioxo-3,4- dihydroquinoxalin-1(2*H*)-yl)methyl)benzoate **(2y)**

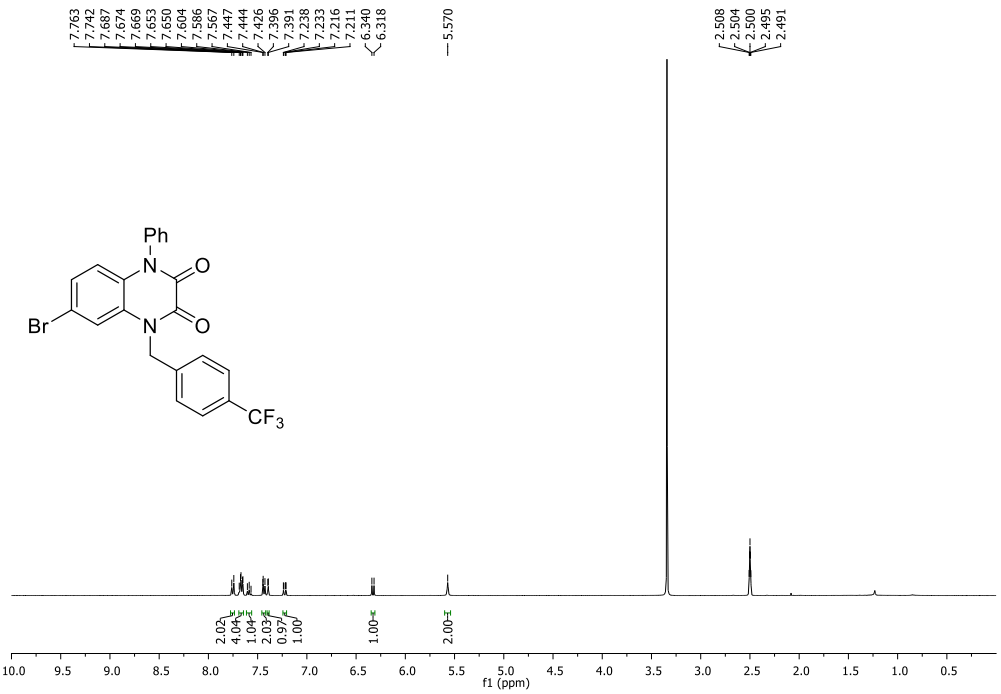

Figure S126. ^{1}H NMR (400 MHz, DMSO-d_6) of 6-bromo-1-phenyl-4-(4-(trifluoromethyl)benzyl)-1,4-dihydroquinoxaline-2,3-dione **(6a)**

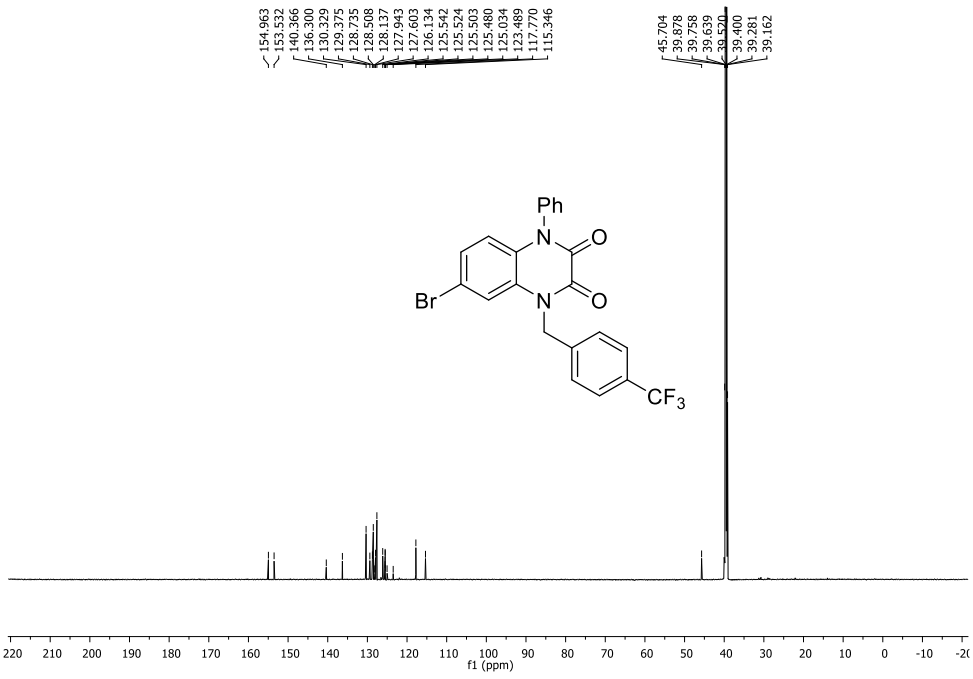

Figure S127. ^{13}C{^{1}H} NMR (100 MHz, DMSO-d_6) of 6-bromo-1-phenyl-4-(4-(trifluoromethyl)benzyl)-1,4-dihydroquinoxaline-2,3-dione (**6a**).

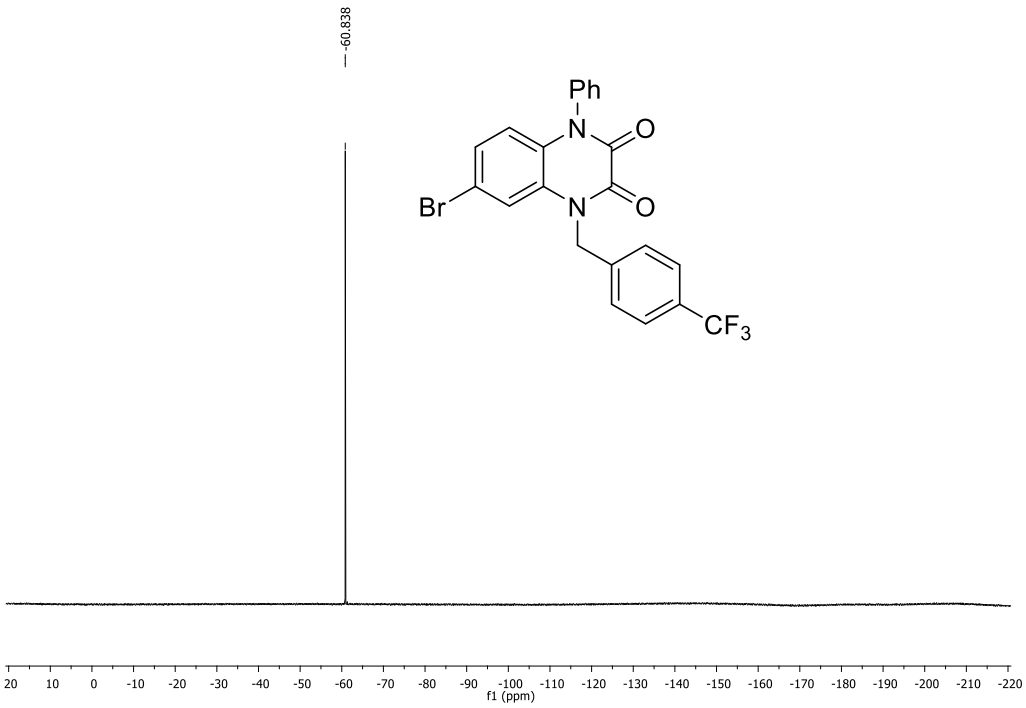

Figure S128. ^{19}F NMR (375 MHz, DMSO-d_6) of 6-bromo-1-phenyl-4-(4-(trifluoromethyl)benzyl)-1,4-dihydroquinoxaline-2,3-dione (**6a**).

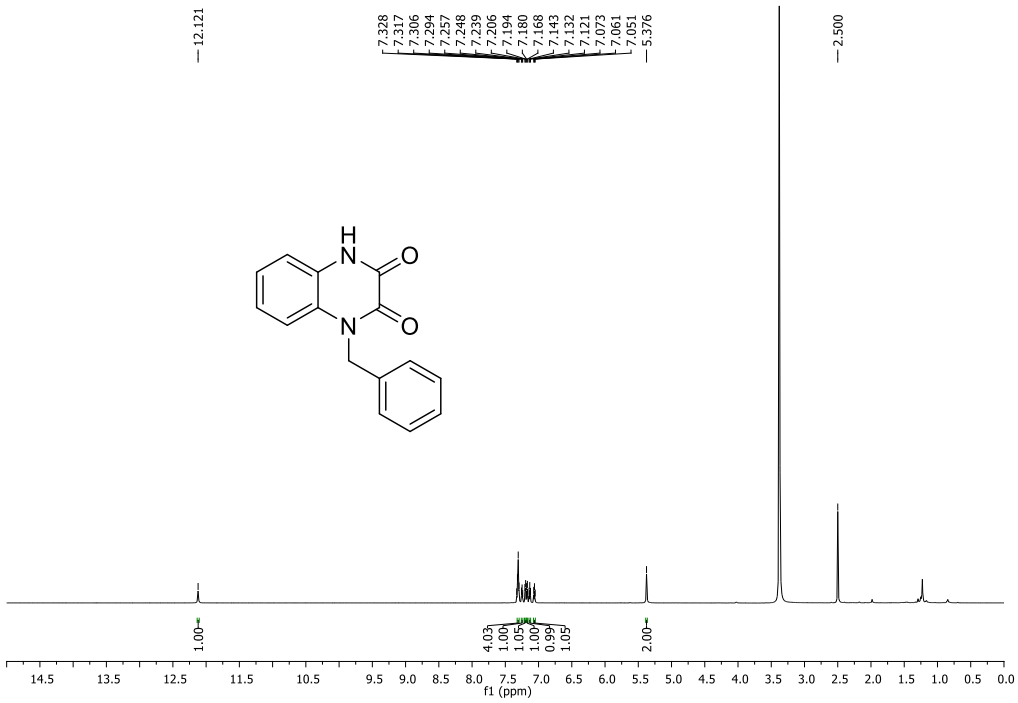

Figure S129. ^{1}H NMR (700 MHz, DMSO-d_6) of 1-benzyl-1,4-dihydroquinoxaline-2,3-dione **(7a).**

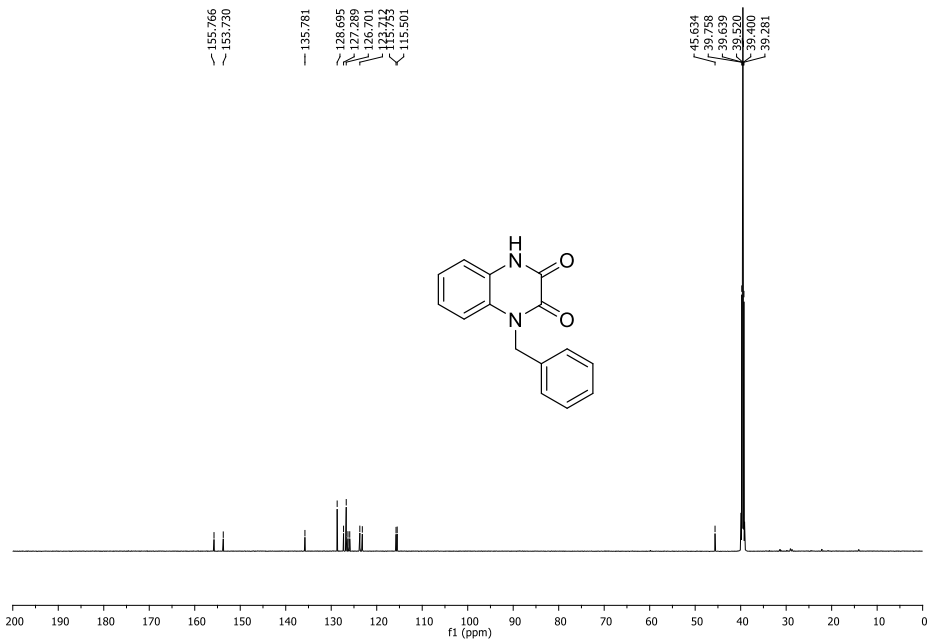

Figure S130. ^{13}C{^{1}H} NMR (175 MHz, DMSO-d_6) of 1-benzyl-1,4-dihydroquinoxaline-2,3-dione **(7a).**

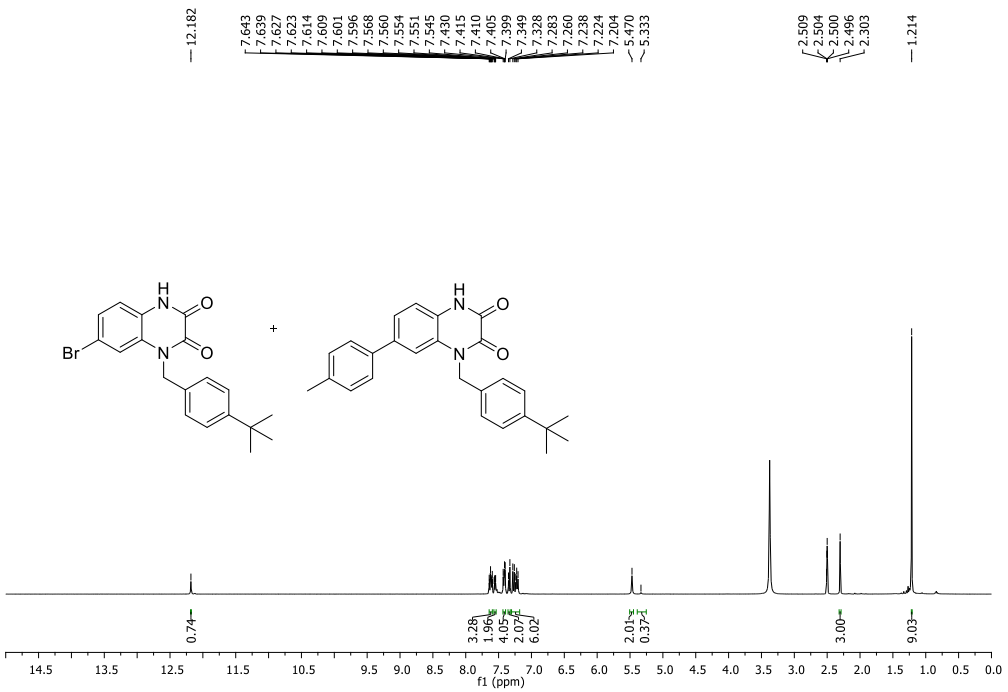

Figure S131. ^{1}H NMR (700 MHz, DMSO-d_6) of 1-(4-(*tert*-butyl)benzyl)-7-(p-tolyl)-1,4-dihydroquinoxaline-2,3-dione **(8a)** and **2i.**

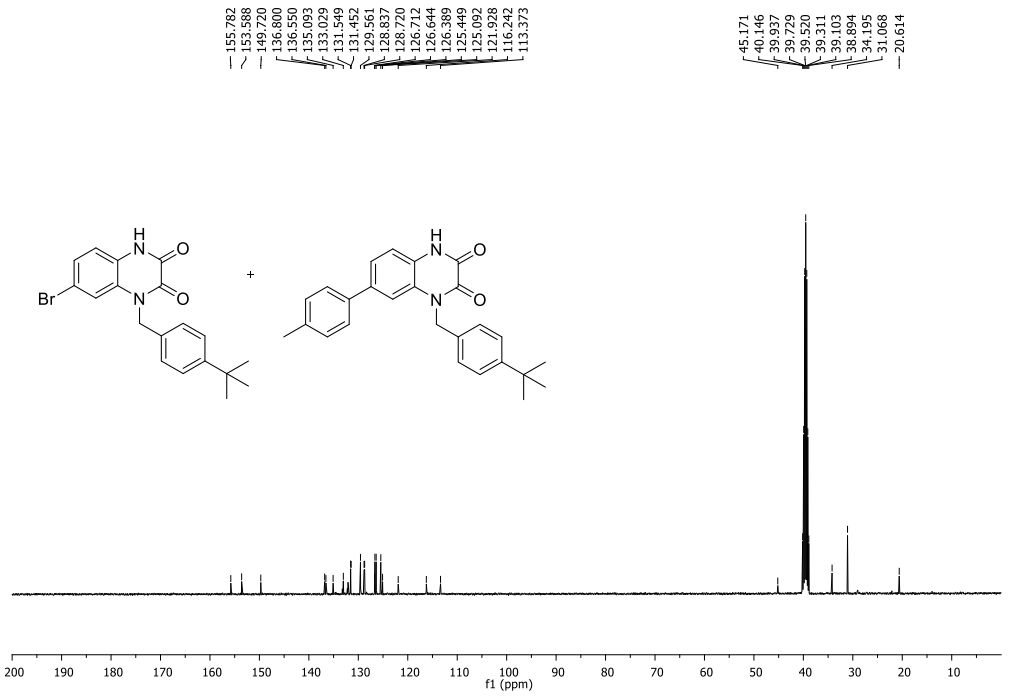

Figure S132. ^{13}C{^{1}H} NMR (175 MHz, DMSO-d_6) of 1-(4-(*tert*-butyl)benzyl)-7-(p-tolyl)-1,4-dihydroquinoxaline-2,3-dione **(8a)** and **2i.**

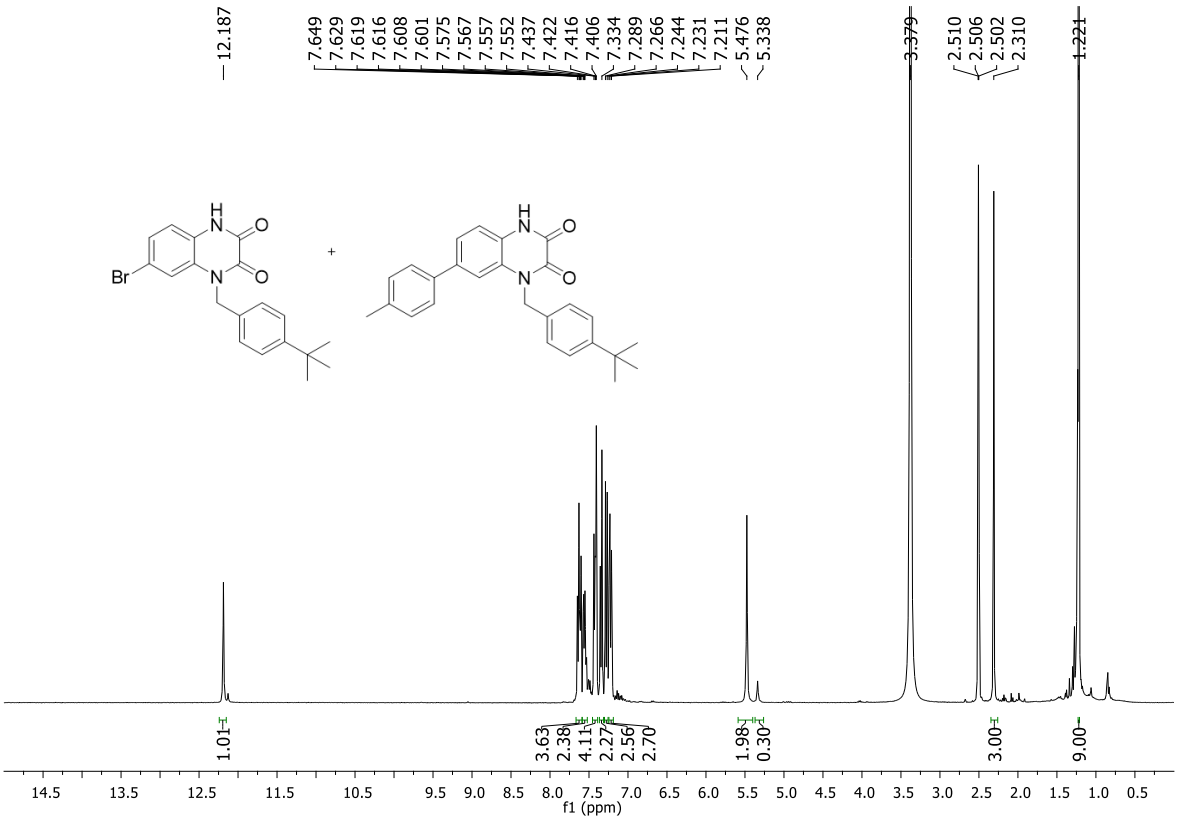

Figure S133. ^{1}H NMR (700 MHz, DMSO-d_6) of 1-(4-(*tert*-butyl)benzyl)-7-(p-tolyl)-1,4-dihydroquinoxaline-2,3-dione **(8a)** and **2i** (after 72 h).

REFERENCES

1. I. Ghosh, T. Ghosh, J. I. Bardagi and B. König, Reduction of aryl halides by consecutive visible light-induced electron transfer processes, *Science*, 2014, **346**, 725-728.
2. B. Pal and P. Mal, Thermocontrolled Radical Nucleophilicity vs Radicophilicity in Regiodivergent C–H Functionalization, *Org. Lett.*, 2025, **27**, 978-983.
3. S. Cao, J.-X. Chen, X.-L. Zhang, X. Song, W.-Y. Song, Y.-S. Wu, Y.-H. Zhang and Z. Liu, Merging Quinoxalin-2(1*H*)-ones Excitation with Cobaloxime Catalysis: C_3 Alkylation of Quinoxalin-2(1*H*)-ones with Unactivated Alkyl Iodides and Carboxylic Acids under Light, *Org. Lett.*, 2024, **26**, 5833-5838.
4. S. Sau and P. Mal, Visible-Light Promoted Regioselective Oxygenation of Quinoxalin-2(1*H*)-ones Using O_2 as an Oxidant, *J. Org. Chem.*, 2022, **87**, 14565-14579.
5. C. Caristi, G. Cimino, A. Ferlazzo, M. Gattuso and M. Parisi, Unusual behaviour of N-bromosuccinimide. Conversion of *N*,*N*-dimethylamides to *N*-methyl,*N*-succinimidomethylamides, *Tetrahedron Lett.*, 1983, **24**, 2685-2688.
6. T. K. Dinda, A. Manna and P. Mal, En Route to Recyclable Semi-Heterogeneous Photocatalysis with Photoinert $CeCl_3$, *ACS Catal.*, 2024, **14**, 7664-7673.
7. S. Mahata, T. K. Dinda, S. R. Sahoo, N. Polley, D. Topwal, P. Mal and N. Goswami, Organic Photocatalysis by In Situ Polymerized Gold Nanocluster-Polydopamine Networks, *ACS Appl. Mater. Interfaces*, 2025, **17**, 59410-59421.
8. SAINT+, Bruker AXS Inc., Madison, Wisconsin, USA, 1999 (Program for Reduction of Data collected on Bruker CCD Area Detector Diffractometer V. 6.02.)
9. SADABS, Bruker AXS, Madison, Wisconsin, USA, 2004
10. G. Sheldrick, A short history of SHELX, *Acta Crystallogr. A*, 2008, **64**, 112-122.
11. S. Sau, S. Takizawa, H. Y. Kim and K. Oh, Visible Light-Induced Radical Cascade Functionalization of Quinoxalin-2(1*H*)-ones: Three-Component 1,2-Di(hetero)arylation Approach with Styrenes and Thianthrenium Salts, *Org. Lett.*, 2024, **26**, 8821-8826.
12. V. S. Patil, G. Chunduri, B. K. Avasarala, G. L, P. Yoganand, K. Srinivas, M. Koparala and N. Devunuri, The Lacunae identified in processing, analyzing and finding means of catalyst-free Oxone mediated through C_3-oxidation of *N*-alkyl quinoxalin-2(1*H*)-one, *Synth. Commun.*, 2024, **54**, 694-708.

13. S. Sau, S. Sahoo, A. Manna and P. Mal, Moisture-resistant radical anions of quinoxalin-2(1*H*)-ones in aerial dioxygen activation, *Org. Biomol. Chem.*, 2024, **22**, 4662-4666.
14. V. V. Khade, A. Bhowmick, A. S. Thube and R. G. Bhat, Direct Access to Strained Fused Dihalo-Aziridino Quinoxalinones via C_3-Alkylation Followed by Tandem Cyclization, *J. Org. Chem.*, 2023, **88**, 8010-8023.
15. S. Song, X. Peng, B. Zhou, L. Zheng, J. Sun, Z. Chen and J. Li, Acid-Promoted Self-Photocatalyzed Regioselective Oxidation: A Novel Strategy for Accessing Quinoxaline-2,3-diones, *Chem. Eur. J.*, 2024, **30**, e202402848.
16. S. Sau and P. Mal, C−H Hydroxylation of Quinoxalin-2(1*H*)-ones through ipso-Substitution Using *tert*-Butyl Nitrite, *Eur. J. Org. Chem.*, 2022, e202200425.
17. S. B. Goud, R. L. Dhakar and S. Samanta, Switching Copper(II)-Catalytic Process for the Selective Access to C_3-Imidazolyl- and Pyridylquinoxalin-2(1*H*)-ones, *J. Org. Chem.*, 2026, **91**, 2575-2596.
18. G. Badhani, V. M. Biramya and S. Adimurthy, Ionic liquid-catalysed regioselective oxygenation of quinoxalin-2(1*H*)-ones under visible-light conditions, *New J. Chem.*, 2023, **47**, 21596-21599.